UNIVERSIDAD AUTÓNOMA DE MADRID

FACULTAD DE CIENCIAS

DEPARTAMENTO DE BIOLOGÍA MOLECULAR

INSIGHTS INTO THE GENETICS AND BIOCHEMISTRY OF SIGNALING ADAPTOR MODULES AND NK CELL RECEPTORS FROM STUDY OF PRIMARY IMMUNODEFICIENCY

Thesis dissertation submitted for the degree of Doctor of Philosophy

Alfonso Blázquez Moreno

Degree in Biotechnology
Master in Molecular and Cellular Biology

Supervised by Hugh Reyburn, BVMS, PhD, MRCVS

Carried out at the National Center for Biotechnology (CNB-CSIC)
Madrid, Spain

The research presented in this thesis was carried out in the Department of Immunology and Oncology of the National Centre for Biotechnology (CNB-CSIC) in Madrid, under the supervision of Hugh Reyburn, PhD. Thesis research was supported by PhD studentship SVP-2014-068263 and grant SAF-2014-58752 from MINEICO.

**“ Son los problemas sin resolver, no los resueltos,
los que mantienen activa la mente ”**

Erwin Guido Kolbenheyer

ABSTRACT

Many immune cell receptors are modular in design; the ligand binding function and signaling capacity are separated into two different elements. One common signaling adaptor molecule expressed in both Natural Killer and T cells is CD247.

The opportunity to study immune cells from a CD247 deficient patient let us analyze the effects of the lack of this adaptor module on human lymphocyte biology. In the absence of CD247, T cell receptor assembly was compromised and its expression at the cell surface markedly diminished, abrogating antigen-specific immune responses by the patient and increasing susceptibility to infections. With regard to NK cells, surface expression of CD247-coupled receptors and their function after specific ligation was compromised. Moreover, as well as these direct effects, the absence of functional T cells also impaired NK cell development and proper maturation indirectly.

Consistent with prior studies on CD247-deficient patients, it was possible to detect revertant T and NK cells in this particular patient. Subsequent genetic analyses of the patients T cells, after brief *in vitro* expansion, revealed two classes of revertant cells: a true back mutation and a compensatory mutation, both compatible with restored CD247 protein expression and T cell receptor assembly. This reversion phenomenon has been reported for only a set of genes affected in PIDs. Further informatics analysis of the genetic variation in other PID genes where reversion has been reported showed a higher rate of missense variants in the coding sequence of these genes compared to PID affected genes with no reversion cases or control genes, leading to the hypothesis that the occurrence of somatic mutations that reconstitute genetic defects in PID is related to an increased propensity of those genes to mutate.

To date, the interactions that mediate CD247 assembly with counterpart receptors depend on contacts between single transmembrane residues of opposing charge. However, CD16A does not contain a positively charged residue in its transmembrane domain. Detailed biochemical study of CD16A receptor complex formation revealed a novel mode of assembly based on multiple polar and aromatic interactions that could be extended to other Fc receptors, CD64 and FcεR1α.

Altogether, our results illustrate how the human immune system adapts, escapes by reversion of genetic defects and the biochemical plasticity of CD247 signaling adaptor module demonstrated by the ability to couple many receptors by different mechanisms.

RESUMEN

La gran mayoría de los receptores inmunes tienen un diseño modular; la capacidad de unirse a sus ligandos y de señalizar recae en subunidades diferentes. CD247 es un módulo de señalización común a células T y Natural Killer.

La ocasión de estudiar el sistema inmunitario de un paciente deficiente en CD247 ha permitido analizar las consecuencias de la ausencia de esta molécula adaptadora en la biología de los linfocitos humanos. En ausencia de CD247, el ensamblaje del TCR se ve comprometido y su expresión en superficie es prácticamente nula, impidiendo las respuestas antígeno específicas y aumentando la susceptibilidad a infecciones del paciente. En cuanto a las células NK, la expresión en superficie y la respuesta a través de receptores que se asocian a CD247 está disminuida. Además de estos efectos directos, la ausencia de células T funcionales afecta de manera indirecta al correcto desarrollo y maduración de las células NK.

Al igual que en los pacientes deficientes en CD247 previamente descritos, detectamos células T y NK revertientes. El análisis genético de células T del paciente, tras una breve expansión *in vitro*, reveló la existencia de dos clases de revertientes: una retromutación y una mutación compensatoria, permitiendo ambas recuperar la expresión de la proteína CD247 y el ensamblaje del TCR. Se han encontrado eventos de reversión en solo algunos de los genes afectados en inmunodeficiencias primarias (IDPs). El análisis de la variación genética en el resto de genes revertientes mostró una mayor tasa de mutaciones sin sentido en la región codificante, comparado a otros genes afectados en IDPs sin eventos de reversión descritos o en genes control. Este hallazgo hizo plantear como hipótesis que la probabilidad de revertir un defecto genético está relacionada con la propensión intrínseca de dicho gen a mutar.

Hasta la fecha, la asociación de CD247 a sus receptores se basa en una única interacción mediada por residuos de carga opuesta. Sin embargo, CD16A no contiene un residuo cargado positivamente en su región transmembrana. El estudio bioquímico de la interacción de CD16A con sus módulos de señalización reveló un nuevo modelo de ensamblaje basado en múltiples interacciones polares y aromáticas. Además, se demostró que este modelo podría aplicarse a otros receptores de Fc, CD64 y FcεR1α.

En resumen, estos resultados ilustran como el sistema inmunitario se adapta, revierte los defectos genéticos y demuestra la plasticidad del módulo de señalización CD247 para unirse a distintos receptores mediante diferentes mecanismos.

INDEX

23 INTRODUCTION

ABBREVIATIONS

Ab	Antibody
ADA	Adenosine deaminase
ADCC	Antibody dependent cell cytotoxicity
BCR	B cell receptor
CARD11	Caspase recruitment domain 11
CD	Cluster of differentiation
cDNA	Complementary deoxyribonucleic acid
CID	Combined Immunodeficiency
CNV	Copy number variation
CO2	Carbon dioxide
CXCR4	C-X-C chemokine receptor type 4
DMEM	Dulbecco´s Modified Eagle medium
DNA	Deoxyribonucleic acid
DOCK8	Dedicator of cytokinesis 8
EGFP	Enhanced green fluorescence protein
ER	Endoplasmic reticulum
F	Forward
FAS	First apoptosis signal
Fc	Fragment crystallizable
FcR	Fc receptors
FCS	Foetal calf serum
FcαR	Fc-alpha receptors
FcγR	Fc-gamma receptors
FcεR	Fc-epsilon receptors
FynT	Fyn tyrosine
GeoMFI	Geometric mean fluorescence intensity
GlcNAc	β-N-acetylglucosamine
GPI	Glycosylphosphatidylinositol
Grb2	Growth factor receptor-bound protein 2
HCMV	Human cytomegalovirus
HIV	Human immunodeficiency virus
HLA	Human leukocyte antigen

HSC	Hematopoietic stem cell
ICOS	Inducible T cell co-stimulator
IDP	Inmunodeficiencia primaria
IFN	Interferon
Ig	Immunoglobulin
IgAD	Immunoglobulin A deficiency
IKBKG	Inhibitor of kappa B kinase gamma
IL	Interleukin
IL-R	Interleukin - receptor
IP_3	Inositol triphosphate
IP_4	Inositol tetrakisphosphate
IRAK4	Interleukin-1 receptor-associated kinase 4
IRF8	Interferon regulatory factor 8
ISG15	Interferon (IFN)-stimulated gene 15
ITAM	Immunoreceptor tyrosine based activating motif
ITIM	Immunoreceptor tyrosine-based inhibition motif
IUIS	International Union of Immunological Societies
IVT	In vitro transcription
JAK3	Janus Kinase 3
KIR	Killer-cell immunoglobulin-like receptors
LIG1	Ligase 1
mAb	Monoclonal antibody
MALT	Mucosa-associated lymphoid tissue
MCMV	Mouse cytomegalovirus
Med-Golgi	Medial-Golgi
MFI	Mean fluorescence intensity
MHC	Major histocompatibility complex
min	Minutes
MIP1a/B	Macrophage Inflammatory Proteins
MIRR	Multisubunit immune-recognition receptor
mL	Milliliter
mM	Millimolar

MMR	Mismatch repair
mRNA	Messenger Ribonucleic acid
NCR	Natural Cytotoxicity Receptor
NEMO	Nuclear factor-κB essential modulator
NK	Natural Killer
nm	Nanometre
NMR	Nuclear magnetic resonance
PBA	PBS-azide
PBMC	Peripheral blood mononuclear cell
PBS	Phosphate-buffered saline
PCR	Polymerase chain reaction
PE	Phycoerythrin
PI3K	Phosphatidylinositol-4,5-bisphosphate 3-kinase
PID	Primary Immunodeficiency
PM	Plasma membrane
qPCR	Quantitative polymerase chain reaction
R	Reverse
RAG 1/2	Recombination-activating gene enzymes 1/2
RNA	Ribonucleic acid
RT	Reverse transcription
SAP	SLAM associated protein
SD	Standard deviation
SH2	Src homology 2
SH2D1A	SH2 domain–containing protein 1A
SHIP	SH2-containing polyinositol phosphatase
SHP-1/2	SH2-containing protein tyrosine phosphatase 1/2
SLE	Systemic lupus erythematosus
SMFS	Single-molecule force spectroscopy
SNP	Single nucleotide polymorphisms
STAT1	Signal transducer and activator of transcription 1
TCR	T cell receptor
TGF	Transforming growth factor

TGFBR1	TGF-beta receptor type-1
TGN	Trans-Golgi network
TM	Transmembrane
TMD	Transmembrane domain
TNF	Tumor necrosis factor
TRAPS	TNF - Receptor-Associated Periodic Syndrome
TWEAK	TNF - related weak inducer of apoptosis
U	Unit
v/v	Volume/volume
w/v	Weight/Volume
WAS	Wiskott–Aldrich syndrome protein
wt	Wild type
ZAP70	Zeta-chain-associated protein kinase 70
ºC	Degree Celsius

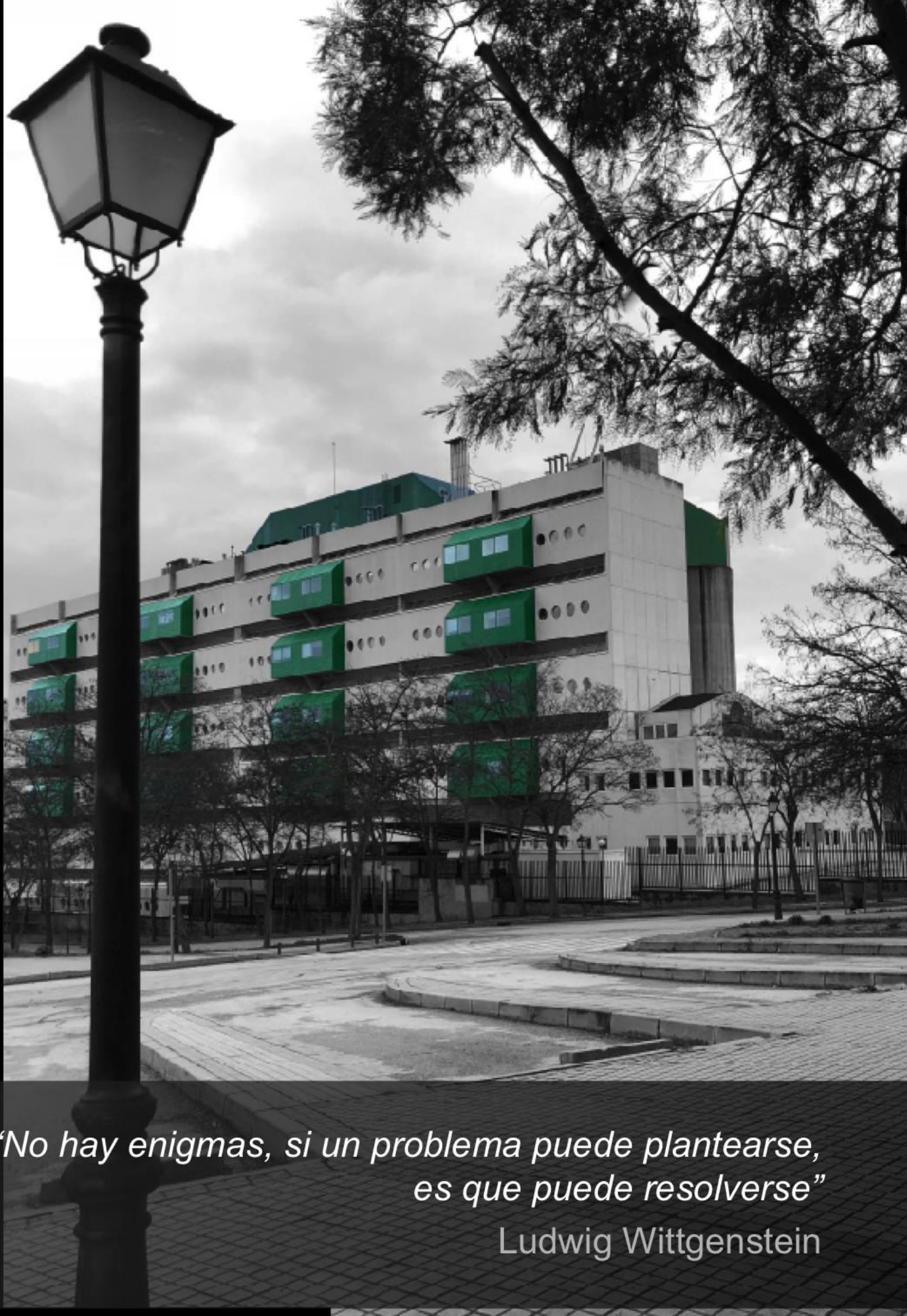

“No hay enigmas, si un problema puede plantearse,
es que puede resolverse”

Ludwig Wittgenstein

INTRODUCTION

1. PRIMARY IMMUNODEFICIENCIES:

1.1. Definition and classification:

Primary immunodeficiency diseases (PID) are a group of more than 300 rare, chronic disorders in which part of the body's immune system is missing or functions improperly [1]. These diseases are not contagious, rather they are caused by hereditary or spontaneous genetic defects, and, although most disorders present at birth or in early childhood, the disorders can manifest themselves at any age.

In contrast, secondary immunodeficiencies occur during certain viral infections, after immunosuppression to prevent graft rejection after transplantation, during treatment of systemic autoimmune disease, and in association with cancer and chemotherapy [1].

Some PIDs affect a single part of the immune system, while others may affect one or more components of the system. Although, the specific symptoms may differ between diseases, they all share an increased susceptibility and severity to infection. Moreover, common features often include immune dysregulation with autoimmune disease, lymphoproliferation, aberrant inflammatory responses and malignancy [1].

With the exception of IgA deficiency (IgAD), which occurs with a high incidence of 1:500 newborns [2], all other forms of PID are rare and have an overall prevalence of approximately 1:10,000 live births; however, a much higher rate is observed among populations with high rates of consanguinity or among genetically isolated populations. PIDs are classified according to the component of the immune system that is primarily involved. The Expert Committee for Primary Immunodeficiency of the International Union of Immunological Societies (IUIS) classified PIDs into 8 general categories affecting either adaptive or innate immune responses (Table 1): (1) combined immunodeficiencies (CIDs), (2) well-defined syndromes with immunodeficiency, (3) predominantly antibody deficiencies, (4) diseases of immune dysregulation, (5) congenital defects of phagocyte number, function, or both, (6) defects in innate immunity, (7) autoinflammatory disorders, and (8) complement deficiencies [3, 4].

In the last years, advances in molecular genetics and immunology have resulted in the identification of a growing number of genes causing primary

immunodeficiencies in human subjects and a better understanding of the pathophysiology of these disorders. Characterization of the molecular mechanisms of PIDs have also facilitated the development of novel diagnostic assays based on analysis of the expression of the protein encoded by the PID-specific gene. Pilot newborn screening programs for the identification of infants with severe combined immunodeficiency have been initiated and appropriate protocols to PID diagnosis and management [1]. Furthermore, significant advances have been made in the treatment of PIDs based on the use of subcutaneous immunoglobulins, hematopoietic cell transplantation from unrelated donors and cord blood, and gene therapy [5].

Finally, PID provide a unique opportunity to study the phenotypic and functional consequences of a single gene defect for human immunology and this is important since there are many differences between mice and human immune system, in particular with regard to the NK cell compartment [6].

2. MUTATIONS CAUSING PRIMARY IMMUNODEFICIENCIES:

2.1. Nature of gene defects:

Mutations causing primary immunodeficiencies are mostly recessive and often require homozygosity to significantly affect immune cells and responses. Since most PIDs are inherited in an autosomal recessive pattern, inbreeding has a huge impact on PID incidence due to the higher probability for offspring of consanguineous parents to be homozygous by descent and to inherit two copies of the same single mutated allele than for those born to non-consanguineous parents [7]. However, genetic characterization of some PID patients has also shown that *de novo* mutations can also be the cause of disease [8].

2.2. Reversion of PID gene defects:

Similar to somatic mosaicism due to *de novo* mutations during embryogenesis, mosaicism due to reversions to normal of an inherited mutation have been discovered because of milder than expected clinical course and/or presence of both phenotypically normal and abnormal cells *in vivo* and *in vitro* [9]. A revertant is a mutant that has regained, partially or completely, the wild type phenotype by either a genetic or a non-genetic mechanism [10].

2.3. Genotypic revertants classification:

Genetic revertants fall into two different classes:

1) True revertants, which represent a genuine reversal of the original mutational event. A so-called back or reverse mutation changes the original deleterious mutation either back to the original base or to a third one, thereby restoring the amino acid sequence of the wild-type polypeptide. The genetic mechanisms involved in reversion are true back mutation (reverse point mutation), crossing-over, and gene conversion [11, 12].

2) Revertants resulting from second site mutations or compensatory mutations, which take either place inside or outside the mutated gene, without changing the nucleotide of the original mutation. Such mutations restore the activity of the mutated gene but frequently lead only to partial reversion. The mechanism of second site mutations include base pair addition or deletion, suppressor mutation, and chromosomal loss or gain [11, 12].

Table 1: Human primary immunodeficiencies: Classification and affected genes.

Nº affected genes (% total)	Example	Reported revertants		
		Yes/No	Nº genes (% total)	Genes
(1) **Combined immunodeficiencies**				
98 (31%)	JAK3, CD3γ, CD3ε,	Yes	6 (46.1%)	IL2RG, CD247, RAG1, ADA, DOCK8, TGFBR1
(2) **Well-defined syndromes with immunodeficiency**				
58 (18.4%)	LIG1, GATA2	Yes	1 (7.7%)	WAS
(3) **Antibody deficiencies**				
44 (13.9%)	CD19, ICOS, TWEAK	Yes	2 (15.4%)	FANCA, FANCC
(4) **Diseases of immune dysregulation**				
43 (13.6%)	CARD11, FAS, ILR10	Yes	1 (7.7%)	SH2D1A
(5) **Congenital defects of phagocyte number, function, or both**				
43 (13.6%)	IL18, ISG15, IRF8	Yes	1 (7.7%)	CD18
(6) **Defects in innate immunity**				
22 (6.9%)	STAT1, IRAK4, CXCR4	Yes	2 (15.4%)	IKBKG, NEMO
(7) **Autoinflammatory disorders**				
19 (6.03%)	TRAPS, CIAS1, IL1R	No	-	-
(8) **Complement deficiencies**				
31 (9.84%)	Factor B, C2, C3,C4	No	-	-
Total				
315			13	

The spontaneous occurrence of somatic mutations that either reverse or compensate the deleterious effects of the original genetic defect is a feature of a minimal set of genes affected in PID (Table 1), including those ones for germ-line mutations of the adenosine deaminase [13], interleukin-2 receptor γc [14], recombination-activating gene 1 [15], the Wiskott–Aldrich syndrome protein [16], dedicator of cytokinesis 8 [17], nuclear factor-κB essential modulator (NEMO, or IKKγ) [18], TGFBR1 [19], IKBKG [20], SH2D1A [21], leukocyte adhesion integrin CD18 [22], FANCA/ FANCC [23-25] and CD247 [26-28] genes. To date, no plausible mechanisms to explain why only some PID genes undergo reversion events has been proposed, work in this thesis now identifies a potential genetic feature that explains why certain genes have higher probabilities to revert gene defects [29].

3. T CELL RECEPTOR CHAIN GENE DEFECTS CAUSING PID:

Mature T lymphocytes detect the presence of antigens by way of a variable surface disulphide-linked heterodimer (either αβ or γδ) termed the T-cell receptor (TCR) [30]. In humans, TCR molecules form a complex with two invariant heterodimers called CD3γε and CD3δε and a single invariant homodimer termed CD247 (also called TCRζ or CD3ζ) [31-34]. These invariant proteins participate in assembly of the whole TCR complex, which takes place in the ER before the complex reaches the Golgi system, and occurs in a precise and defined order (Figure 1) [35-38]. In fact, only correctly assembled receptors can reach the cell surface and pre-assembled TCR complexes lacking the CD247 subunit are shunted to degradation [39, 40] (Figure 1). TCR assembly and cell surface expression constitute not only a critical landmark during thymocyte development, but are also key for the delivery of intracellular signals that drive T-cell maturation or apoptosis in the thymus, and T-cell activation, proliferation, and effector function or anergy/apoptosis after antigen recognition [41].

TCR complex deficiencies in humans are very rare autosomal recessive diseases characterized by impaired expression of the TCR at the cell surface and selective T lymphopenia and hypofunction [42]. Primary immunodeficiencies affecting total or partially T cell receptor complex subunits have been previously described for TCRα [43], CD3γ [44-47], CD3δ [48-52], CD3ε [49, 53] and CD247 [26-28]. Given that the different chains appear to vary in importance for TCR assembly (Figure 1), the lack of each

particular subunit produces different degrees of TCR surface expression defects and disease severity [54].

Mutations in TCRα and the CD3γδε chains that are specifically expressed together in T cells affect T, but not B and NK cells. However, the CD247 chain is found in other cell types, including Natural Killer (NK) cells [55, 56], where it also acts as a signaling molecule for several NK cell receptors as well as Fc receptors [56]. As a consequence, work in this thesis shows for the first time how CD247 deficiency affects Natural Killer cell receptor biochemistry, function, maturation and development [57].

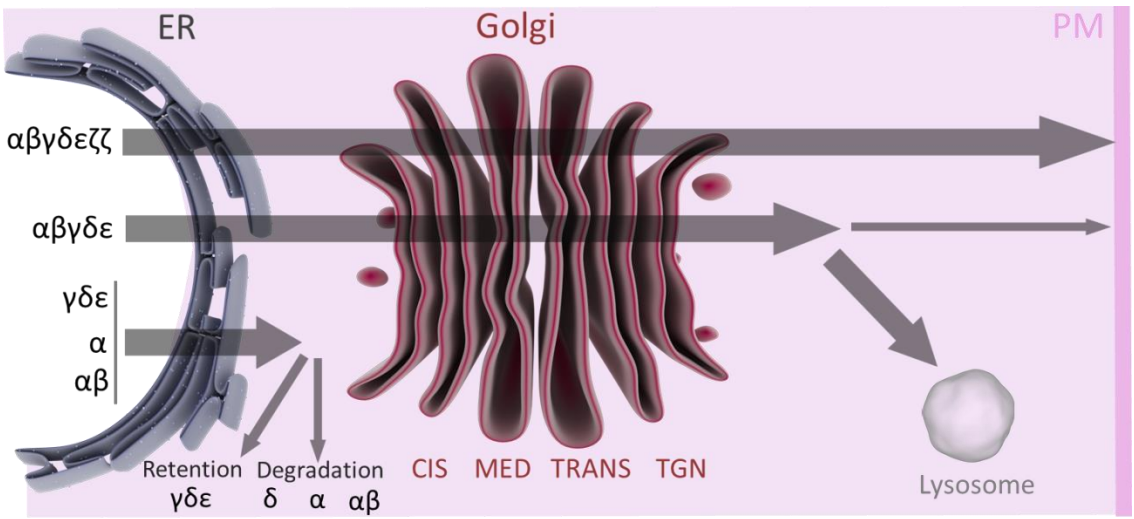

Figure 1: Intracellular fate of the TCR and its partial complexes: A schematic diagram of T cell receptor assembly illustrating the fate of partially assembled complexes: cis, cis-Golgi, med, medial-Golgi; trans, trans-Golgi; TGN, Trans-Golgi network; PM, plasma membrane. Redesigned based on [40]. Organelles pictures taken from: *http://www.somersault1824.com/resources/*

4. NATURAL KILLER CELLS:

In the early 1970s, Natural Killer cells were identified as lymphocytes with the ability to mediate spontaneous cytotoxic activity against transformed tumor cells without any requirement for prior priming [58, 59]. NK cells constitute from 5 to 15% of the peripheral blood lymphocyte population [60] and, after T and B cells, are the third major lineage of lymphocytes. However, NK cells also reside in a variety of tissues including the liver, spleen, bone marrow, decidua, lungs, uterus, thymus, mucosa-associated lymphoid tissue (MALT) and lymph nodes in humans [61-64]. NK cells responses have been traditionally associated with innate immunity, since they can release cytotoxic granules containing perforin and granzyme and secrete cytokines

such as IFNγ, TNFα, RANTES, MIP1a/B on recognition of virus-infected and tumor cells in the absence of prior priming, and because the response was not dependent on antigen-specific receptors. NK cells are able to recruit and amplify inflammatory responses by regulating the function of other immune system cells such as T cells, dendritic cells and macrophages [65-68].

4.1. Origin, maturation and education of NK cells:

Natural Killer originate, together with T and B lymphocytes, from a common $CD34^+$ hematopoietic progenitor [69, 70], but also can be generated from myeloid progenitors [71]. NK cell development starts in the fetal liver, but after birth, it occurs mainly in the bone marrow [72] and minimally in lymph nodes, thymus, gut and liver [73-76] in well characterized discrete stages [63, 77].

Human peripheral blood NK cells are phenotypically characterized as $CD3^-$ $CD56^+$ and are divided into two main groups: a major NK cell population defined by low levels of CD56, but high expression of CD16, called "$CD56^{dim}$"; and a minor "$CD56^{bright}$" NK population with high levels of CD56 and lacking CD16. Regarding NK cell development, after several precursor stages, immature NK cells gain expression of CD56, CD94/NKG2A, and several activating receptors including NKp46, NKp30, and NKG2D (Figure 2). These cells, called $CD56^{bright}$ NK cells, are highly proliferative, capable of producing high amounts of IFNγ, and express IL-7Rα and c-KIT [78-80].

In humans, $CD56^{bright}$ NK cells have been hypothesized to give rise to $CD56^{dim}$ NK cells [81]. This hypothesis is supported both by the observations that $CD56^{bright}$ NK cells have longer telomeres than $CD56^{dim}$ [79], and that *in vitro* stimulation of $CD56^{bright}$ NK cells with IL-2 results in acquisition of CD16 and KIR expression at the same time that IL-7Rα and c-KIT expression is lost [79]. During this process, NK cells also downregulate CD56 expression and acquire KIR inhibitory receptors [77, 82]. $CD56^{dim}$ NK cells are potently cytotoxic, but have lower proliferative capacity and cytokine secretion than $CD56^{bright}$ subpopulation. Although plausible, the idea that $CD56^{dim}$ derive from $CD56^{bright}$ in humans has not been established definitely. Indeed, recent studies in macaques using genetic barcoding of hematopoietic stem cells strongly suggested distinct developmental precursors for both NK cell subpopulations [83].

CD57 and CD62L are, among others, other important developmental NK cell markers. CD57 expression is limited to $CD56^{dim}CD16^+$ cells, and absent from $CD56^{bright}$

NK cells, meanwhile CD62L is first expressed by $CD56^{bright}$ cells and gradually lost during the processes of education and differentiation (Figure 2) [84-87].

Diversity is an essential characteristic of the immune system, and NK cells comprise a highly heterogeneous population. High-resolution analyses techniques like mass cytometry have shown that somewhere between 6000 to 30,000 phenotypic populations exist within an individual [88]. This extensive repertoire flexibility, although presumably expanding the range of target cell recognition, if carried to excess may decrease the flexibility of the antiviral response and even increase the risk of viral infection [89].

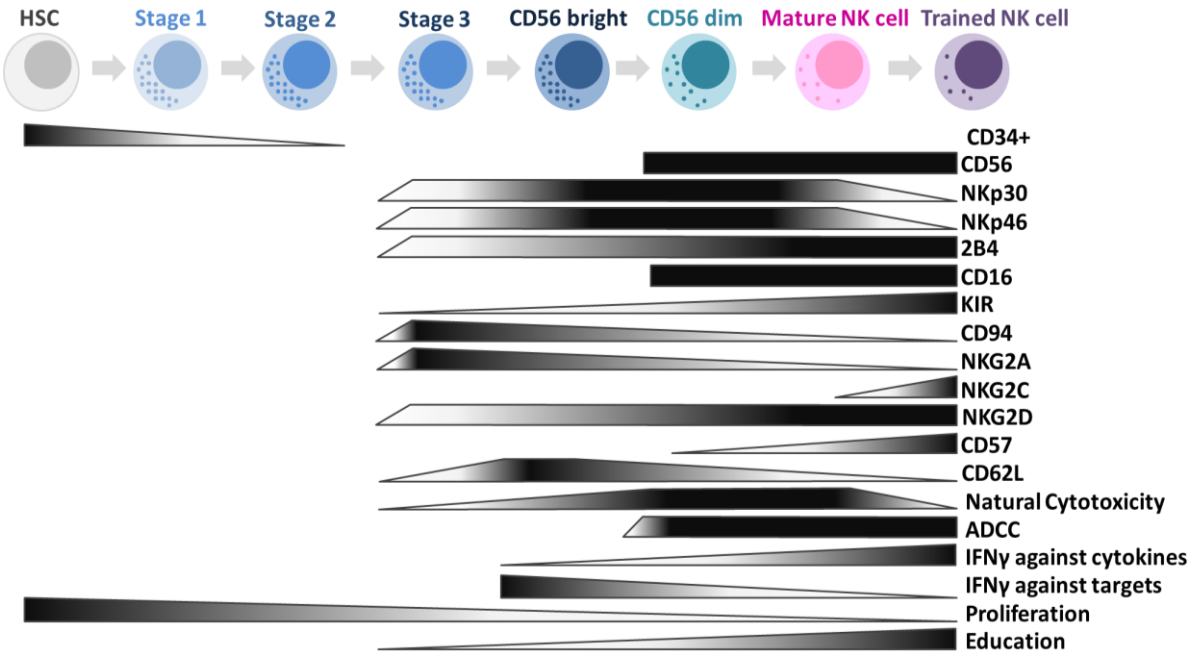

Figure 2: Schematic representation of human NK cell development and terminal differentiation: The development of human NK cells from a common lymphoid progenitor over NK cell precursors to terminally differentiated NK cells is depicted from left to right. The acquisition and loss of indicated surface markers and functional properties for human NK cell are indicated by the bars. Protein expression levels are depicted as black for high expression and white for no expression, gray indicates intermediate levels.

4.2. Natural Killer cells, further innate immunity horizon:

Recently, novel populations of NK cells that possess adaptive immune features such as long-life, qualitatively different responses [90-93] and even antigen specificity in the case of mice [94] and macaques [95] NK cells have been described.

Although previously NK cells were considered unable to differentiate into memory cells, accumulating evidence demonstrates that some NK cells can undergo

antigen-specific expansion and differentiation into a long-lived memory subset [96-100].

In some mouse models, NK cells are activated after exposure to pathogens, antigens, and cytokines, and subsequently differentiate into long-lived memory or memory-like NK cells with augmented effector functions in response to a variety of secondary stimuli, as compared with naive NK cells [96-98]. It has been demonstrated that mouse NK cells bearing the activating Ly49H receptor, which specifically recognizes the m157 mouse cytomegalovirus (MCMV) glycoprotein on the infected cells [101, 102], undergo activation, expansion, contraction, differentiation into memory NK cells, and persist for several months after MCMV infection [98, 103]. These MCMV-specific memory NK cells are capable of mounting a recall response and provide more effective host protection against rechallenge with MCMV than naive NK cells [98].

Moreover, this phenomenon has also been demonstrated in a rhesus macaque model of SIV infection, where NK cells directly target Gag and Env epitopes and provide protection for upwards of months [95]. The existence of memory NK cells in humans is supported by the specific expansion and lifelong persistence of NKG2C^{high} NK cells after human cytomegalovirus (HCMV) infection [100, 104-107], or HCMV reactivation after superinfection with other viruses such as HIV-1, Hantavirus, Chikungunya virus, hepatitis B and C. These “adaptive” NK cells are characterized by a longer lifespan and mediate enhanced responses through antibody dependent cell cytotoxicity (ADCC) and IFNγ production.

4.3. NK cell function:

Natural Killer cells fulfill their roles by recognizing sets of specific ligands expressed on the target cell with an array of germline-encoded cell surface receptors. These receptors are independent of the recombination activating gene enzymes (RAG1 and 2), that are essential for expression of the T and B cell receptors that require rearrangement [108, 109].

4.3.1. The inhibition-activation paradigm in Natural Killer cells:

Multiple checkpoints have been identified that function to insure an orderly progression through an immune response and thereby prevent the generation of self-

destructive processes. A common theme that has emerged from the study of these checkpoints is the requirement for the establishment of discrete thresholds that define narrow windows of response. One mechanism to achieve these thresholds is for the co-expression of receptors with common ligand binding properties but divergent signaling capacities, coupling activating receptors with an inhibitory counterpart, thereby setting thresholds for immune cell activation.

The activation of Natural Killer cells is regulated by the integration of signals from activating and inhibitory receptors expressed on the NK cell after ligation, or not, by ligands on the target cell [110, 111]. However, it has been observed that not all NK cells respond equally to the same stimulus. The responsiveness of any given NK cell is determined during its development in a process referred to as NK cell “licencing” or “education” [112, 113].

NK cell education renders potentially auto-reactive NK cells tolerant to the surrounding environment by adjusting the responsiveness of NK cell to ensure self-tolerance while maintaining the possibility of useful reactivity against potential threats. NK cell expressed MHC-specific inhibitory receptors play a major role establishing this equilibrium, but signaling from activating receptors is also important, suggesting that the integration of signals from both types of receptors is critical. This process is still only incompletely understood and a further complication is that NK cell responsiveness can be re-set, if for example the MHC environment changes [114, 115].

Moreover, the inflammatory conditions often associated with infections can over-ride the regulated responsiveness of NK cells to modulate their activity [116, 117] raising questions such as whether viruses and tumor cells manipulate NK cell responsiveness to evade immune-recognition [118, 119]. As knowledge of the underlying processes grows, the possibility of modulating NK cell responsiveness for therapeutic benefit may also become possible [117, 120].

5. NATURAL KILLER CELL RECEPTORS:

5.1. Inhibitory receptors:

Most of the inhibitory receptors expressed by NK cells recognize classical self MHC class I molecules and this is believed to be a key mechanism by which NK cells sense perturbations in the self-HLA environment. The majority of NK cells express at least one inhibitory receptor, known as KIR, for at least one self-HLA molecule [121]. Genes encoding for KIR receptors present multiple alleles and different number of genes along the population [122, 123], which generates a broad diversity of inhibitory panel of receptors and NK cell reactivity against each host.

However, significant proportions of NK cells do not express any self-specific inhibitory KIR, and to compensate for this, KIR-negative cells express CD94/NKG2A heterodimer that specifically interacts with non-classical HLA-E [124-126]. Furthermore, other non-MHC inhibitory receptors including KLRG1, TIGIT, Siclecs, LAIR-1 or CEACAM1 are present on NK cells.

Thus the cellular loss of MHC class I expression due to pathogen infection can lead to NK cell activation through the loss of inhibitory signals; this process is known as missing self [127].

5.2. Activating receptors of NK cells:

Natural Killer cells express many activating receptors including Natural Cytotoxicity Receptors (NCR), Fc receptors, NKG2 family receptors and others. The following section will focus on those receptors that are particularly relevant for the work presented in this thesis:

5.2.1. Natural Cytotoxicity Receptors:

Three NCRs, discovered in the late 1990s, are expressed on human NK cells: NKp46 (NCR1; CD335) [128], NKp44 (NCR2; CD336) [129], and NKp30 (NCR3; CD337) [130]. They are grouped together as all of them were able to activate NK cells and they were important for the killing of tumor cells *in vitro*. However, despite their similar functional abilities, NCRs do not share significant similarities in either their amino acid sequence or in their structure. They are type I transmembrane proteins belonging to the immunoglobulin superfamily and are composed of one or two extracellular immunoglobulin-like domains, which are responsible for ligand binding. In addition,

they contain a transmembrane domain with a positive-charged amino acid that can interact with signaling adaptor proteins containing immunoreceptor tyrosine-based activation motifs (Figure 3).

NKp46: This particular receptor was the first NCR to be identified and is the most specific marker of NK cells reported so far, regardless of their activation status [128, 131]. The NKp46 gene is located on chromosome 19 and encodes two N-terminal C2-type Ig domains connected by a hinge region, followed by a stalk domain, a single transmembrane domain and a short cytoplasmic region lacking a signaling motif. An arginine residue in the NKp46 TM allows its association with the FcεR1γ and CD247 signaling modules.

NKp30: NKp30 is expressed in all mature NK cells [130]. There are six different NKp30 isoforms, generated by alternative splicing after transcription of a single gene located in the class III region of the human MHC. Three isoforms possess a C-type Ig extracellular domain [132]; meanwhile the most frequent NKp30 isoforms (NKp30 I/c, NKp30 II/b and NKp30 III/a) encode V-type extracellular domains and associate through a positively charged arginine residue with either FcεR1γ or CD247 molecules.

Surprisingly, although coupled to the same signaling adaptors, engagement of each isoform has been shown to trigger different cellular functions and differences in the repertoire of isoforms expressed has been linked to prognosis of several cancers, autoimmune diseases and reproduction [133-138].

NKp44: The NKp44 receptor is only expressed in activated NK cells [129]. It is encoded on chromosome 6 (6p21.1.) and encodes a single extracellular V-type Ig domain, connected via a 64-amino acid-long stalk domain, to a single transmembrane domain and a short cytoplasmic tail [139, 140] containing an immunoreceptor tyrosine-based inhibitory motif, shown to be functional after binding to certain ligands [141, 142]. The specific location of a transmembrane sequence lysine residue renders NKp44 unable to bind FcεR1γ or CD247, and instead, it interacts with the DAP12 signaling dimer.

5.2.2. Fc receptors:

Fc receptors interact with antibodies or antibody-antigen complexes interactions and are expressed on the surface of certain immune cells, including,

among others, B lymphocytes, follicular dendritic cells, Natural Killer cells, macrophages, neutrophils, eosinophils, basophils, human platelets and mast cells. The name, Fc receptor, is derived from their binding to a part of an antibody known as the Fc (fragment, crystallizable) region [143, 144].

Upon binding the Fc portion of Ig bound to infected cells or invading pathogens, these receptors trigger a wide range of effector functions such as antibody-dependent cell cytotoxicity by NK cells, mast cell degranulation, antibody secretion, and phagocytosis as well as the induction of immunomodulatory signals regulating lymphocyte proliferation and antibody secretion, which contribute to the protective functions of the immune system.

There are several different types of Fc receptors (FcR), which are classified based on the type of antibody that they recognize. For example, those that bind the most common class of antibody, IgG, are called Fc-gamma receptors (FcγR), those that bind IgA are called Fc-alpha receptors (FcαR) and those that bind IgE are called Fc-epsilon receptors (FcεR). The classes of FcR's are also distinguished by the cells that express them (macrophages, granulocytes, natural killer cells, T and B cells), structural similarities and the signaling properties of each receptor [145].

Fc-α receptors: Only one Fc receptor belongs to the FcαR subgroup, which is called FcαRI (or CD89) [10]. FcαRI is found on the surface of neutrophils, eosinophils, monocytes, some macrophages (including Kupffer cells), and some dendritic cells [146]. It is composed of two extracellular Ig-like domains, and is a member of both the immunoglobulin superfamily and the multi-chain immune recognition receptor (MIRR) family [147]. It signals by associating with two FcεR1γ signaling chains [146]. Another receptor can also bind IgA, although it has higher affinity for IgM [148]. This receptor is called the Fc-alpha/mu receptor (Fcα/μR) and is a type I transmembrane protein. With one Ig-like domain in its extracellular portion, this Fc receptor is also a member of the immunoglobulin superfamily [149].

Fc-ε receptors: Two types of FcεR are known: [147] The high-affinity receptor FcεRI is a member of the immunoglobulin superfamily (it has two Ig-like domains). FcεRI is found on epidermal Langerhans cells, eosinophils, mast cells and basophils [150, 151]. As a result of its cellular distribution, this receptor plays a major role in controlling allergic responses. FcεRI is also expressed on antigen-presenting cells, and

controls the production of important immune mediators called cytokines that promote inflammation [152]. The low-affinity receptor FcεRII (CD23) is a C-type lectin molecule. FcεRII has multiple functions as a membrane-bound or soluble receptor; it controls B cell growth and differentiation and blocks IgE-binding of eosinophils, monocytes, and basophils [153].

Fc-γ receptors: All of the Fcγ receptors (FcγR) belong to the immunoglobulin superfamily and are the most important Fc receptors for inducing phagocytosis of opsonized microbes [147]. This family includes several activating members: FcγRI (CD64, present on monocytes and macrophages [154, 155]), FcγRIIA (CD32A, found on monocytes, neutrophils and eosinophil platelets), FcγRIIIA (CD16A, expressed on mature NK, NKT, subsets of monocyte/macrophages and γδ T cells) and FcγRIIIB (CD16B, GPI anchored, expressed on neutrophils); and the inhibitory FcγRIIB (CD32B, expressed in monocyte, neutrophils, macrophages, basophils, eosinophils, Langerhans cells, B-cells, platelets cells and epithelial placenta cells). The genes encoding these receptors are located on chromosome 1 [156-158], and display high variability between individuals due to single nucleotide polymorphisms (SNP) and copy number variation (CNV) [159, 160] that directly affects receptor expression level. As might be expected from the importance of these molecules, variability in these receptors has been associated with susceptibility to autoimmunity and several infectious diseases [161-164]. Moreover, family members differ in their antibody affinities due to their different molecular structure [165]. For instance, FcγRI binds to IgG more strongly than FcγRII or FcγRIII does. FcγRI also has an extracellular portion composed of three immunoglobulin (Ig)-like domains, one more domain than FcγRII or FcγRIII has. This property allows FcγRI to bind monomeric IgG molecules, but all Fcγ receptors must bind multiple IgG molecules within an immune complex to be activated [166].

The Fc-gamma receptors differ in their affinity for IgG and likewise the different IgG subclasses have unique affinities for each of the Fc gamma receptors [167]. These interactions are further tuned by specific post-translational modifications at Fc IgG portion. The Fc glycan has a heptasaccharide core structure that can be modified by the addition of specific residues; these modifications are dynamic and regulate the

biological activity of IgGs. Modifications at certain positions of this glycan core are critical for proper FcR function (see later for CD16A).

Another FcR is expressed on multiple cell types and is similar in structure to MHC class I. This receptor also binds IgG and is involved in preservation of this antibody [168]. However, since this Fc receptor is also involved in transferring IgG from a mother either via the placenta to her fetus or in milk to her suckling infant, it is called the neonatal Fc receptor (FcRn) [169, 170]. This receptor is generally thought to play a role in the homeostatic regulation of serum IgG levels.

Within the spectrum of FcγRs, CD16A (FcγRIIIA) is the low affinity receptor for IgG and appears to be specialized for the recognition of multimeric immune complexes, such as those found on virus-infected cells, to mediate ADCC, a major pathway involved in the clearance of infectious pathogens and tumor cells. Like many immune activating receptors, CD16A associates at the cell surface with signaling adaptor molecules, in humans, FcεR1γ and CD247 [55, 171-174]. Interestingly, the composition of the CD16A receptor complex varies between NK cell subpopulations, in particular FcεR1γ expression is silenced epigenetically in adaptive NK cells [90] so that in these cells only CD247 is available to pair with CD16A.

Stimulation of CD16A on NK cells with ligands results in a rapid rise in [Ca^{2+}], and the hydrolysis of membrane phosphoinositides, resulting in the production of both inositol 1, 4, 5 triphosphate (IP_3) and IP_4 [175]. Further cross-linking of the receptor augments these responses. Part of the initial [Ca^{2+}], rise depends on mobilization from intracellular stores, but sustained [Ca^{2+}] levels require the influx of extracellular calcium. NK-cell activation, mediated by CD16A crosslinking, also results in transcriptional activation of specific cytokines like IFNγ and TNFα [176].

As already mentioned, N-linked glycan modifications in the IgG-Fc markedly affect the affinity of IgG binding to CD16A; and so, the robustness of the cellular immune response. For example, binding of human IgG1 to CD16A is highly sensitive to the presence of a single N-linked glycosylation site [177], so that deglycosylation results in a complete loss of receptor binding [178]. In contrast, Ig-Fc with N-linked sugars lacking galactose and terminating instead with GlcNAc moieties, bind CD16A with increased affinity [167]. Similarly, glycan modifications to remove a fucose core also enhance binding affinity for CD16A [179]. This particular modification has been

applied to engineered monoclonal antibody therapies [180]. Importantly, a recent report showed that early in Dengue infection a global shift in IgG Fc glycan structure occurs, triggering a decrease in antibody fucosylation, and consequently, a higher affinity of Ig for CD16A, which has been associated with an increased risk of severe disease [181].

5.2.3. Clinical relevance of Fc receptors:

Since the first successful use of a monoclonal antibody for the treatment of lymphoma in 1982, several antibodies, that bind molecules such as CD20, CD22, CD40, PD1 and CTLA-4, have been incorporated into standard treatment protocols for cancer. Among these therapies, ADCC is emerging as an important function for tumour clearance by recognition of therapeutic antibodies by immune cell FcRs [182]. Thus, FcRs represent a link between the specificity of the adaptive immune system and the powerful cytotoxic effector responses triggered by the innate effector cells. A better understanding to allow modulation of the interactions of antibodies with FcRs is one obvious strategy to obtain stronger anti-tumor responses and improve monoclonal antibody based therapies. In this sense, several groups have succeeded in generating antibody variants with increased CD16A affinity by either alanine scanning mutagenesis or by computer-based prediction models [183, 184].

5.2.4. Other activating NK cell receptors:

2B4: 2B4 (CD244) is a cell surface glycoprotein of the Ig-superfamily structurally related to CD2-like molecules [185, 186]. Extracellularly, 2B4 is composed of one membrane-distal Ig-V–like domain and one membrane proximal Ig-C2–like domain. 2B4 has a long, tyrosine-rich cytoplasmic tail. Whereas 2B4 functions mainly as an activating receptor on human NK cells [187], on murine NK cells 2B4 has been shown to exert both activating and inhibitory effects on the cytotoxic activity of NK cells [188]. Upon 2B4 ligation, the SH2-containing adaptor molecule SAP is recruited to 2B4 cytoplasmic tyrosines, which mediates signal transduction by recruiting the Src-family kinase FynT [189], which then phosphorylates downstream signaling molecules, e.g., phospholipase C-γ or Vav-1 [190, 191], and trigger NK cell cytotoxic response [192].

6. BIOLOGICAL MEMBRANES AND TRANSMEMBRANE DOMAINS:

Cellular membranes are biological membranes that separate the interior of the cells from the extracellular environment. Plasma membranes (PM) are composed of a mixture of different lipids including phospholipids, glycolipids and sterols.

These lipids are amphipathic and thus plasma membranes constitute as bilayers; hydrophilic phosphate heads are always arranged so that they are near water molecules, intracellular and extracellular fluids, while hydrophobic tails of membrane phospholipids are organized to the inner part of the bilayer, keeping away from water molecules and generating a hydrophobic environment [193].

Plasma membranes are structurally and functionally asymmetric. In addition to lipids, membranes present carbohydrates in the extracellular and are loaded with proteins integrally, or partially, embedded in the plasma membrane. In fact, proteins account for roughly half the mass of most cellular membranes. Many of these proteins are embedded into the membrane and stick out on both sides; these are called transmembrane proteins. Furthermore, membrane fluidity allows these embedded molecules to flow within the lipid bilayer [193].

The plasma membrane not only regulates the exchange of materials between a cell and its surroundings, but also represents an actual physical barrier. Therefore, extracellular information has to be transmitted through the membrane into the appropriate signal-transducing network. In the particular case of modular receptors, this process relies in different proteins connected through their transmembrane regions; thus precise receptor connection to appropriate signaling module is essential to activate the required cellular response [193].

The lipid bilayer environment strongly limits the range of possible structures for transmembrane proteins and the protein portion embedded into the lipid bilayer, called the transmembrane domain, reflects the physical properties of the bilayers in which it resides. In fact, transmembrane domain sequences have certain particularities and can be predicted as they are enriched in aliphatic and hydrophobic residues that constitute an α helix [194]. Usually, a helix of 18–21 amino acid length is sufficient to span the usual width of a lipid bilayer.

The stability of helices is a consequence of the hydrophobic effect and main-chain hydrogen bonding [195]. The interactions that connect the different subunits of

modular receptors are mediated by amino acid side chains exposed to the outer part of each subunit helix.

7. INTEGRATION OF EXTRACELLULAR SIGNALS INTO SIGNALING TRANSDUCING NETWORKS AND CELLULAR RESPONSES:

7.1. Modular design receptors:

A large proportion of the receptors that most directly control primary immune effector functions: arming and clonal expansion of T and B lymphocytes, activation of natural killer cells, and secretion of cytokines and antibodies; belong to a broad class of modular activating immune receptors, also known as multi-subunit immune-recognition receptors (MIRRs). In this sense, ligand-binding and signal-transducing functions are contributed by separate protein modules within the receptor complex subunits. These receptors share a distinctive molecular architecture in which a broad array of ligand-recognition specificities modules assemble non-covalently with one or more of a small group of dimeric signal-transducing modules to form functional membrane-embedded receptor complexes [31].

Because extracellular ligand binding and intracellular signaling functions are encoded by separate genes, this modular design creates a platform in which receptors can rapidly evolve new ligand specificities, associate with multiple signaling modules, and even exchange one signaling pathway for another through relatively small changes. In some cases, this functional diversification has clearly been driven by the selective pressures of pathogen immune-evasion strategies [196]. The flexibility is facilitated by the fact that the molecular interactions governing the assembly of these modules into functional receptors are largely restricted to their transmembrane domains, where specific residues in the receptor mediate stable interactions with residues at the signaling module within the lipid bilayer.

While most of the interaction is concentrated at the transmembrane domain, in some particular cases there are also some assembly contributions from residues in the extracellular or intracellular sequences. For instance, it has been shown directly and indirectly that extracellular regions from CD3 subunits can interact and affect the assembly and function of the T cell receptor [197-203].

7.2. Signaling adaptor molecules:

Modular activating immune receptors incorporate one or more of seven different dimeric signaling modules, including CD247/CD3ζ/TCRζ, CD3γ, CD3ε, CD79, DAP12, DAP10 and FcεR1γ. CD3γδε and CD79 modules associate exclusively with the variable T and B cell antigen receptors, respectively, and associate principally through interactions between their transmembrane domain. In contrast, CD3ζ, FcεR1γ and DAP12 are employed by many receptors from different protein families, and they share with the more restricted DAP10 signaling module a lack of folded extracellular domains. These are predominantly homodimeric and contain stabilizing intermolecular disulfide bonds.

In order to trigger cell responses through intracellular signals, these molecules have one (for the case of FcεRIγ and DAP12), or several (CD247) immunoreceptor tyrosine based activating motifs (ITAM) or a YINM motif for DAP10. ITAMs consist of conserved sequences of amino acids that contain two appropriately spaced tyrosines separated from a leucine or isoleucine by any two other amino acids. Two of these signatures are typically separated by between 6 and 8 amino acids in the tail of the molecule (YxxL/Ix6-8YxxL/I, where x denotes non-conserved residues). Following receptor engagement, phosphorylation of ITAM tyrosine residues represents one of the earliest events in the signaling cascade.

The adaptor molecules of particular interest for this thesis are CD247 and FcεR1γ and will be presented in more detail.

CD247 was first discovered as a disulfide-linked homodimer of two 16kDa non-glycosylated peptides [204] and contains 8 amino acids in its extracellular domain, followed by a single transmembrane domain, and a long 113-115 amino acid cytoplasmic tail [205] containing three ITAM domains. FcεR1γ has a similar structure, but a shorter cytoplasmic domain with only one ITAM domain. Comparison of the genes for FcεR1γ [206] and CD3ζ [205, 207, 208] chains indicates that they belong to the same family and are likely to have arisen by duplication. Both genes are located on mouse and human chromosome 1 and show analogous organization of their exons. FcεR1γ contains five exons while CD247 contains eight [208]. It has been demonstrated that CD247 and FcεR1γ not only form homodimers, but can also interact to assemble heterodimers [209].

7.3. Signal transduction networks:

After ligand recognition by activating receptors, Src family kinases are activated and phosphorylate ITAM tyrosine residues on signaling modules [210]. This phosphorylation triggers the activation and recruitment of protein tyrosine kinases such as Syk, or ZAP70 to ITAM signaling modules; or PI3K and Grb2-Vav1, to the YINM motif in DAP10. Finally, signaling cascades induce processes involved in cytoskeleton reorganization, which is required for NK cell polarization and the release of lytic granules, as well as transcription of cytokine and chemokine genes [110, 211]. In particular cases, ligand-induced receptor oligomerization is employed as a key factor in receptor triggering [212, 213].

In the case of inhibitory receptors, despite considerable diversity in extracellular domains, all share Immunoreceptor tyrosine-based inhibitory motif (ITIM) in their cytoplasmic tail. Thus, when an inhibitory receptor recognizes its ligand, Src-family kinases, likely those recruited to the activating receptors, phosphorylate the ITIM element and recruit of phosphatases such as SHP-1, SHP-2 or SHIP which dephosphorylate proteins implicated in NK cell activation, so blocking NK cell activation at an early-stage [211]. Strikingly, this inhibition is a local effect that does not affect NK cell response to other activating stimuli [214].

7.4. Transmembrane domain mediated interactions between subunits:

To date, the best characterized mechanisms of receptor complex assembly are those that depend on single interactions in the transmembrane domain (TMD) between the different elements of multi-subunit immune-recognition receptors.

First described for T cell receptor assembly, association occurs via precise interactions between basic and acidic residues localized at precise positions of the transmembrane domains of the different subunits in the complex [31]. Formation of the appropriate receptor structure is therefore dependent on proper placement of a total of three basic and six acidic TM residues (Figure 3).

Detailed studies, using site-directed mutagenesis of these residues, demonstrated that these specific interactions were necessary, and often sufficient, for complex assembly [34], and mutation of these amino-acids led to an assembly defect.

Subsequent studies on the assembly of NK cell receptor complexes, such as NKG2D-DAP10 [215] or NKG2C-DAP12 [216], have shown that the association of the subunits in these complexes also depends on similar structural arrangements, where pairs of aspartic acids in the adaptor molecules interact with either an arginine or lysine residue in the receptor TM domain. Indeed, for KIR2DS2 or NKG2D, all residues of the receptor TM domain can be mutated to valine or leucine, and the interactions of the lysine of KIR2DS2, or the arginine of NKG2D, with aspartic acids in DAP12 and DAP10, respectively, are sufficient to maintain the complex formation [217] (Figure 3). Therefore, membrane-localized assembly mechanism is relevant for activating receptors expressed by many different cell types of hematopoietic origin. In this sense, the placement and precise chemical nature of polar residues determine specificity of assembly and which signaling module is able to interact with each particular receptor.

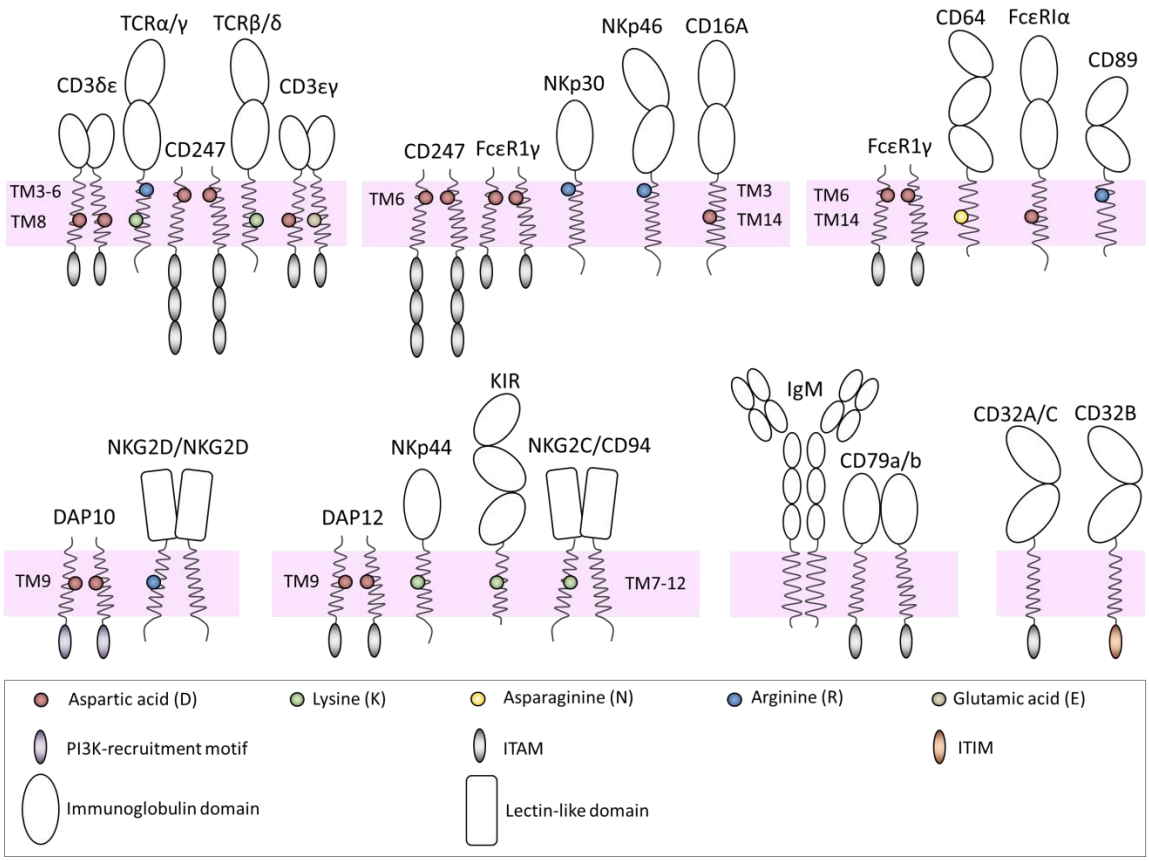

Figure 3: Assembly and architecture of modular activating immune receptors: Schematic representation showing the mechanism for selective assembly of a diverse group of receptors and their signaling modules. Key residues involved in receptor association are shown in different colors at the particular transmembrane (TM) position. Pink rectangles represent the plasma membrane.

However, the mechanisms by which several receptors such as the BCR, CD16A, CD64 and FcεR1α associate with their particular signaling modules through the transmembrane is still unknown. These molecules lack oppositely charged residues suggesting that their assembly with adaptors depends on other modes of other interaction. We now define the interacting interface for CD16A and a novel interaction mode for Fc receptors that bind FcεR1γ [218].

“Sólo aquellos que se arriesgan a ir muy lejos,
pueden llegar a saber lo lejos que pueden ir”

Thomas Stearns Eliot

OBJECTIVES

Modular activating receptors represent a complex scenario in which extracellular input signal sensing and intracellular signal transduction rely on at least two different elements. CD247 is a highly important signaling module shared with different receptors important for both the T and the NK cell compartments. Given the opportunity to analyse a new CD247 deficient patient, the phenotype and functional consequences of the absence of CD247 for NK cells was investigated, as were the genetics underlying patient mutation and the biochemistry of CD247-associated NK cell receptors.

The main objectives of the work presented in this thesis were:

1. Analyse the phenotypic and functional alterations of Natural Killer cells in a new primary immunodeficient patient lacking CD247 expression.

2. Investigate the genetics underlying the mutation, specifically the genetic reversion, observed in this CD247 deficient patient.

3. Biochemical study of how CD16A NK cell receptor mediates association with FcεR1γ and CD247 signaling modules despite the lack of transmembrane arginine or lysine residues.

“El experimentador que no sabe lo que está buscando, no comprenderá lo que encuentra”

Claude Bernard

MATERIALS & METHODS RESULTS

ARTICLE 1

NATURAL KILLER CELL HYPORESPONSIVENESS AND IMPAIRED DEVELOPMENT IN A CD247-DEFICIENT PATIENT

CD247 is a signaling adaptor molecule important for different receptor complexes such as the T cell receptor and several NK cell activating receptors. The opportunity to study a CD247-deficient PID patient allowed us to detailed analyze for the first time the phenotypic and functional consequences of the lack of this protein in human NK cells.

Here we report a new CD247 patient with a novel inherited mutation in homozygosis affecting the CD247 initiation codon, which prevents protein synthesis. We observed that CD247 protein was absent in this patient and that protein levels were segregated with genotype when mutation carriers in heterozygosis were compared with control individuals.

Surface expression analysis of patient NK cells showed that NKp30 and CD16A expression was compromised when this adaptor molecule was absent. Receptor levels also correlated with CD247 protein levels among genotypes. However, the expression levels of other NK cell receptors, such as NKp46 and 2B4 receptor remained comparable to healthy controls.

Natural Killer cell function was compromised when cells were activated in retargeted lysis experiments stimulating different NK cell receptors. However, in response to a receptor independent stimulus, PMA/Ionomycin, NK cell response was normal, which confirmed a problem in NK receptor-driven activation in the absence of CD247. When the NK cell response was evaluated in other CD3 deficiencies, no differences were observed compared to age matched controls, which further support that the altered NK cell activation response was specific for CD247 deficiency.

Phenotypically, patient NK cells expressed increased levels of CD56, decreased levels of KIR2D and an increased proportion of $CD94^{+}$/NKG2A, suggesting a maturation impairment and defective NK cell differentiation.

In conclusion, although CD247 deficiency is a rare disease, the identification of this new case has allowed a detailed evaluation of the role of CD247 in human NK biology.

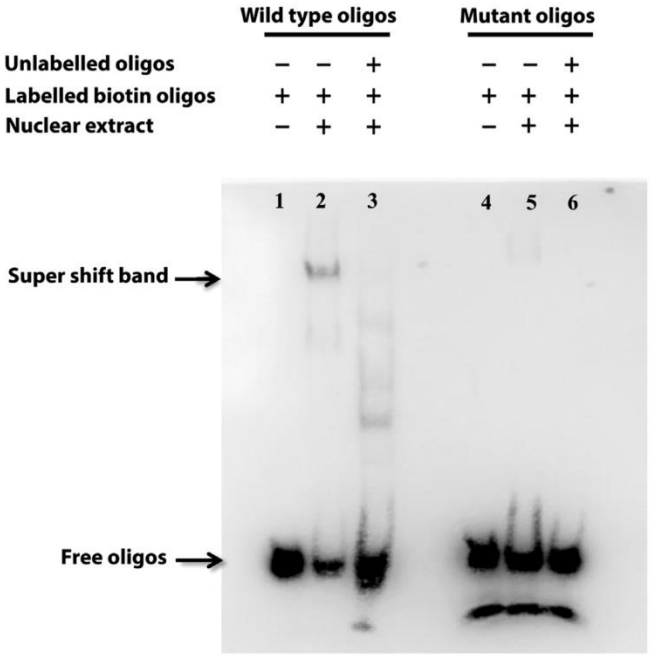

FIG 2. Electrophoretic mobility shift assay. Biotin-labeled wild-type or mutant oligonucleotides incubated without nuclear extracts (*lanes 1* and *4*), with nuclear extracts (*lanes 2, 3, 5,* and *6*), and in the absence (*lanes 2* and *5*) or presence (*lanes 3* and *6*) of an excess of unlabeled oligonucleotides. A supershift DNA/protein complex band is detected and marked. The free-labeled oligonucleotide is indicated.

means of hematopoietic stem cell transplantation or gene therapy. Furthermore, our finding highlights the potential role of mutations in gene regulatory regions as a cause of significant primary immunodeficiencies.

We thank Niek P. van Til, Department of Hematology, Erasmus University Medical Center, Rotterdam, The Netherlands, for providing the wild-type gcPRO plasmid.

Anita Chandra, MRCP, FRCPath, PhD[a,b,f]*
Fang Zhang, PhD[c]*
Kimberly C. Gilmour, FRCPath, PhD[d]
David Webster, FRCPath[e]
Vincent Plagnol, PhD[h]
Dinakantha S. Kumararatne, FRCPath, DPhil[a]
Siobhan O. Burns, MB, PhD, MRCPI(Paeds)[e,i]
Sergey Nejentsev, MD, PhD[f]
Adrian J. Thrasher, MRCP, PhD[c,g]

From [a]the Department of Clinical Biochemistry and Immunology, Cambridge University Hospitals NHS Foundation Trust, Cambridge, United Kingdom; [b]Lymphocyte Signalling & Development, Babraham Institute, Cambridge, United Kingdom; [c]Molecular and Cellular Immunology, Institute of Child Health, University College London, London, United Kingdom; [d]the Department of Immunology, Great Ormond Street Hospital NHS Foundation Trust, London, United Kingdom; [e]University College London Institute of Immunity and Transplantation, London, United Kingdom; [f]the Department of Medicine, University of Cambridge, Cambridge, United Kingdom; [g]Great Ormond Street Hospital NHS Foundation Trust, London, United Kingdom; [h]University College London Genetics Institute, University College London, London, United Kingdom; and [i]the Department of Immunology, Royal Free London NHS Foundation Trust, London, United Kingdom. E-mail: anita.chandra@doctors.org.uk.

*These authors contributed equally to this work.

S.N. is a Wellcome Trust Senior Research Fellow in Basic Biomedical Science (095198/Z/10/Z). S.N. is also supported by the European Research Council Starting grant 260477 and the EU FP7 collaborative grant 261441 (PEVNET project) and a National Institute for Health Research (NIHR) Cambridge Biomedical Research Centre. F.Z. is funded by an EU FP7 grant: CELL-PID—Advanced Cell-based therapies for the treatment of primary immunodeficiencies (reference no. FP7-261387). A.C. has a Wellcome Trust Postdoctoral Training Fellowship for Clinicians (103413/Z/13/Z). A.J.T. is a Wellcome Trust Principal Fellow.

Disclosure of potential conflict of interest: A. Chandra and D. S. Kumararatne received travel support from Shire. S. O. Burns received travel support from Immunodeficiency Canada, CSL Behring. and Baxalta US. The rest of the authors declare that have no relevant conflicts of interest.

REFERENCES

1. Modell V, Gee B, Lewis DB, Orange JS, Roifman CM, Routes JM, et al. Global study of primary immunodeficiency diseases (PI)—diagnosis, treatment, and economic impact: an updated report from the Jeffrey Modell Foundation. Immunol Res 2011;51:61-70.
2. Puck JM, Pepper AE, Henthorn PS, Candotti F, Isakov J, Whitman T, et al. Mutation analysis of IL2RG in human X-linked severe combined immunodeficiency. Blood 1997;89:1968-77.
3. Ochs HD. Common variable immunodeficiency (CVID): new genetic insight and unanswered questions. Clin Exp Immunol 2014;178(suppl 1):5-6.
4. Markiewicz S, Bosselut R, Le Deist F, de Villartay JP, Hivroz C, Ghysdael J, et al. Tissue-specific activity of the gammac chain promoter depends upon an Ets binding site and is regulated by GA-binding protein. J Biol Chem 1996;271:14849-55.
5. Niemela JE, Puck JM, Fischer RE, Fleischer TA, Hsu AP. Efficient detection of thirty-seven new IL2RG mutations in human X-linked severe combined immunodeficiency. Clin Immunol 2000;95:33-8.
6. Estévez OA, Ortega C, Fernández S, Aguado R, Rumbao J, Perez-Navaro J, et al. A novel IL2RG mutation presenting with atypical T(-)B(+)NK+ phenotype: rapid elucidation of NK cell origin. Paediatr Blood Cancer 2014;61:178-9.
7. Kellermayer R, Hsu AP, Stankovics J, Balogh P, Hadzsiev K, Vojcek Á, et al. A novel IL2RG mutation associated with maternal T lymphocyte engraftment in a patient with severe combined immunodeficiency. J Hum Genet 2006;51:495-7.
8. Sharrocks AD. The ETS-domain transcription factor family. Nat Rev Mol Cell Biol 2001;2:827-37.
9. Ciau-Uitz A, Wang L, Patient R, Liu F. ETS transcription factors in haematopoietic stem cell development. Blood Cell Mol Dis 2013;51:248-55.

Available online October 31, 2015.
http://dx.doi.org/10.1016/j.jaci.2015.08.049

Natural killer cell hyporesponsiveness and impaired development in a CD247-deficient patient

To the Editor:

The analysis of single gene defects in patients with primary immunodeficiency has provided important insights into the normal physiology of the immune system and is particularly valuable in those instances where the human and murine immune systems are different.[1] CD247 (T-cell receptor [TCR] ζ/CD3ζ) is one of the invariant chains that, along with CD3γ, CD3δ, CD3ε, and a clonotypic TCR heterodimer (αβ or γδ), forms the TCR antigen receptor complex expressed at the surfaces of T lymphocytes. However, CD247 is also expressed in natural killer (NK) cells, and although the biology of CD247 in the TCR complex is similar in mice and human subjects, there are marked differences between human and murine NK cells in the expression and association of activating NK receptors (CD16/FcγRIII, natural cytotoxicity receptor (NCR)3/NKp30, and NCR1/NKp46) with CD247.[2,3] Thus analysis of the rare patients deficient in CD247 provides unique insights into the biology of this signaling molecule in NK cells that cannot be obtained from the study of murine models.

Two CD247-deficient patients have been described previously.[4,5] Those studies focused on the effects of this deficiency on T cells, and although a somewhat reduced NK cell activity was noted, this population was not studied in detail. Here we report in-depth analyses of NK cells in a new case of inherited

J ALLERGY CLIN IMMUNOL
VOLUME 137, NUMBER 3

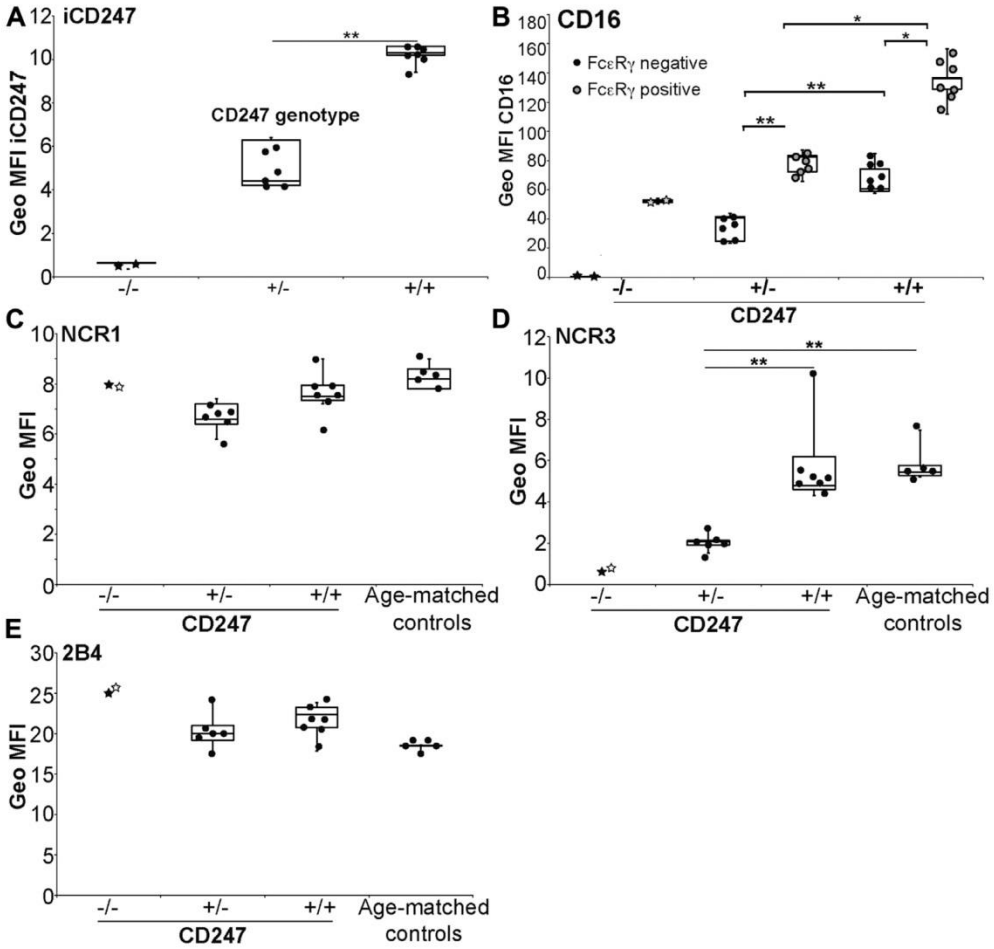

FIG 1. CD247 genotype correlates with expression of CD247 and CD16 and NCR3 expression on NK cells. NK receptor expression levels in $CD3^{-}CD56^{dim}$ NK cells from the $CD247^{-/-}$ patient were compared with those of $CD247^{+/-}$ and $CD247^{+/+}$ relatives or age-matched control subjects for intracellular CD247 **(A)**, CD16 on $Fc\varepsilon R\gamma^{+}$ or $Fc\varepsilon R\gamma^{-}$ cells **(B)**, NCR1 **(C)**, NCR3 **(D)**, and 2B4 **(E)**. Data are shown as geometric mean fluorescence intensity *(Geo MFI)*. ★/☆, First/second sample taken 3 months apart $*P < .05$ and $**P < .01$.

CD247 deficiency (see the Case report in this article's Online Repository at www.jacionline.org) because of loss of the translation initiation codon (see Fig E1, *A*, in this article's Online Repository at www.jacionline.org). NK cells from other family members, who were either heterozygous for the mutation in CD247 or homozygous for wild-type CD247 (see Fig E1, *B*), were also analyzed.

Loss of the initiation codon led to the complete absence of CD247 protein expression in the proband (see Fig E1, *C*), and correlation between levels of CD247 expression in $CD3^{-}CD56^{dim}$ NK cells and genotype was observed in family members (Fig 1, *A*). In human NK cells the CD16, NCR1/NKp46, and NCR3/NKp30 receptors associate with CD247 or FcεRγ.[3] The level of surface CD16 on NK cells, both $Fc\varepsilon R\gamma^{-}$ and $Fc\varepsilon R\gamma^{+}$, segregated with the CD247 genotype of the donor (Fig 1, *B*, and see Fig E2, *A*, in this article's Online Repository at www.jacionline.org), strongly suggesting that the defective expression of CD247 underlies these phenotypic changes.

In contrast, NCR1, but not NCR3, expression in NK cells was comparable in all genotypes (Fig 1, *C* and *D*, and see Fig E2, *B*), suggesting that association with FcεRγ is sufficient for surface expression of NCR1, even in the absence of CD247, whereas NCR3 expression depends principally on CD247. Finally, as expected, surface expression of the 2B4 receptor, which is not known to associate with CD247, was normal in all subjects, irrespective of the CD247 genotype (Fig 1, *E*).

To gain insight into the functional effect of CD247 deficiency on NK cell function, we analyzed degranulation of IL-2–cultured NK cells from the patient and her relatives in response to receptor-mediated signals (shown in Fig 1) by using either specific mAb and P815 cells or K562 cells as targets (Fig 2, *A*). IL-2–cultured NK cells were used for these experiments because NK cell cytotoxicity is greatly reduced compared with that seen in adults in early life; however, exposure to IL-2 can reconstitute NK cell cytotoxic capacity to adult levels,[6] thus permitting a fair comparison of NK cell cytotoxic function from the infant patient and adult family members. The patient's NK cells responded poorly to all receptor-mediated signals, irrespective of their surface expression levels (Fig 2, *A*). However, the patient's NK cells did not have a general defect in cytotoxic machinery because their receptor-independent degranulation induced by phorbol 12-myristate 13-acetate plus ionomycin was normal. Although NK cell degranulation from $CD247^{+/-}$ subjects was always somewhat less than that observed for $CD247^{+/+}$ control subjects,

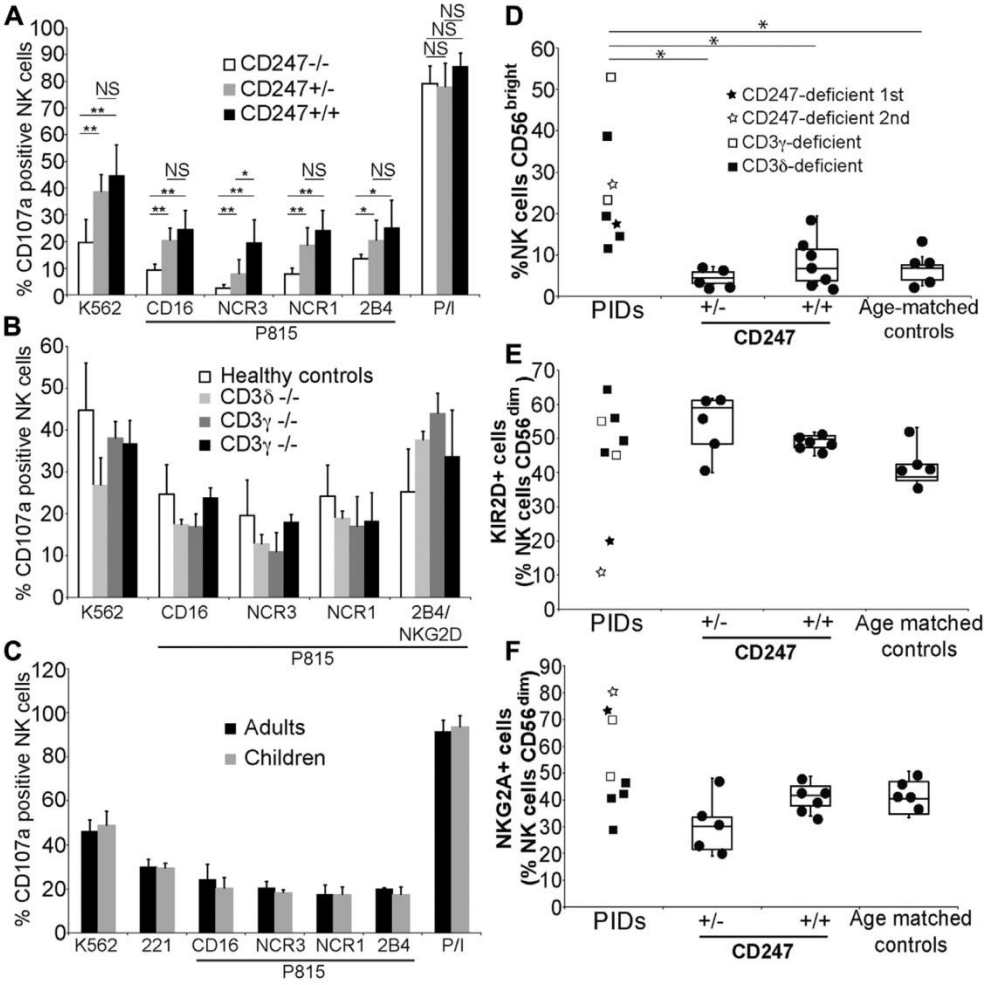

FIG 2. Hyporesponsiveness **(A-C)** and impaired maturation **(D-F)** of CD247-deficient NK cells. Comparative degranulation in response to the indicated stimuli for the 3 CD247 genotypes (Fig 2, *A*), CD3δ- and CD3γ-deficient patients versus healthy control subjects (Fig 2, *B*), and healthy adults versus children (Fig 2, *C*). CD3-deficient *(squares)* and CD247-deficient primary immunodeficiencies were compared among them and with $CD247^{+/-}$ and $CD247^{+/+}$ relatives or age-matched control subjects for peripheral blood $CD56^{bright}$ NK cells (Fig 2, *D*), KIR2D+$CD56^{dim}$ NK cells (Fig 2, E), and CD94/NKG2A+$CD56^{dim}$ NK cells (Fig 2, *F*). ★/☆, First/second sample. **P* < .05 and ***P* < .01.

these differences only reached statistical significance for stimulation through NCR3 (Fig 2, *A*), again suggesting that CD247 is particularly important for NCR3 expression and signaling.

The observed receptor-mediated NK cell hyporesponsiveness was specific for CD247 deficiency because it was not seen for NK cells from patients with CD3γ or CD3δ deficiencies (Fig 2, *B*) and was unrelated to age (Fig 2, *C*).

Given the hyporesponsiveness of NK cells from the CD247-deficient patient, her NK cell differentiation was compared with that of other family members and age-matched control subjects. Peripheral blood NK cells can be divided into 2 subsets: $CD56^{bright}$ and $CD56^{dim}$ cells. $CD56^{bright}$ NK cells produce cytokines after monokine stimulation and are considered progenitors of the $CD56^{dim}$ NK cells, which are more specialized for cytotoxicity.[7] Although the total number of $CD3^{-}CD56^{+}$ NK cells was comparable in the CD247-deficient patient and other family members and control subjects (data not shown), the proportion of $CD56^{bright}$ NK cells was considerably higher (Fig 2, *D*), suggesting defective NK cell differentiation. Consistent with this hypothesis, flow cytometric analysis of expression of additional surface markers in the $CD56^{dim}$ NK cell subset also revealed impaired NK cell maturation in the patient. In particular, late stages of the differentiation of $CD56^{dim}$ NK cells are characterized by a switch from CD94/NKG2A expression to killer immunoglobulin-like receptor (KIR) expression.[7] As expected, the majority of $CD56^{dim}$ NK cells from control subjects expressed KIR2D receptors, as did NK cells from patients with CD3γ or CD3δ deficiencies. However, only approximately 20% of $CD56^{dim}$ NK cells from the CD247-deficient patient expressed KIR2D (Fig 2, *E*), whereas greater than 80% of these cells expressed the CD94/NKG2A heterodimer (Fig 2, *F*), demonstrating a specific block in the late differentiation stages of $CD56^{dim}$ NK cells in this patient.

Our data suggest that CD247 deficiency affects NK cell development and function both directly and indirectly. In particular, an increased proportion of peripheral blood $CD56^{bright}$ NK cells was noted in all CD3/CD247-deficient patients

J ALLERGY CLIN IMMUNOL
VOLUME 137, NUMBER 3

examined, suggesting that the absence of functional T cells, rather than specifically CD247, affects NK differentiation. This observation is consistent with data from patients undergoing stem cell transplantation (SCT) in whom the first NK cells to repopulate the periphery have an immature phenotype and are less able to mediate cytotoxicity before T-cell recovery.[8] Interestingly, the ability of peripheral blood NK cells from the CD247-deficient patient to proliferate in mixed lymphocyte cultures *in vitro* was severely limited (see Fig E3 in this article's Online Repository at www.jacionline.org), but this phenotype could be reversed by IL-2 addition.

During differentiation, the ability of NK cells to respond to stimulation is finely tuned in function of the repertoire of inhibitory and activating receptors expressed by each NK cell.[9] Because CD247 deficiency causes decreased expression and function of a range of activating NK receptors, impaired signaling might underlie the partial block of NK cell differentiation and NK cell hyporesponsiveness, which were observed in the CD247-deficient patient. Importantly, similar changes in NK cell phenotype and function have not been seen in children with symptomatic congenital human cytomegalovirus (CMV) infection,[10] arguing against the hypothesis that the changes observed in the CD247-deficient patient are a consequence of CMV infection.

Our observations have direct implications for the clinical management of immunodeficient patients. Even when not directly fatal, episodes of infectious disease delay transplantation and negatively affect the outcome. Thus, because NK cells play a critical role in antiviral immunity, the potentiation of NK cell function, for example by means of low-dose therapy with IL-2, could be a useful strategy to minimize infections and aid in the management of these patients until SCT.

We thank all of the subjects who have contributed blood samples for these studies and Drs M. Lopez-Botet, J. Gil-Herrera, and M. L. Toribio for helpful discussion and advice.

Mar Valés-Gómez, PhD[a]*
Gloria Esteso, PhD[a]*
Cigdem Aydogmus, MD[b]
Alfonso Blázquez-Moreno, BSc[a]
Ana V. Marín, BSc[c]
Alejandro C. Briones, BSc[c]
Beatriz Garcillán, PhD[c]
Eva-María García-Cuesta, BSc[a]
Sheila López Cobo, BSc[a]
Sule Haskologlu, MD[d]
Manuela Moraru, MD[e]
Funda Cipe, MD[b]
Kerry Dobbs, BS[f]
Figen Dogu, MD[d]
Silvia Parolini, PhD[g]
Luigi D. Notarangelo, MD[f]
Carlos Vilches, MD, PhD[e]
Maria J. Recio, PhD[c]
José R. Regueiro, PhD[c]
Aydan Ikinciogullari, MD[d]
Hugh T. Reyburn, PhD[a]

From [a]the Department of Immunology and Oncology, National Centre for Biotechnology, CSIC, Madrid, Spain; [b]the Department of Pediatric Immunology, Istanbul Kanuni Sultan Süleyman Hospital, Istanbul, Turkey; [c]the Department of Immunology, Complutense University School of Medicine and Hospital 12 de Octubre Health Research Institute, Madrid, Spain; [d]the Department of Pediatric Immunology-Allergy, Ankara University School of Medicine, Ankara, Turkey; [e]Immunogenetics-HLA, Instituto de Investigación Sanitaria Puerta de Hierro, Madrid, Spain; [f]the Division of Immunology, Boston Children's Hospital, Boston, Mass; and [g]the Department of Molecular and Translational Medicine, University of Brescia, Brescia, Italy. E-mail: mvales@cnb.csic.es. Or: htreyburn@cnb.csic.es.

*These authors contributed equally to this work.

Supported by grants from the Fondo de Investigación Sanitaria (PI11/00298, PS09/00181, FIS2011-00127 and PI08/1701), MINECO (SAF2011-24235, SAF2012-32293, SAF2010-22153-C03-03, SAF2014-54708-R and SAF2014-58752-R), the Comunidad de Madrid (grant S2010/BMD-2326 to M.V.-G. and S2010/BMD-2316 to J.R.R.), and the National Institutes of Health (grant 5R01AI100887-03 to L.D.N.).

Disclosure of potential conflict of interest: M. Vales-Gomez has received research support from the Regional Government of Madrid, MINECO, and Instituto Carlos III. A. C. Briones, B. Garcillan, E. -M. Garcia-Cuesta, S. Lopez-Cobo, M. J. Recio, and J. R. Regueiro have received research support and travel support from the Spanish Ministerio de economía y competitividad (MINECO). G. Esteso, A. Blazquez-Moreno, and H. T. Reyburn have received research support from Instituto Carlos III and MINECO. A. V. Marin, M. Moraru, and C. Vilches have received research support from MINECO. L. D. Notarangelo has received research support from the National Institutes of Health (NIH) and the March of Dimes; is a board member for the *Journal of Allergy and Clinical Immunology*, the *Journal of Clinical Immunology*, and Novimmune; is employed by Boston Children's Hospital Pediatric Associates; and has received royalties from UpToDate. The rest of the authors declare that they have no relevant conflicts of interest.

REFERENCES

1. Casanova JL, Conley ME, Seligman SJ, Abel L, Notarangelo LD. Guidelines for genetic studies in single patients: lessons from primary immunodeficiencies. J Exp Med 2014;211:2137-49.
2. Hollyoake M, Campbell RD, Aguado B. NKp30 (NCR3) is a pseudogene in 12 inbred and wild mouse strains, but an expressed gene in *Mus caroli*. Mol Biol Evol 2005;22:1661-72.
3. Lanier LL. Up on the tightrope: natural killer cell activation and inhibition. Nat Immunol 2008;9:495-502.
4. Rieux-Laucat F, Hivroz C, Lim A, Mateo V, Pellier I, Selz F, et al. Inherited and somatic CD3zeta mutations in a patient with T-cell deficiency. N Engl J Med 2006; 354:1913-21.
5. Roberts JL, Lauritsen JP, Cooney M, Parrott RE, Sajaroff EO, Win CM, et al. T-B+NK+ severe combined immunodeficiency caused by complete deficiency of the CD3zeta subunit of the T-cell antigen receptor complex. Blood 2007;109: 3198-206.
6. Guilmot A, Hermann E, Braud VM, Carlier Y, Truyens C. Natural killer cell responses to infections in early life. J Innate Immun 2011;3:280-8.
7. Luetke-Eversloh M, Killig M, Romagnani C. Signatures of human NK cell development and terminal differentiation. Front Immunol 2013;4:499.
8. Nguyen S, Dhedin N, Vernant JP, Kuentz M, Al Jijakli A, Rouas-Freiss N, et al. NK-cell reconstitution after haploidentical hematopoietic stem-cell transplantations: immaturity of NK cells and inhibitory effect of NKG2A override GvL effect. Blood 2005;105:4135-42.
9. Shifrin N, Raulet DH, Ardolino M. NK cell self tolerance, responsiveness and missing self recognition. Semin Immunol 2014;26:138-44.
10. Noyola DE, Fortuny C, Muntasell A, Noguera-Julian A, Munoz-Almagro C, Alarcon A, et al. Influence of congenital human cytomegalovirus infection and the NKG2C genotype on NK-cell subset distribution in children. Eur J Immunol 2012;42:3256-66.

Available online November 2, 2015.
http://dx.doi.org/10.1016/j.jaci.2015.07.051

Anti–IFN-γ autoantibodies are strongly associated with HLA-DR*15:02/16:02 and HLA-DQ*05:01/05:02 across Southeast Asia

To the Editor:

Neutralizing anti–IFN-γ autoantibodies (nAIGAs) are a recently recognized mechanism of infection with disseminated nontuberculous mycobacteria and other intracellular opportunists, with the phenotype being similar to genetic disruption of IFN-γ immunity.[1-3] In the last decade, there has been a high prevalence of nAIGAs, nearly completely restricted to patients from Southeast Asia, mostly from Thailand and Taiwan,[4,5]

CASE REPORT

A Turkish girl born in 2012, the first child of first-degree cousins (Fig E1), was healthy until 2 months of age, when she was admitted for sepsis because of a 10-day fever after routine vaccination (DaPT-polio/Hib and BCG). Immunoglobulin levels were normal (IgG, 1.260 mg/dL; IgA, 41 mg/dL; and IgM, 138 mg/dL). Paleness, bone marrow aspiration performed because of pancytopenia, and high transaminase and ferritin levels were compatible with hemophagocytic lymphohistiocytosis, and therefore she was started on steroids. On determination of CMV antigenemia (3000 copies/mL), she received intravenous ganciclovir and intravenous immunoglobulin. An underlying primary immunodeficiency was suspected because of consanguinity and hemophagocytic lymphohistiocytosis.

Lymphocyte subsets determined after cessation of steroid treatment were as follows: 0.5% $CD3^+CD16^-CD56^-$, 0.3% $CD3^+CD4^+$, 0.1% $CD3^+CD8^+$, 23% $CD19^+$, 23% $CD20^+$, 31% HLA-DR^+, and 36% $CD3^-CD16^+CD56^+$ cells and 2% recent thymic emigrants (RTE) cells evaluated as $CD4^+CD45RA^+CD31^+$ cells. T-lymphocyte activation in response to PHA was extremely low (5.5% $CD3^+CD25^+$ and 5.9% $CD3^+CD69^+$ cells). The patient's T cells showed a severe surface TCR expression defect, with partial defects in parents and some family members compatible with Mendelian inheritance. The patient's lymphocytes lacked intracellular CD247, and a final diagnosis of CD247 deficiency was reached by using molecular analyses (Fig E1).

Before hematopoietic stem cell transplantation (HSCT), she received antiviral treatment: ganciclovir, foscarnet, and CMV hyperimmunoglobulin for 17 months because of CMV antigenemia and ribavirin for 5 months because of recurring pneumonia associated with type 3 parainfluenza.

At 19 months of age, maternal haploidentical HSCT was performed after fully HLA-compatible donor screening failed within and outside her family. She received 14×10^6 $CD34^+$ cells/kg after protocol D nonmyeloablative conditioning in inborn errors according to the European Society for Blood and Marrow Transplantation 2011 guidelines for graft-versus-host disease (GvHD) prophylaxis (150 mg/m^2 fludarabine, 42 g/m^2 treosulfan, 10 mg/kg thiotepa, and 3 mg/kg/d cyclosporine).

The first week after HSCT, she had fever with CMV reactivation, severe oral and genital mucositis, and veno-occlusive disease and received foscarnet and defibrotide. Myeloid and platelet engraftment were detected at 11 and 16 days after HSCT, respectively. However, she had pneumonia with type 3 parainfluenza and rhinovirus, hypertension caused by renal failure, and biopsy-proved grade 2 skin acute GvHD afterward. Cyclosporine was stopped because of persistent high blood pressure. Because of ongoing acute GvHD despite steroid and mycophenolate mofetil administration, mesenchymal stem cells (2.6×10^6/kg) were infused at 32 and 49 days. Thereafter, infections regressed, CMV disappeared, and foscarnet was stopped. Blood pressure returned to normal levels, antihypertensive drugs were thus discontinued, and the patient was discharged at 83 days after HSCT. At 94 days, she was readmitted with urine flow reduction. Peritoneal dialysis was performed for 15 days because of 6.7 mg/dL creatinine and 119.6 mg/dL blood urea nitrogen. Renal functions and urine flow reached normal levels, and she was discharged, but a renal biopsy was compatible with tubulointerstitial nephropathy.

Six months after HSCT, she was readmitted with pneumonia. Her thorax computed tomographic scan revealed paratracheal, aortopulmonary, subcranial, and bilateral hilar microlymphadenopathies and bilateral nonspecific consolidations. Antimicrobial agents and antireflux treatment were started on determination of gastroesophageal reflux disease (GERD) with pH monitoring. At 7 months after HSCT, she had BCGitis, and therefore isoniazid, rifampin, and clofazimine were started. A month later, she was readmitted with pneumonia.

One year after HSCT, she presented with respiratory problems and hypoxemia. No bacteria, respiratory tract viruses, CMV, or EBV antigenemia were detected. Immune system evaluation revealed normal cellular and humoral parameters: total lymphocyte count, 6,100/mm^3; total neutrophil count, 8,500/mm^3; total eosinophil count, 1,100/mm^3; IgG, 1.300 mg/dL; IgA, 84.5 mg/dL; IgM, 181 mg/dL; 61% $CD3^+CD16^-CD56^-$ cells (normal range, 55% to 79%); 18% $CD3^-CD16^+CD56^+$ cells (normal range, 5% to 28%); 20% $CD3^+CD4^+$ cells (normal range, 26% to 49%); 41% $CD3^+CD8^+$ (normal range, 9% to 35%); 16% $CD19^+$ and $CD20^+$ (normal range, 11% to 30%); 21% HLA-DR (normal range, 18% to 38%); and 31% RTE cells, with a reasonable donor chimerism (97%). However, her lung radiographs showed bilateral perihilar infiltration, and a thoracic computed tomographic scan revealed widespread soft tissue densities, atelectasis, pleural thickenings, air-trapped areas in the lungs, and decreased volume in left lung. Bronchoscopic examination did not confirm any significant pathology, microorganism, or mycobacteria. Cytological investigation excluded GvHD. A biopsy performed on GERD findings, reduced food intake, and weight loss did not support such a diagnosis, and she did not respond to GERD treatment. Pulmonary hypertension and left ventricular hypertrophy were detected on cardiologic evaluation. She was treated with oxygen, salbutamol, intravenous steroids, wide-spectrum antibiotics, and antimycobacterial agents. However, her respiratory difficulty and bronchospastic attacks did not respond to any treatment modality. At 13 months after HSCT, she died of respiratory failure despite mechanical ventilation and administration of extracorporeal membrane oxygenation in the intensive care unit.

The work described here was carried out over a 6-month period (corresponding to 10-16 months of age), during which 3 blood samples were available for analysis. Age-matched control samples were obtained during the clinical work-up of a diverse group of children (17-24 months of age) admitted to the hospital in Istanbul for a variety of reasons, including respiratory tract infections, urinary tract infections, and gastroenteritis. PBMCs deficient in CD3δ or CD3γ were frozen samples from previously described patients.[E1,E2]

The study was conducted according to the principles expressed in the Declaration of Helsinki and approved by the Institutional Research Ethics Committees of the various hospitals involved. All participants or their guardians provided informed consent for the collection of samples and subsequent analyses.

REFERENCES

E1. Gil J, Busto EM, Garcillán B, Chean C, García-Rodríguez MC, Díaz-Alderete A, et al. A leaky mutation in CD3D differentially affects αβ and γδ T cells and leads to a Tαβ-Tγδ+B+NK+ human SCID. J Clin Invest 2011;121:3872-6.

E2. Recio MJ, Moreno-Pelayo MA, Kiliç SS, Guardo AC, Sanal O, Allende LM, et al. Differential biological role of CD3 chains revealed by human immunodeficiencies. J Immunol 2007;178:2556-64.

J ALLERGY CLIN IMMUNOL
VOLUME 137, NUMBER 3

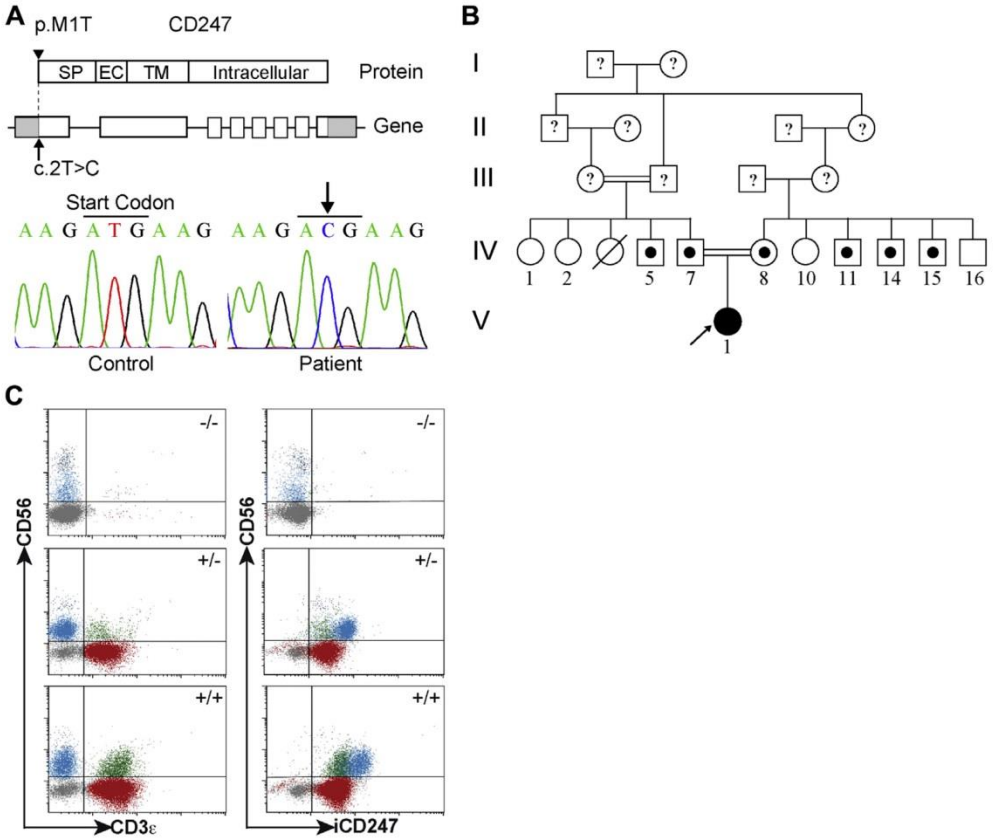

FIG E1. Genetic and phenotypic characterization of CD247 deficiency. **A,** The index patient inherited a CD247 mutation affecting the start codon that is shown within the CD247 protein (p.M1T or p.0) and gene (c.2T>C, g.147T>C) structure, as well as in the comparative chromatograms *(arrows)*. *EC*, Extracellular region; *SP*, signal peptide; *TM*, transmembrane region. **B,** Genetic pedigree. *Circles* indicate female subjects, and *squares* indicate male subjects (*slashes* indicate deaths). *Dotted* and *full symbols* indicate heterozygosity and homozygosity for the mutation, respectively. *Empty symbols* and *symbols marked with ?* indicate noncarrier and unknown mutation status, respectively. Only tested subjects are numbered. **C,** PBMCs from the CD247$^{-/-}$ patient, a relative heterozygous for the CD247 initiation codon mutation (+/−) and a family member homozygous for nonmutant CD247 sequence (+/+) were stained with directly labeled mAbs specific for CD3ε and CD56. The cells were then fixed, permeabilized, blocked with mouse serum, and stained with a directly labelled mAb specific for the cytoplasmic tail of CD247. The flow cytometric data were analyzed by using the Kaluza program (Beckman Coulter, Fullerton, Calif). *Red*, CD3ε^{+}CD56^{-} T cells; *green*, CD3ε^{+}CD56^{+} T cells; *light blue*, CD3ε^{-}CD56^{dim} NK cells; *dark blue*, CD3ε^{-}CD56^{bright} NK cells; *gray*, non-NK/non-T cells.

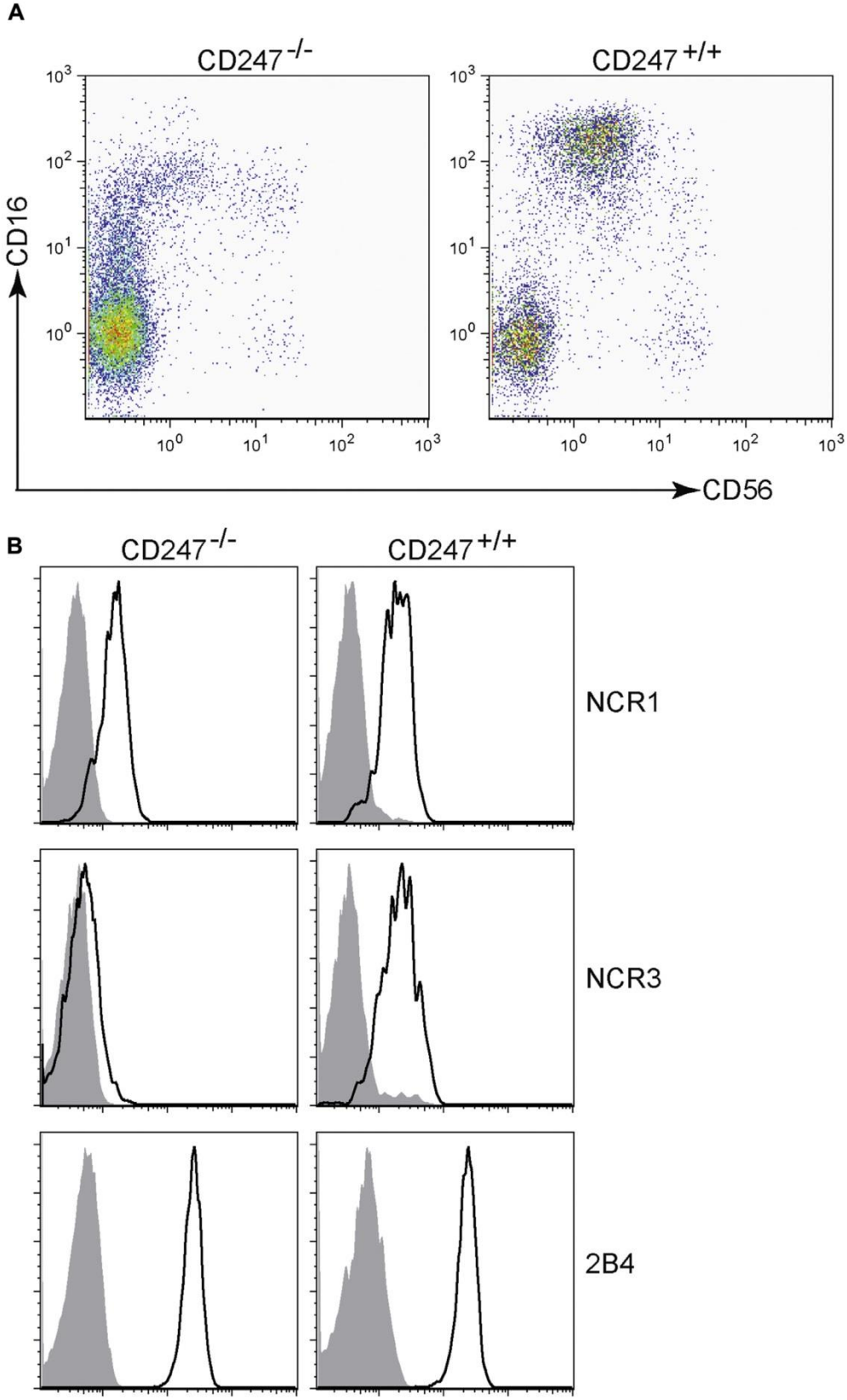

FIG E2. A, Representative dot plots showing staining for CD56 and CD16 on $CD3^-$ lymphocytes of the $CD247^{-/-}$ patient and a healthy control subject. **B,** Overlay histograms showing levels of NCR1, NCR3, and 2B4 expression on $CD3^-CD56^{dim}$ NK cells in the $CD247^{-/-}$ patient and a healthy control subject. *Shaded gray plots*, Isotype control staining; *solid black line*, NCR1, NCR3, or 2B4 staining.

J ALLERGY CLIN IMMUNOL
VOLUME 137, NUMBER 3

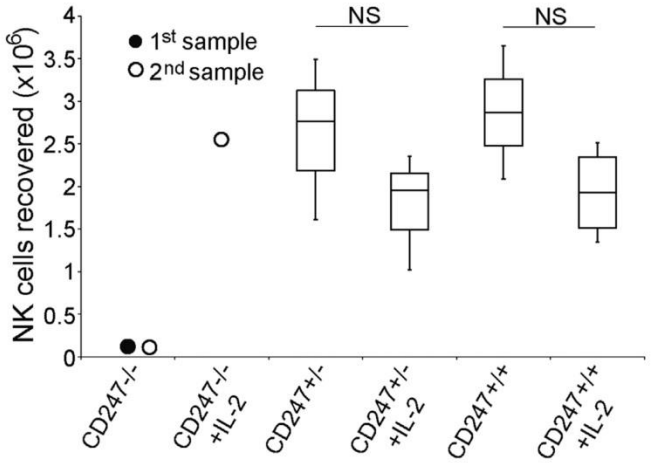

FIG E3. Deficient expansion of NK cells of the CD247$^{-/-}$ patient during *in vitro* culture can be remedied by addition of IL-2. PBMCs were purified by means of centrifugation on Ficoll-Hypaque and then placed in culture in RPMI 1640 medium with 10% AB^{-} human serum and irradiated (40 Gy) feeder cells (RPMI 8866, Daudi, and 221/AEH cells) in the presence or absence of 50 IU/mL rIL-2. After 7 days of culture, half the medium was removed and replaced with fresh medium (with or without IL-2). On day 10, the cells were harvested and counted, and aliquots of the cultures were stained with directly labeled mAbs specific for CD3 and CD56.

ARTICLE 2

ANALYSIS OF THE RECOVERY OF CD247 EXPRESSION IN A PID PATIENT: INSIGHTS INTO THE SPONTANEOUS REPAIR OF DEFECTIVE GENES

T cell receptor complex assembly is a precise and ordered process involving eight different components, and is essential for development and function of T cells. In fact, in the absence of CD247 protein, TCR is unable to reach cell surface and pre-assembled complexes are blocked at cis-Golgi and shunted to degradation.

Most of the T cells present in CD247-deficient patients are essentially negative for cell surface TCR; however, a minimal proportion of revertant cells with normal levels of TCR at the plasma membrane can be identified. Close examination of flow cytometry analyses of NK and T cells from patient PBMCs revealed phenotypic revertants that had recovered intracellular expression of CD247 and normal TCR levels at the cell surface, respectively. Further stimulation of patient PBMCs with CD3/CD28 mAbs showed an expansion of these revertant cells *in vitro*, supporting that these TCR complexes were fully functional.

Sequence analysis of CD247 transcripts from cell cultures containing revertant cells revealed that CD247 reversion was due to a true back mutation but also a compensatory mutation encoding for a CD247 version with an elongated signal peptide. Both of which restored gene transcription and were able to support TCR assembly and surface expression when introduced into Ma5.8 CD247-deficient cell line using lentiviruses. Moreover, a high rate of sequence variation was observed in CD247 compared to other genes located close on chromosome 1.

Reversion phenomena have been reported not only for CD247 deficient patients, but also for other genes affected in PID. However, they only represent a small proportion of affected genes and it is still unclear why reversion only happens in these particular genes. With the data of high variation within CD247 gene as a clue, the variation rate of all the PID affected genes that have been reported to suffer somatic reversion was analyzed. An increased number of missense variants in the coding sequence of these genes, compared to others where no reversion has been found or control genes, was found, leading to the hypothesis that high intrinsic gene variability increases the chance of PID gene mutants to revert.

Brief Report

blood

IMMUNOBIOLOGY AND IMMUNOTHERAPY

Analysis of the recovery of CD247 expression in a PID patient: insights into the spontaneous repair of defective genes

Alfonso Blázquez-Moreno,[1] Adriana Pérez-Portilla,[1] Miriam Agúndez-Llaca,[1] Daniela Dukovska,[1] Mar Valés-Gómez,[1] Cigdem Aydogmus,[2] Aydan Ikinciogullari,[3] José R. Regueiro,[4] and Hugh T. Reyburn[1]

[1]Department of Immunology and Oncology, National Center for Biotechnology and Spanish National Research Council, Madrid, Spain; [2]Department of Pediatric Immunology, Istanbul Kanuni Sultan Süleyman Hospital, Istanbul, Turkey; [3]Department of Pediatric Immunology-Allergy, Ankara University School of Medicine, Ankara, Turkey; and [4]Department of Immunology, Complutense University School of Medicine, Hospital 12 de Octubre Health Research Institute, Madrid, Spain

Key Points

- The propensity of genes to mutate influences the probability of spontaneous reversion of genetic defects in PID.

Mutations in T-cell antigen receptor (TCR) subunit genes cause rare immunodeficiency diseases characterized by impaired expression of the TCR at the cell surface and selective T lymphopenia. Here, detailed analyses of spontaneously arising somatic mutations that recover CD247, and thus TCR expression, in a newly identified CD247-deficient patient are described. The recovery of CD247 expression in some patient T cells was associated with both reversion of the inactivating mutation and a variant with a compensating mutation that could reconstitute TCR expression, but not as efficiently as wild-type CD247. Multiple mutations were found in CD247 complementary DNAs (cDNAs) cloned from the patient as well as in cDNA and genomic DNA from other individuals, suggesting that genetic variation in this gene is frequent. Analyses of other genes mutated in primary immunodeficiency diseases (PIDs) where reversions have been described also revealed a higher rate of mutation than that observed for genes mutated in PIDs where revertants have not been identified or control genes. These data support the hypothesis that the occurrence of somatic mutations that may reconstitute genetic defects in PID is related to an increased propensity of those genes to mutate. (*Blood*. 2017;130(10):1205-1208)

Introduction

Spontaneous somatic mutations that repair genetic defects have been documented in a range of primary immunodeficiency diseases (PIDs), including CD247 deficiency,[1-4] Wiskott-Aldrich syndrome,[5] X-linked IL2RG,[6,7] and leukocyte adhesion deficiency,[8] among others.[9] Although genetic reversion of a deleterious mutation is unlikely, if the mutation confers a selective advantage, these rare clones may expand.[9] However, the mechanisms underlying these somatic changes and why they occur in only some PIDs are unclear. Here, a detailed analysis of spontaneously arising somatic mutations that recover CD247, and thus T-cell antigen receptor (TCR) expression, in a CD247-deficient patient is presented. Genetic variation in CD247 is frequent, and this characteristic is shared with other PID genes in which reversion occurs. We suggest that the intrinsic mutability of a gene determines the likelihood of the emergence of somatic revertants on which selection subsequently acts.

Study design

In vitro T-cell culture

Purified peripheral blood mononuclear cells (PBMCs) were stimulated either with irradiated, autologous PBMCs and phytohemagglutinin or with immobilized CD3- and CD28-specific monoclonal antibodies (mAbs). In both cases, interleukin-2 (Peprotech) was added to 50 U/mL.

The study was conducted following the Declaration of Helsinki principles and approved by the institutional research ethics committees involved. All participants, or their guardians, consented to the collection of samples and subsequent analyses.

Sequencing of CD247, CD16A, and FcεRIγ cDNAs

Total RNA and genomic DNA were isolated using the RNeasy Mini kit and DNeasy kit, respectively (QIAGEN). Complementary DNA (cDNA) was synthesized using random hexamers and Superscript II (Life Sciences). Specific exons and full-length cDNAs were amplified using the Expand long-template polymerase chain reaction (PCR) system (Roche) and specific primers (supplemental Table 1, available on the *Blood* Web site), cloned (CloneJET PCR Cloning Kit), and sequenced (GATC Biotech).

Lentivirus transduction of Ma5.8 cells

Lentiviruses were generated by transfection of 293T cells with the plasmids pCMVdR8.74, pMD2G, and either wild-type CD247 or the mutant with an elongated signal peptide subcloned into pHR-sin.[10] The CD247-deficient murine T-cell hybridoma Ma5.8[11] was transduced as described previously.[10]

CD247 immunoblotting

Cells were lysed in buffer containing 1% Triton X-100/DOC and 0.1% sodium dodecyl sulfate. Then, 30 μg lysate was separated by 12% sodium dodecyl sulfate-polyacrylamide gel electrophoresis, transferred to a polyvinylidene

Submitted 17 January 2017; accepted 18 July 2017. Prepublished online as *Blood* First Edition paper, 25 July 2017; DOI 10.1182/blood-2017-01-762864.

The online version of this article contains a data supplement.

The publication costs of this article were defrayed in part by page charge payment. Therefore, and solely to indicate this fact, this article is hereby marked "advertisement" in accordance with 18 USC section 1734.

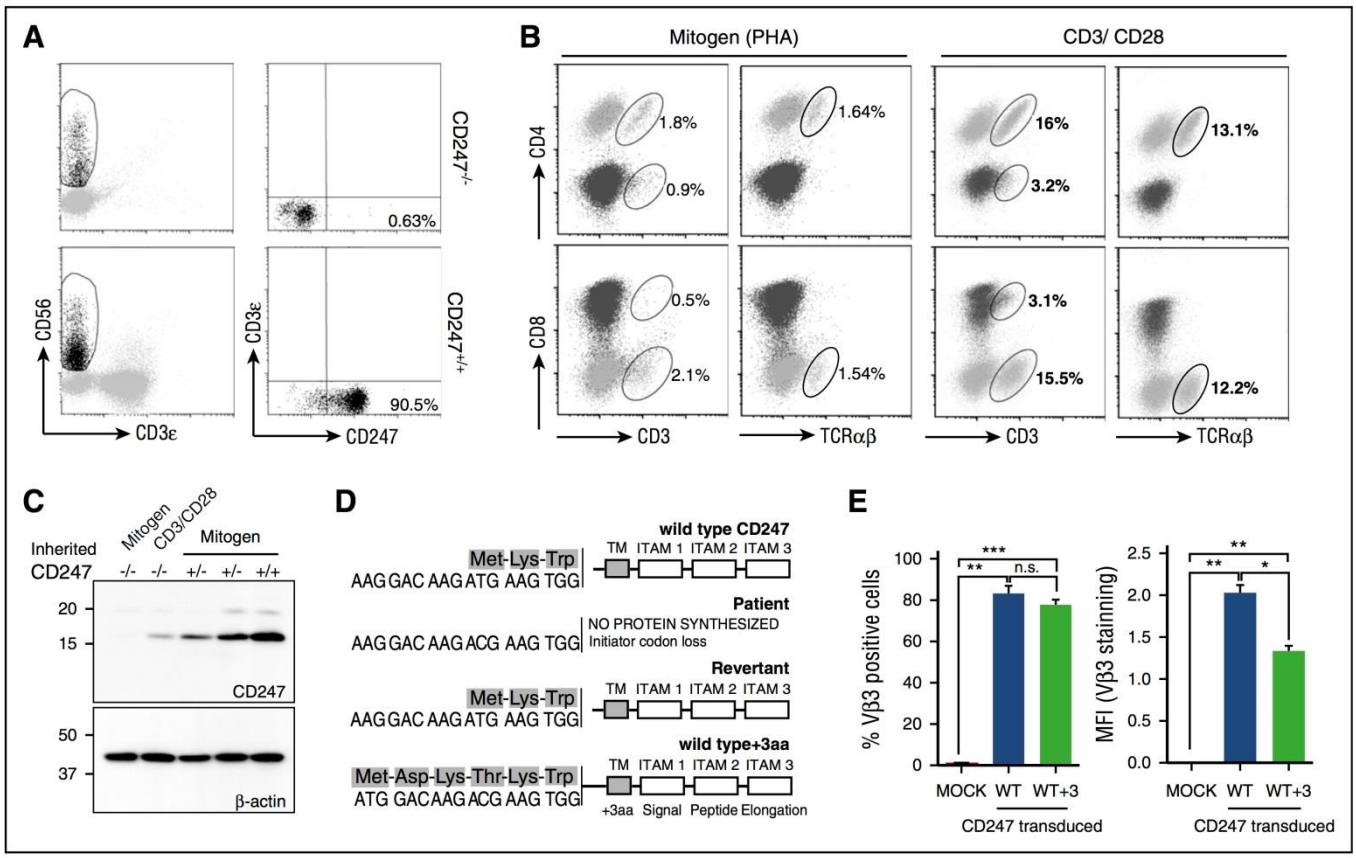

Figure 1. Characterization of CD247 revertants. (A) Freshly isolated CD247$^{-/-}$ patient PBMCs were stained, and rare CD247 revertant NK cells were observed. (B-C) Mitogen- and antigen receptor–stimulated PBMCs from a patient were analyzed by flow cytometry (B) and western blot (C) for TCR and CD247 expression. (D-E) Somatic mutants recovering CD247 expression were sequenced (D), and their ability to restore surface TCR expression was analyzed using the CD247-deficient Ma5.8 cell line (E). *$P < .05$; **$P < .01$; ***$P < .001$; n.s. (not significant), $P > .05$. ITAM, immunoreceptor tyrosine-based activation motif; PHA, phytohemagglutinin; TM, transmembrane; WT, wild-type.

difluoride (Millipore) membrane, and probed with CD247-specific[12] and β-actin–specific (Sigma) antibodies.

Flow cytometry

PBMCs were stained with labeled antibodies for CD3, CD56, CD4, CD8 (BioLegend), and TCRαβ (BD Pharmingen). Ma5.8 cells were stained with a phycoerythrin-labeled mAb specific for Vβ3 (BD Pharmingen). For intracellular staining, cells were fixed with paraformaldehyde and permeabilized with saponin before incubation with mAb specific for CD247 (eBioscience), CD3-ε, or -γ (Abcam). Data were acquired using a Gallios cytometer and analyzed using the Kaluza program (Beckman Coulter).

Gene variation analysis

Gene variation data were obtained from the 1000 Genomes Project (http://browser.1000genomes.org). For comparison of missense and synonymous variation, the data were relativized to coding sequence length and plotted as variants per 1000 base pairs. Gene region analysis was carried out by normalizing variants per region to the 5′ untranslated region (UTR), coding sequence, or 3′ UTR length.

Results and discussion

The clinical, genetic, and immunological characteristics of this CD247-deficient patient have been reported previously.[3,4] Although most patient T cells were TCR defective, 0.2% of T cells had recovered CD247 expression and normal levels of cell surface CD3ε.[4] Rare revertant cells (0.63%) were also present among freshly isolated natural killer (NK) cells (Figure 1A).

To study the spontaneous recovery of CD247 expression, patient PBMCs were stimulated with either mitogen (phytohemagglutinin) or immobilized anti-CD3ε/CD28 mAbs. TCR stimulation triggered expansion of these rare CD3^{high}/TCRαβ+ T cells to become ~18% of the lymphocytes in the culture (Figure 1B), confirming the functionality of these TCR complexes. Western blot analysis demonstrated the recovery of CD247 expression (Figure 1C).

Sequencing of CD247 transcripts cloned from the cultured lymphocytes revealed the presence of the T to C transition eliminating the initiation codon and a revertant, c.2T>C>T, that reconstituted the wild-type initiation codon (Figure 1D). A second mutation, c.-8A>T, producing a new methionine codon permitting synthesis of a mutant CD247 with a 3-amino-acid extension of the signal peptide (WT+3) (Figure 1D), was also identified. Transfection of cell-surface TCR-negative Ma5.8 cells[11] with wild-type CD247 or the WT+3 variant restored TCR expression (Figure 1E). However, the MFI for TCR staining was significantly lower for cells expressing the WT+3 variant (Figure 1E).

The sequencing analysis also revealed that mutations occurred not only around the initiation codon but also throughout the CD247 transcript so that 15 sequences were found among 20 full-length cDNA clones sequenced (supplemental Table 2). In contrast, no variation was noted in transcripts of the FcγRIIIA and FcεR1γ genes (data not shown) also encoded on chromosome 1. Multiple, distinct CD247 cDNA clones were also isolated from 3 other individuals (Figure 2A; supplemental Table 2), but again, no sequence variation was noted for FcεR1γ. Sequence analysis of CD247 exons amplified from genomic DNA isolated from purified granulocytes confirmed the frequent sequence variation in CD247 (supplemental Table 3). In control

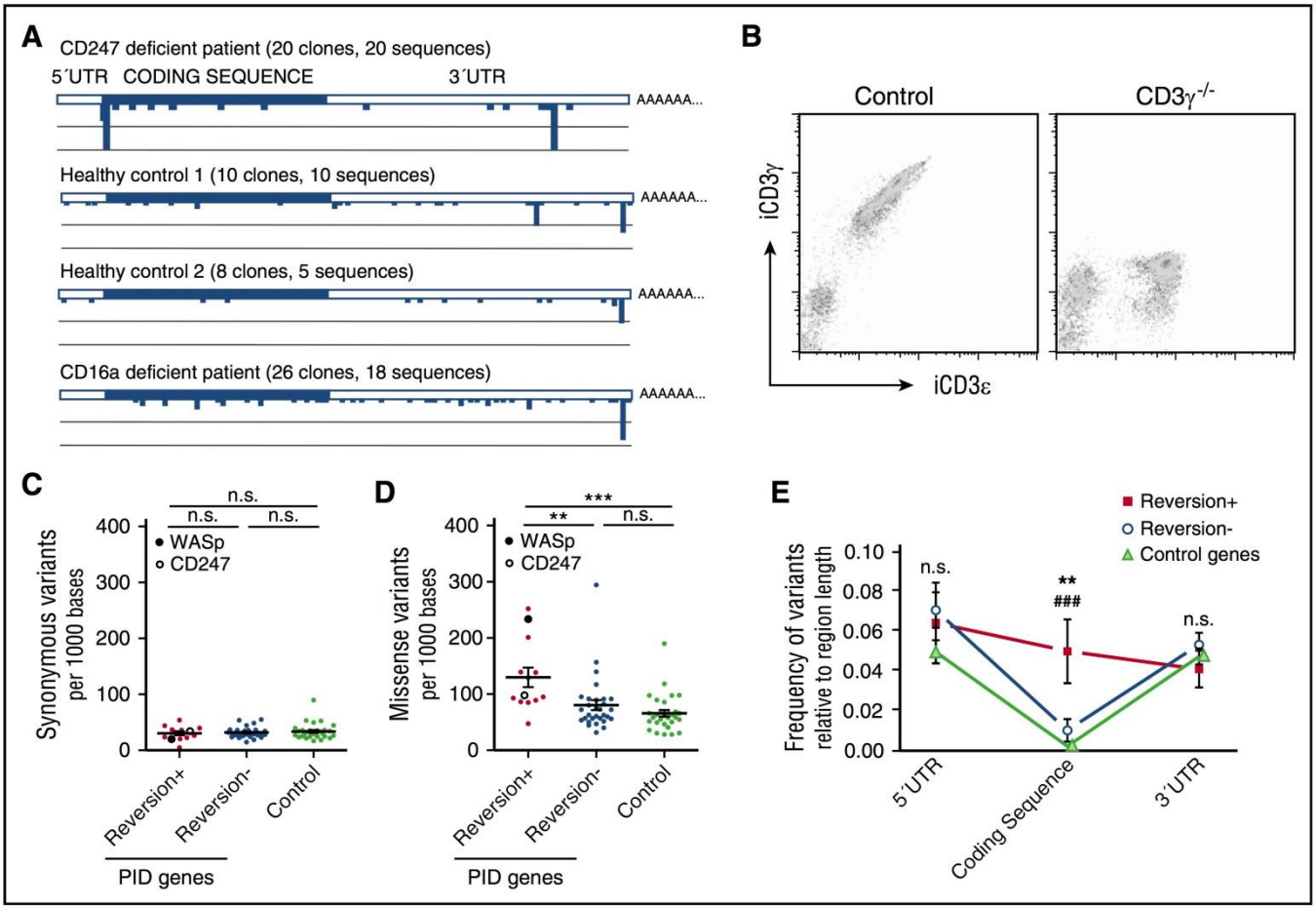

Figure 2. Gene variation and reversion probability in PIDs. (A) CD247 sequence analysis of samples from the patient and controls revealed high genetic variability. (B) Freshly isolated PBMCs from a CD3$\gamma^{-/-}$ patient and control were stained and analyzed by flow cytometry. (C-E) Analysis of data from the 1000 Genomes Project revealed no differences in the occurrence of synonymous mutations (C), but an increased frequency of missense mutations (D) in the coding region (E) was observed for PID genes where reversion has been described compared with PID genes with no reversion described or control genes. CD247 and WASp are specifically indicated in panels C and D. Statistical significance was calculated using a 1-way analysis of variance for synonymous and missense variation rates and a 2-way analysis of variance for variation vs gene region analysis comparing the 3 different groups of genes (**$P < .01$; ***$P < .001$; n.s., $P > .05$).

experiments, no revertants were noted in freshly isolated T cells of CD3γ-deficient patients[13] (Figure 2B). No revertant clones were identified after sequencing CD3γ cDNA clones prepared from in vitro–activated T cells; indeed, the majority of sequences were invariant, with only 3 single-nucleotide variants identified (data not shown).

Previous molecular characterization of revertant cells has generally revealed one or, rarely, a few revertant genotypes.[9] However, these observations likely underestimate genotypic diversity, since direct sequence analysis of PCR-amplified DNA will only identify genotypes that have undergone sufficient clonal expansion to reach a detectable frequency. Similar considerations undermine the suggestion that CD247 was not a mutational hot spot, since somatic mutants were only found in patient T cells.[1] CD247 is only expressed in T and NK cells that can undergo sufficient clonal expansion for the mutant genotype to be detectable. Our data show that CD247 mutants are frequent, although functional consequences are hard to quantify, since these mutations likely occur in single cells in heterozygosis.

Consistent with the idea that genetic diversity in PID might be greater than often appreciated, direct PCR analysis of purified WASp-expressing T cells from a WASp-deficient patient identified 1 mutation, whereas 25 putative revertant genotypes were identified when 45 allospecific T-cell clones were analyzed.[5] This diversity of WASp sequences in revertant T cells was confirmed by high-resolution electrophoretic analysis of WASp RNA from another WASp-deficient patient.[14]

Thus, the occurrence of revertant or compensating mutations in certain PIDs might reflect a more general tendency of those genes to mutate (ie, more mutation means more chance of a reversion/compensation event that might confer a selective advantage). To test this hypothesis, we compared the genetic variability of a set of control genes, PID genes where reversion has been described, and PID genes without revertants. Here, it should be remembered that these are rare diseases, so it is possible that as more patients are described in detail, the definition of some PIDs as "nonrevertant" might change. This analysis is fundamentally different from those above, since genetic variability within a population is being studied, whereas Figure 2A reports CD247 variation within individuals. The rate of missense, but not synonymous, mutations observed in PID genes where reversion has been described was significantly higher than that found for nonrevertants or control genes (Figure 2C-D). These observations support the hypothesis that certain PID genes are more mutable than others and that an increased mutation rate makes it more likely that reversion or compensating mutations may occur. The nature of the gene mutated and the degree of recovery of function will affect these data, since they will influence the possibilities of clonal expansion and thus detection. However, the possible impact of these mutations on gene function, as assessed by the Gene Damage Index algorithm,[15] was not significantly different (supplemental Table 4). Since genes important for lymphocyte growth are found among both PID genes with revertant and nonrevertant PID genes (supplemental Table 4), we suggest that the frequency of

mutation is a key first influence on the emergence of candidate revertants that subsequently are the objects of selection that may lead to clonal expansion. Interestingly, variation in the coding sequence was significantly greater for revertant genes than for nonrevertant or control genes but similar at UTR flanking regions (Figure 2E). The genetics underlying the intrinsic mutability of PID genes where reversion occurs is unknown. The presence of CpG islands was somewhat more frequent in revertant than nonrevertant PID genes (supplemental Table 4), but it is also possible that local chromatin structure and accessibility for DNA repair could influence mutation.

Acknowledgments

The authors thank Hisse van Santen and Balbino Alarcón for gifts of CD247-specific antibody and Ma5.8 cells and Almudena R. Ramiro for critical reading of the manuscript.

This work was supported in part by grants SAF2014-58752-R (H.T.R.), SAF2014-54708-R (J.R.R.), and SAF2015-69169-R (M.V.-G.) from the Ministerio de Economia y Competitividad and by PhD studentships to A.B.-M. (MINECO SVP-2014-068263) and A.P.-P. (National Secretary of Higher Education, Science, Technology and Innovation, SENESCYT, Ecuador).

Authorship

Contribution: A.B.-M. performed research, analyzed data, and wrote the paper; A.P.-P., M.A.-L., and D.D. performed research and analyzed data; M.V.-G. and J.R.R. analyzed data and wrote the paper; C.A. contributed vital new reagents or analytical tools; A.I. contributed vital new reagents or analytical tools and wrote the paper; and H.T.R. designed research, performed research, analyzed data, and wrote the paper.

Conflict-of-interest disclosure: The authors declare no competing financial interests.

Correspondence: Hugh T. Reyburn, CNB-CSIC, Darwin 3, Campus de CantoBlanco, 28049 Madrid, Spain; e-mail: htreyburn@cnb.csic.es.

References

1. Rieux-Laucat F, Hivroz C, Lim A, et al. Inherited and somatic CD3zeta mutations in a patient with T-cell deficiency. *N Engl J Med*. 2006;354(18):1913-1921.
2. Roberts JL, Lauritsen JP, Cooney M, et al. T-B+NK+ severe combined immunodeficiency caused by complete deficiency of the CD3zeta subunit of the T-cell antigen receptor complex. *Blood*. 2007;109(8):3198-3206.
3. Vales-Gomez M, Esteso G, Aydogmus C, et al. Natural killer cell hyporesponsiveness and impaired development in a CD247-deficient patient. *J Allergy Clin Immunol*. 2016;137(3):942-945.
4. Marin AV, Jimenez-Reinoso A, Briones AC, et al. Primary T-cell immunodeficiency with functional revertant somatic mosaicism in CD247. *J Allergy Clin Immunol*. 2017;139(1):347-349.
5. Davis BR, Dicola MJ, Prokopishyn NL, et al. Unprecedented diversity of genotypic revertants in lymphocytes of a patient with Wiskott-Aldrich syndrome. *Blood*. 2008;111(10):5064-5067.
6. Stephan V, Wahn V, Le Deist F, et al. Atypical X-linked severe combined immunodeficiency due to possible spontaneous reversion of the genetic defect in T cells. *N Engl J Med*. 1996;335(21):1563-1567.
7. Speckmann C, Pannicke U, Wiech E, et al. Clinical and immunologic consequences of a somatic reversion in a patient with X-linked severe combined immunodeficiency. *Blood*. 2008;112(10):4090-4097.
8. Uzel G, Tng E, Rosenzweig SD, et al. Reversion mutations in patients with leukocyte adhesion deficiency type-1 (LAD-1). *Blood*. 2008;111(1):209-218.
9. Hirschhorn R. In vivo reversion to normal of inherited mutations in humans. *J Med Genet*. 2003;40(10):721-728.
10. Demaison C, Parsley K, Brouns G, et al. High-level transduction and gene expression in hematopoietic repopulating cells using a human immunodeficiency [correction of imunodeficiency] virus type 1-based lentiviral vector containing an internal spleen focus forming virus promoter. *Hum Gene Ther*. 2002;13(7):803-813.
11. Sussman JJ, Bonifacino JS, Lippincott-Schwartz J, et al. Failure to synthesize the T cell CD3-zeta chain: structure and function of a partial T cell receptor complex. *Cell*. 1988;52(1):85-95.
12. San José E, Borroto A, Niedergang F, Alcover A, Alarcón B. Triggering the TCR complex causes the downregulation of nonengaged receptors by a signal transduction-dependent mechanism. *Immunity*. 2000;12(2):161-170.
13. Recio MJ, Moreno-Pelayo MA, Kiliç SS, et al. Differential biological role of CD3 chains revealed by human immunodeficiencies. *J Immunol*. 2007;178(4):2556-2564.
14. Lutskiy MI, Park JY, Remold SK, Remold-O'Donnell E. Evolution of highly polymorphic T cell populations in siblings with the Wiskott-Aldrich syndrome. *PLoS One*. 2008;3(10):e3444.
15. Itan Y, Shang L, Boisson B, et al. The human gene damage index as a gene-level approach to prioritizing exome variants. *Proc Natl Acad Sci USA*. 2015;112(44):13615-13620.

Supplementary text:

Materials and Methods

In vitro culture and expansion of CD3^{high} T cells from CD247- and CD3γ-deficient patients

PBMC were purified by centrifugation on Ficoll-Hypaque and cultured in RPMI-1640 medium (Lonza) supplemented with 10% FBS, 10% male AB negative human serum (the first week, and later with 5% FBS, 5% Human Serum), 4 mM L-glutamine, 0.1 mM nonessential amino acids, 1 mM sodium pyruvate, 100U/ml penicillin, 100U/ml streptomycin, 10mM Hepes, 50mM β-mercaptoethanol (Biowest). Cells were stimulated either by culture in 24 well plates coated with anti-CD3 (5ug/ml) and anti-CD28 mAbs (10ug/ml) or in the presence of irradiated feeder cells (autologous PBMCs, Daudi and RPMI-8866 B cell lines) and PHA (0.5ug/ml). In both cases the cultures were supplemented by the addition of 50U/ml recombinant IL-2 (Peprotech).

The study was conducted according to the principles expressed in the Declaration of Helsinki and approved by the Institutional Research Ethics Committees of the various hospitals involved. All participants, or their guardians, provided informed consent for the collection of samples and subsequent analyses.

Cloning and sequencing of the CD247, CD3γ, CD16 and FcεRIγ genes

Total RNA was isolated from cultures of lymphocytes from the patient and a healthy relative control using the RNeasy Mini Kit (Qiagen). cDNA synthesis was carried out using random hexamer primers and Superscript II (Life Sciences). Transcripts for each gene were amplified by PCR using the Expand long template PCR system (a mixture of the proof reading polymerase Pwo and Taq Polymerase, Roche) and specific primers (Table 1) and purified using the Qiagen QIAquick PCR purification kit. Purified PCR products were cloned into pJET 1.2 (CloneJET PCR Cloning Kit) and transformed into *E. coli* DH5α strain. Colonies containing recombinant plasmids, identified by restriction digestion, were sequenced (Parque Científico de Madrid and GATC Biotech).

CD247 construct generation

Selected clones of full length wild-type CD247 molecule and the mutant with an elongated signal peptide were subcloned from pJET sequencing vector into the lentiviral vector pHR-SIN [219] for functional evaluation after lentiviral transduction into the CD247-deficient murine T cell hybridoma Ma5.8 [220].

Cell lines

All cell lines were maintained at 37ºC and 5% CO2 in a humidified incubator and split as necessary. Ma5.8 cells (a gift of Drs Hisse M. van Santen and Balbino Alarcón, CBMSO, Madrid) were maintained in RPMI medium with 5% foetal calf serum (FCS). The 293T packaging cell line was cultured in Dulbecco´s Modified Eagle medium (DMEM) with 10% FCS. All media were supplemented with 2mM L-Glutamine, 0.1mM non essential amino-acids, 10mM HEPES, 1mM sodium pyruvate, 100U/mL penicillin, 100U/mL streptomycin, 50µM β-mercaptoethanol.

Lentivirus generation and transduction of Ma5.8 cells

Lentiviruses were generated by transfection of the 293T cell line with a mixture of the plasmids pCMVdR8.74, pMD2G and pHR-SIN [219] containing a specific insert, using Lipofectamine Plus (Invitrogen) and Optimen (Gibco). Culture supernatants containing lentiviral particles were recovered after 48h, filtered (0.22µm) and stored at -80ºC. For transduction of Ma5.8 cells, $0.5x10^6$ cells were pelleted, resuspended in 0.5mL virus containing supernatant with polybrene (Sigma) at 8µg/mL and plated in one well of a 24-well plate. This plate was centrifuged 90 min at 800 rpm at RT, transferred to an incubator and cultured for 4 to 6 hours at 37ºC, 5% CO2. After this time 0.5ml of medium was removed and replaced with 0.5ml fresh medium (RPMI 5% FCS). Transduction efficiency was tested by flow cytometry by assay of fluorescence in FL-1 channel (CD247-FITC intracellular staining).

CD247 Immunoblotting

Cells were collected, washed once with PBS and lysed in RIPA lysis buffer (1% Triton X-100, 1% DOC, 0.1% SDS, 50mM Tris HCl pH 7.5, 150 mM NaCl, phosphatase inhibitors (1mM $NaVO_3$ and NaF, 2mM EDTA) with protease inhibitors (1µM Pepstatin A, 1µM Leupeptin) and 0.5mM Iodo-acetamide for 30 min on ice. The lysates were centrifuged for 5 min at 13,000rpm to pellet insoluble material and then the protein concentration was determined by Bradford Assay. 30µg of each lysate were separated in 12% SDS reducing polyacrylamide gel electrophoresis followed by transfer to PVDF (Immovilon-P, Millipore). Membranes were blocked in 5% dried skimmed milk (1h, 25ºC), washed three times in 0.05% Tween/TBS and incubated (overnight, 4ºC) with rabbit polyclonal anti-CD247 (gift of Prof. B Alarcon) to visualise CD247. The membranes were then stripped using Restore Western Blot Stripping buffer (Thermo Scientific), re-blocked and developed using mouse monoclonal anti-β-actin (1:15000, Sigma) in 0.05% Tween/TBS.

Flow cytometry

PBMCs either freshly isolated, or cultured, were stained with directly labelled antibodies specific for CD3, CD56, CD4, CD8 (all from Biolegend) and TCR$\alpha\beta$ (BD Pharmingen). Ma5.8 cells were stained with PE-labelled mAb specific for Vβ3 (Pharmingen). For staining, cells were washed and incubated in PBS/0.5% (w/v) Bovine serum albumin/1% (v/v) Fetal bovine serum/0.1% Sodium azide buffer (PBA buffer) with specific antibodies. All the staining was performed on ice, and the labelled cells were maintained on ice until analysis. For intracellular CD247 staining, cells were first stained on ice, if necessary, and then washed with PBA and fixed using 2% para-formaldehyde (PFA). After fixation, cells were washed twice with PBA, and resuspended in 0.2% Saponin/PBA (permeabilization buffer) for 15 min on ice in the dark. After permeabilization, cells were washed once in permeabilization buffer and incubated with CD247-FITC (eBiosciences) antibody in the dark for 30 min on ice, washed and resuspended in PBA for analysis. Cells were analysed using either a FACSCalibur (BD Biosciences) or Gallios (Beckman Coulter) cytometer. Data were analysed with Kaluza Flow Cytometry Analysis.

Gene variation analysis

Data on genes affected in primary immunodeficiencies where reversion events have or have not been described as well as nucleotide variation in control genes information was extracted from publicly available 1000 genomes project data (http://browser.1000genomes.org), with date 21/09/15. Selected information about missense, synonymous and coding variation for each gene, as well as the variation information referred to 5´UTR and 3´UTR regions was also extracted. For missense and synonymous comparison, variation numbers from database were relativized to each gene coding sequence length and plotted as variants described per 1000 base pairs for each gene. On the other hand, region analysis was carried out normalising variants found at each region to the length of 5´UTR, coding sequence or 3´UTR of each gene. Statistical significance was calculated using one way ANOVA test for synonymous and missense variation rates and two way ANOVA for variation vs. gene region analysis comparing the three different group of genes (*, $P<0.05$; **, $P<0.01$; ***, $P<0.001$; n.s. not significant, $P>0.05$). GDI values were extracted for the indicated genes using the GDI server and software (lab.rockefeller.edu/casanova/GDI)[221]. The presence or absence of CpG dinucleotides in the vicinity of the indicated genes was determined using the UCSC Gene Browser.

1. Demaison C, Parsley K, Brouns G, et al. High-level transduction and gene expression in hematopoietic repopulating cells using a human immunodeficiency virus type 1-based lentiviral vector containing an internal spleen focus forming virus promoter. *Hum Gene Ther*. 2002;13(7):803-813.

2. Sussman JJ, Bonifacino JS, Lippincott SJ, et al. Failure to synthesize the T cell CD3-zeta chain: structure and function of a partial T cell receptor complex. *Cell*. 1988;52(1):85-95.

3. Itan Y, Shang L, Boisson B, et al. The human gene damage index as a gene-level approach to prioritizing exome variants. *Proc Natl Acad Sci U S A*. 2015;112(44):13615-13620.

Supplementary table 1: Primer sequences used for amplification of CD247, CD3γ, CD16 and FcεRIγ, as well as for sequencing.

Primers used for PCR and sequencing

Gene	Forward primer	Reverse primer
CD247 cDNA	GGAGATCTCCACAGTCCTCCACTTCCTG	GATCGCGGCCGCATAGGAAGGCTTTAGCATGCC
CD247 Exon1	ACACCCCAAACCCTCAAACCTC	AGGAGGGCAGGATTTGAAGGAG
CD247 Exon2	GGTCAGTCAGTCCTAGTGCCA	CCTTGCTTTGCTCCTGGATAC
CD247 Exon3	GTTAGTTGCCAAGGAGCGGAG	CCTAAACCCAAGACTCTGGCG
CD247 Exon4	CTGTCATGTTAAGGCGTGTTCTC	TGGGTCTCCATCTCTTCTCTTG
CD247 Exon6	AGGTTTGGAGCCTTGATTGTG	ATTTGCAGCTGGGATGAGAAG
CD3γ cDNA	AGTCTAGCTGCTGCACAGGCT	CCCCAAATTTGCTCTGATGGC
CD16A cDNA	GGGGATCCGCCACCATGTGGCAGCTGCTCCTCCC	GCGCGGCCGCTCATTTGTCTTGAGGGTCCTTTCTC
FcεRIγ cDNA	GGGGATCCAGAACGGCCGATCTCCAG	GATCGCGGCCGCGAGTCCAGTCCATGGCAGTT
Sequencing primers used for pJET1.2 and pBlueScript vectors		
pJET1.2	CGACTCACTATAGGGAGAGCGGC	AAGAACATCGATTTTCCATGGCAG
M13	GTAAAACGACGGCCAGT	GCGGATAACAATTTCACACAGG

Supplementary table 2: Summary of several parameters for each CD247 gene variant found in cDNA clones sequenced from the CD247 deficient patient, a CD16A deficient patient and healthy controls. Gene position corresponds to nucleotide base number in full length CD247. CDS denotes coding sequence region.

CD247 deficient Patient

	Gene Mutation	Position	Gene region	Codon Change	Incidence
Original mutation	T>C	147	CDS	Met>Thr	18/20
Revertant mutation	C>T	147	CDS	Stop>Met	2/20
Compensatory mutation	A>T	138	CDS	No aa>Met	6/20
Variation 1	C>T	174	CDS	Ala>Val	1/20
Variation 2	C>A	224	CDS	Leu>Met	1/20
Variation 3	G>C	280	CDS	Ile>Ile	1/20
Variation 4	A>G	342	CDS	Gln>Arg	1/20
Variation 5	C>T	346	CDS	Gly>Gly	1/20
Variation 6	A>G	488	CDS	Arg>Gly	1/20
Variation 7	C>T	617	CDS	Gln>Stop	1/20
Variation 8	T>A	921	3´UTR	-	1/20
Variation 9	A>G	1291	3´UTR	-	1/20
Variation 10	C>A	1338	3´UTR	-	1/20
Variation 11	A>G	1444	3´UTR	-	1/20
Variation 12	T>C	1450	3´UTR	-	1/20
Variation 13	A>G	1466	3´UTR	-	1/20
Variation 14	A>T	1481	3´UTR		20/20
Variation 15	C>T	1527	3´UTR	-	1/20

CD16A deficient Patient

	Gene Mutation	Position	Gene region	Codon Change	Incidence
Variation 1	A>-	155	CDS	Frame shift	1/27
Variation 2	C>T	174	CDS	Ala>Val	2/27
Variation 3	T>C	237	CDS	Leu>Pro	3/27
Variation 4	T>C	303	CDS	Val>Ala	3/27
Variation 5	A>G	356	CDS	Arg>Arg	1/27
Variation 6	T>C	369	CDS	Val>Pro	3/27
Variation 7	G>T	378	CDS	Gly>Val	1/27
Variation 8	G>T	389	CDS	Glu>Stop	2/27
Variation 9	A>G	498	CDS	Lys>Met	1/27
Variation 10	A>G	573	CDS	Gln>Arg	1/27
Variation 11	A>G	605	CDS	Asp>Gly	1/27
Variation 12	C>T	617	CDS	His>His	1/27
Variation 13	C>T	620	CDS	Gln>Stop	1/27
Variation 14	A>G	704	3´UTR	-	1/16
Variation 15	T>C	725	3´UTR	-	1/16
Variation 16	A>G	740	3´UTR	-	1/16
Variation 17	T>C	804	3´UTR	-	1/16
Variation 18	A>G	824	3´UTR	-	1/16
Variation 19	T>A	835	3´UTR	-	1/16
Variation 20	T>G	871	3´UTR	-	1/16
Variation 21	G>A	881	3´UTR	-	1/16
Variation 22	T>C	882	3´UTR	-	1/16
Variation 23	T>A	912	3´UTR	-	1/16
Variation 24	A>G	997	3´UTR	-	2/16
Variation 25	T>C	1005	3´UTR	-	1/16
Variation 26	T>C	1010	3´UTR	-	1/16

Variation 27	G>A	1039	3´UTR	-	2/16
Variation 28	G>A	1160	3´UTR	-	1/16
Variation 29	G>A	1176	3´UTR	-	1/16
Variation 30	C>G	1256	3´UTR	-	4/16
Variation 31	G>A	1265	3´UTR	-	1/16
Variation 32	C>G	1333	3´UTR	-	1/16
Variation 33	T>C	1369	3´UTR	-	1/16
Variation 34	G>A	1425	3´UTR	-	1/16
Variation 35	A>G	1456	3´UTR	-	1/16
Variation 36	A>T	1481	3´UTR	-	16/16
Variation 37	A>G	1505	3´UTR	-	1/16
Variation 38	A>G	1561	3´UTR	-	1/16
Variation 39	T>A	1600	3´UTR	-	1/16

Healthy control 1

	Gene Mutation	Position	Gene region	Codon Change	Incidence
Variation 1	A>G	19	5´UTR	-	1/9
Variation 2	A>G	95	5´UTR	-	1/9
Variation 3	C>T	419	CDS	Arg>Trp	1/9
Variation 4	A>G	492	CDS	Lys>Arg	1/9
Variation 5	T>C	907	3´UTR	-	1/9
Variation 6	T>C	955	3´UTR	-	1/9
Variation 7	T>C	1064	3´UTR	-	1/9
Variation 8	G>A	1125	3´UTR	-	1/9
Variation 9	T>C	1268	3´UTR	-	1/9
Variation 10	A>G	1344	3´UTR	-	1/9
Variation 11	T>C	1427	3´UTR	-	1/9
Variation 12	T>C	1454	3´UTR	-	2/9
Variation 13	A>T	1481	3´UTR	-	9/9

Healthy Control 2

	Gene Mutation	Position	Gene region	Codon Change	Incidence
Variation 1	A>G	19	5´UTR	-	1/10
Variation 2	G>T	62	5´UTR	-	1/10
Variation 3	G>A	98	5´UTR	-	1/10
Variation 4	A>G	189	CDS	Gln>Arg	1/10
Variation 5	T>C	239	CDS	Leu>Pro	1/10
Variation 6	A>C	314	CDS	Cys>Arg	1/10
Variation 7	C>T	394	CDS	Arg>Arg	3/10
Variation 8	C>G	634	CDS	Arg>Gly	1/10
Variation 9	A>-	660	3´UTR	-	2/10
Variation 10	A>-	673	3´UTR	-	1/10
Variation 11	->C	714	3´UTR	-	1/10
Variation 12	G>A	827	3´UTR	-	1/10
Variation 13	G>A	984	3´UTR	-	1/10
Variation 14	A>G	987	3´UTR	-	1/10
Variation 15	T>C	1013	3´UTR	-	1/10
Variation 16	G>A	1225	3´UTR	-	1/10
Variation 17	C>T	1245	3´UTR	-	1/10
Variation 18	C>G	1256	3´UTR	-	6/10
Variation 19	G>A	1276	3´UTR	-	1/10
Variation 20	T>C	1391	3´UTR	-	1/10
Variation 21	A>G	1456	3´UTR	-	1/10
Variation 22	A>T	1481	3´UTR	-	9/10
Variation 23	G>A	1484	3´UTR	-	1/10

Supplementary table 3: Summary of the number of variants found for some specific CD247 exons in clones amplified from genomic DNA isolated from non-CD247 expressing polymorphonuclear (PMN) cells.

Gene	Exon	Clones analyzed	Total variants	Genomic CD247 length amplified (bp)	Variants per 1000bp read	Patients somatic mutation	Reversion of patients mutation
CD247	1	15	12	405	1,97	1	Yes Present Report
	2	10	2	401	0,49	1	Yes[1]
	3	7	8	263	4,34	-	-
	4	10	16	425	3,76	1	Not analyzed[2]
	6	10	0	302	0	-	-

Supplementary Table 4

Primary immunodeficiency genes where revertants have been described

Gene Name	Transcript ID	Nucleotide ID	Synonymous variants	Missense variants	5´UTR variants	3´UTR variants	5´UTR length	CDS length	3´UTR length	Gene Damage Index - GDI Phred	CpG present
IL2RG	ENST00000374202	NM_000206	25	223	1	4	93	1109	358	0.26766	-
CD247	ENST00000392122	NM_000734	17	48	14	44	146	491	1050	NA	154
ADA	ENST00000372874	NM_000022	48	152	3	20	129	1091	346	5.60704	83
WAS	ENST00000376701	NM_000377	30	352	2	1	58	1508	278	1.13817	-
DOCK8	ENST00000432829	NM_203447	250	543	31	45	113	6299	1058	18.28926	101
TGFBR1	ENST00000374994	NM_004612	52	120	6	421	118	1411	4887	0.58837	142
IKBKG	ENST00000369606	NM_001099857	6	117	1	0	415	1259	605	0.09337	168
NEMO	ENST00000407008	NM_016231	51	75	27	47	213	1583	1759	NA	168
SH2D1A	ENST00000371139	NM_001114937	9	95	7	20	362	377	1775	0.04688	-
CD18	ENST00000355153	NM_001127491	125	219	18	27	224	2309	430	NA	61
FANCA	ENST00000389301	NM_000135	158	605	3	120	43	4367	1050	7.80511	140
FANCC	ENST00000289081	NM_000136	34	149	9	130	263	1676	2673	3.37227	136
RAG1	ENST00000299440	NM_000448	83	405	2	97	125	3131	3451	8.76351	-

Primary immunodeficiency genes with no revertants described

Gene Name	Transcript ID	Nucleotide ID	Synonymous variants	Missense variants	5´UTR variants	3´UTR variants	5´UTR length	CDS length	3´UTR length	Gene Damage Index - GDI Phred	CpG present
RFX5	ENST00000290524	NM_000449	41	105	3	42	222	1850	1546	4.54115	18
IKBA	ENST00000216797	NM_020529	30	51	16	42	111	953	515	NA	111
IRAK4	ENST00000431837	NM_001145256	19	92	32	93	357	1010	2838	5.19884	41
ICOS	ENST00000316386	NM_012092	17	24	4	61	68	599	1985	1.51225	-
CD19	ENST00000538922	NM_001178098	50	100	4	20	63	1673	233	2.61413	35
TNFRSF13B	ENST00000261652	NM_012452	32	123	0	30	14	881	482	5.14551	-
TWEAK	ENST00000293825	NM_003809	23	42	11	18	97	749	561	NA	50
TYK2	ENST00000525621	NM_003331	110	257	24	16	379	3563	320	7.41708	135
WIPF1	ENST00000392547	NM_003387	54	110	9	95	101	1511	2988	0.96977	122
STAT3	ENST00000264657	NM_003150	85	185	8	88	219	2309	2425	1.52170	87
CD3G	ENST00000532917	NM_000073	13	45	18	103	81	548	682	10.80204	-
TNFSF5	ENST00000370629	NM_000074	22	231	1	22	73	785	976	NA	-
RHOH	ENST00000381799	NM_001278363	18	36	41	99	737	575	802	0.68348	-
Lck	ENST00000336890	NM_005356	55	114	6	15	139	1529	451	NA	74
OX40	ENST00000379236	NM_003327	37	39	1	17	42	833	245	NA	52
IL7RA	ENST00000303115	NM_002185	67	216	13	144	104	1379	3134	NA	-
CD3D	ENST00000300692	NM_000732	18	49	15	13	138	515	118	0.59015	-
CD3E	ENST00000309424	NM_012099	48	79	24	74	489	1532	1265	1.24983	-

TRAF3	ENST00000367025	NM_025228	40	104	21	7	438	1655	191	8.81729	249
TICAM1	ENST00000248244	NM_182919	58	122	16	16	269	2138	320	6.88939	43
CD16a	ENST00000367969	NM_000569	30	78	13	45	185	872	1349	NA	-
CD16b	ENST00000294800	NM_001244753	23	74	32	60	261	809	1324	NA	-
FCER1G	ENST00000289902	NM_004106	6	13	3	11	26	260	305	0.90665	-
CXCR4	ENST00000409817	NM_001008540	34	65	13	20	305	1070	537	0.28802	-
RPSA	ENST00000301821	NM_002295	13	28	13	4	110	887	1076	0.15368	60
C1QA	ENST00000374642	NM_015991	20	42	5	14	86	737	275	0.31014	-
FCN3	ENST00000270879	NM_003665	26	65	0	4	7	899	253	3.01786	-
STAT5B	ENST00000293328	NM_012448	60	105	3	106	170	2363	2638	1.31577	126
JAK3	ENST00000458235	NM_000215	186	395	6	131	101	3374	1974	3.69742	160
ZAP70	ENST00000264972	NM_001079	100	170	21	39	208	1859	383	1.46999	115

Control genes

Gene Name	Transcript	Nucleotide ID	Synonymous variants	Missense variants	5´UTR variants	3´UTR variants	5´UTR length	CDS length	3´UTR length	Gene Damage Index – GDI Phred	CpG present
ACT	ENST00000331789	NM_001101	60	58	13	43	85	1127	640	NA	245
ARPC	ENST00000259477	NM_030978	15	13	7	40	87	461	493	NA	93
ADRA1A	ENST00000380586	NM_033303	128	271	16	25	437	1427	440	5.12161	202
APOA4	ENST00000357780	NM_000482	59	116	2	14	105	1190	165	3.38677	35
ABHD2	ENST00000352732	NM_152924	43	74	18	308	521	1277	6963	1.24066	59
CDHR1	ENST00000372117	NM_033100	91	231	5	108	127	2579	4082	5.36670	85
CCT6A	ENST00000275603	NM_001762	39	74	14	30	165	1595	922	3.94523	105
COL9A1	ENST00000357250	NM_001851	109	270	10	71	160	2765	880	17.93014	61
CYP1A1	ENST00000395048	NM_000499	36	151	3	42	123	1538	947	8.23125	-
DHX8	ENST00000262415	NM_004941	79	131	7	57	122	3662	485	1.39801	28
DCTN1	ENST00000361874	NM_004082	98	254	11	17	319	3836	363	4.54937	-
E2F1	ENST00000343380	NM_005225	39	66	3	38	141	1313	1268	2.63160	142
ANGPTL1	ENST00000234816	NM_004673	40	94	17	51	477	1475	1603	1.77414	-
KDELC2	ENST00000323468	NM_153705	28	75	4	72	67	1523	2721	3.29002	101
HSP90AA1	ENST00000334701	NM_001017963	90	142	16	45	346	2564	977	2.04609	157
HCAR1	ENST00000432564	NM_032554	36	64	4	77	244	1040	1693	3.33717	-

IFNAR2	ENST00000382241	NM_207585	46	102	18	61	360	1547	1013	4.30687	94
LTBP1	ENST00000418533	NM_001166264	146	348	4	47	142	4061	979	5.77162	164
DUSP1	ENST00000239223	NM_004417	27	45	13	26	249	1103	688	3.19307	172
ACAD9	ENST00000308982	NM_014049	53	102	11	28	203	1865	540	2.84303	55
MYO15A	ENST00000205890	NM_016239	279	620	16	26	339	10592	945	16.09179	275
NFATC1	ENST00000253506	NM_001278669	149	188	16	98	454	2831	1746	8.00523	544
OTUB1	ENST00000538426	NM_017670	24	25	2	46	605	815	890	2.06462	85
PRDX1	ENST00000262746	NM_002574	15	41	20	15	342	599	322	0.75000	64
PSMA1	ENST00000396394	NM_002786	27	24	18	6	147	791	343	0.79430	52
TYRO3	ENST00000263798	NM_006293	96	181	1	31	237	2672	1092	7.27014	20
RYR1	ENST00000355481	NM_001042723	675	1785	10	7	131	15101	144	8.51518	320
ANKS1A	ENST00000360359	NM_015245	110	200	10	104	143	3404	2808	5.26551	61
TSPAN1	ENST00000372003	NM_005727	16	46	13	19	475	725	439	1.21738	-
VAMP1	ENST00000396308	NM_014231	6	10	22	21	369	356	2245	0.16428	76

ARTICLE 3

TRANSMEMBRANE FEATURES GOVERNING FC RECEPTOR CD16A ASSEMBLY WITH CD16A SIGNALING ADAPTOR MOLECULES

Multicomponent immune receptors are those where ligand binding and intracellular signal transduction are mediated by different elements. The physical coupling of both elements is highly important and takes place through their transmembrane (TM) domains.

Previously described interactions for other receptor complexes are based on a single principle: assembly between complex subunits relies on single interactions at precise positions between lysine or arginine residues in the receptor and pairs of aspartic acid, present in the signaling dimer. However, the transmembrane domain sequence of the CD16A NK cell receptor also presents an aspartic acid and yet clearly associates with CD247 since CD16A expression was markedly reduced, in a CD247-genotype dependent manner in the CD247-deficient patient and family NK cells.

Thus, in this article, the biochemistry of the interaction between CD16A and CD247 or FcεR1γ was analyzed in detail to better understand their transmembrane association. Initial *in vitro* transcription, translation and assembly of complexes using multiple CD16A-TM mutants identified the residues involved in this association, which was further supported by the observation of membrane expression defects when these mutants were expressed in NK cell lines. Molecular modeling corroborated that all interacting residues were located within the same receptor interface. In contrast to the well-established “complementary-charge” model, the CD16A transmembrane acid acts principally in protein quality control and complex association depends on multiple polar and aromatic residues along the entire length of CD16A transmembrane domain.

These observations were extended to other Fc receptors that also lack transmembrane positively charge residues and bind same signaling dimer, FcεR1γ, and similar interacting interfaces were identified.

To sum up, all these results show a novel mode of complex formation between immune receptor and signaling adaptor molecules that underlies the ability of the CD247 signaling adaptor molecule to interact with many receptors by different mechanisms.

Transmembrane features governing Fc receptor CD16A assembly with CD16A signaling adaptor molecules

Alfonso Blázquez-Moreno[a], Soohyung Park[b,c], Wonpil Im[b,c], Melissa J. Call[d,e], Matthew E. Call[d,e,1,2], and Hugh T. Reyburn[a,1,2]

[a]Department of Immunology and Oncology, Centro Nacional de Biotecnología-Consejo Superior de Investigaciones Científicas, Madrid 28049, Spain; [b]Department of Biological Sciences, Lehigh University, Bethlehem, PA 18015; [c]Bioengineering Program, Lehigh University, Bethlehem, PA 18015; [d]Structural Biology Division, The Walter and Eliza Hall Institute of Medical Research, Parkville, VIC 3052, Australia; and [e]Department of Medical Biology, University of Melbourne, Parkville, VIC 3052, Australia

Edited by Jeffrey V. Ravetch, Rockefeller University, New York, NY, and approved June 6, 2017 (received for review April 21, 2017)

Many activating immunoreceptors associate with signaling adaptor molecules like FcεR1γ or CD247. FcεR1γ and CD247 share high sequence homology and form disulphide-linked homodimers that contain a pair of acidic aspartic acid residues in their transmembrane (TM) domains that mediate assembly, via interaction with an arginine residue at a similar register to these aspartic acids, with the activating immunoreceptors. However, this model cannot hold true for receptors like CD16A, whose TM domains do not contain basic residues. We have carried out an extensive site-directed mutagenesis analysis of the CD16A receptor complex and now report that the association of receptor with the signaling adaptor depends on a network of polar and aromatic residues along the length of the TM domain. Molecular modeling indicates that CD16A TM residues F^{202}, D^{205}, and T^{206} form the core of the membrane-embedded trimeric interface by establishing highly favorable contacts to the signaling modules through rearrangement of a hydrogen bond network previously identified in the CD247 TM dimer solution NMR structure. Strikingly, the amino acid D^{205} also regulates the turnover and surface expression of CD16A in the absence of FcεR1γ or CD247. Modeling studies indicate that similar features underlie the association of other activating immune receptors, including CD64 and FcεR1α, with signaling adaptor molecules, and we confirm experimentally that equivalent F, D, and T residues in the TM domain of FcεR1α markedly influence the biology of this receptor and its association with FcεR1γ.

activating immunoreceptors | signaling adaptor molecules | Fc receptors | transmembrane interactions

Human FcγRIIIA (CD16A) is a low-affinity receptor for the Fc portion of IgG expressed by human $CD56^{dim}$ natural killer (NK) cells, subsets of monocytes, dendritic cells, and rare T cells. FcγRIIIB (CD16B) is encoded by a distinct gene and is preferentially expressed by neutrophils (1). CD16B is a GPI-anchored glycoprotein whereas CD16A is a type 1 membrane glycoprotein with a single transmembrane (TM) domain and a short cytoplasmic tail whose expression at the cell surface depends on association with the signaling adaptor molecules CD247 (TCRζ) and/or FcεR1γ (1–4). First discovered as components of the TCR:CD3 complex and the high affinity receptor for IgE, respectively (5–7), CD247 and FcεR1γ are integral membrane proteins that have subsequently been found to be obligate signaling adaptors for many immunoreceptors in different cell types. Both adaptors have very short extracellular domains and cytoplasmic tails that contain immunoreceptor tyrosine-based activating motifs (ITAMs) for signal transduction. Moreover, both CD247 and FcεR1γ form dimers in the endoplasmic reticulum (ER) that are stabilized by a disulphide bond at the junction between the extracellular and TM domains so that, at the cell surface, CD247 and FcεR1γ in complex with their client receptors are dimeric. In general, the receptors known to associate with CD247 and FcεR1γ have short intracellular tails and thus are completely dependent on these adaptors to signal, although phosphorylation of a protein kinase C (PKC) motif in the cytoplasmic tail of CD16A can modulate the outcome of receptor ligation (8).

The incorporation of CD247 into the TCR/CD3 complex is the rate-limiting step in the process of assembly of the receptor complex for cell surface expression because incomplete TCR/CD3 complex is otherwise retained in the cis-Golgi and targeted for degradation (9). Similarly, association with the FcεR1γ or CD247 molecules is also required for the correct maturation and expression at the cell surface of the CD16A protein (2–4). The interaction of CD247 with the TCR, like many immunoreceptor complex interactions, occurs via a precise interface involving the TM domains of the different subunits in the complex (10). Detailed analysis of the interactions underlying the associations between the different subunits of the T-cell receptor complex have shown that interactions between basic and acidic residues localized at precise positions of the TM domains of the different subunits are necessary, and often sufficient, for complex assembly (11). Subsequent studies on the assembly of NK cell receptor complexes, such as NKG2D–DAP10 (12) or NKG2C–DAP12 (13), have shown that the association of the subunits in these complexes is also mediated by similar interactions, where pairs of aspartic acids in the adaptor molecules interact with either an

Significance

Many activating immunoreceptors associate, via interactions between transmembrane domains, with adaptor molecules that mediate signaling for leukocyte activation. To date, the best characterized form of receptor complex assembly depends on a single basic transmembrane (TM) domain residue. We now describe a second, completely different solution for TM-mediated receptor assembly, found in three different Fc receptor TM domains, and involving a more complex polar/aromatic interface. Residues in the core of this interaction motif can also regulate receptor protein turnover. Thus, multiple solutions for TM-mediated receptor assembly with signaling modules have evolved. These findings may provide more broadly useful insights into how other immune receptors that do not contain charged residues in their TM domains assemble into complexes with signaling adaptor molecules.

Author contributions: A.B.-M., M.E.C., and H.T.R. designed research; A.B.-M., S.P., and M.J.C. performed research; A.B.-M., S.P., W.I., M.J.C., M.E.C., and H.T.R. analyzed data; and A.B.-M., S.P., W.I., M.J.C., M.E.C., and H.T.R. wrote the paper.

The authors declare no conflict of interest.

This article is a PNAS Direct Submission.

[1]M.E.C. and H.T.R. contributed equally to the supervision of this work.

[2]To whom correspondence may be addressed. Email: htreyburn@cnb.csic.es or mecall@wehi.edu.au.

This article contains supporting information online at www.pnas.org/lookup/suppl/doi:10.1073/pnas.1706483114/-/DCSupplemental.

arginine or lysine residue in the receptor TM domain. Indeed, for KIR2DS2 or NKG2D, all residues of the receptor TM domain can be mutated to valine or leucine, and the interactions of the lysine of KIR2DS2, or the arginine of NKG2D, with aspartic acids in DAP12 and DAP10, respectively, are sufficient to maintain the receptor/adaptor complex (14). Surprisingly, however, the TM domain sequence of CD16A, which is devoid of basic residues and contains an aspartic acid, pairs with FcεR1γ and CD247 which also contain aspartic acids in their TM. Thus, a mechanism of assembly between CD16A and FcεR1γ or CD247, distinct from those known for other immunoreceptor complexes, must exist.

We examined in detail the TM interactions that mediate association of CD16A with FcεR1γ and CD247 signaling molecules and found that multiple polar and aromatic residues, distributed along an extended helical face of the CD16A TM domain, contribute to the receptor/adaptor interaction. Our analysis revealed a particularly important role for the CD16A TM sequence $F^{202}D^{205}T^{206}$ in both assembly with signaling adaptors and intracellular retention/degradation of unassembled CD16A protein. An independent molecular dynamics (MD) simulation approach identified a highly favored TM assembly mode in which nearly all of the CD16A TM residues identified in mutagenesis experiments directly contact the surfaces of FcεR1γ and CD247 signaling dimers. The model that emerged provides a structural rationale for the role of the $F^{202}D^{205}T^{206}$ trio in establishing favorable contacts with signaling dimers and sequestering D^{205}, which constitutes the key CD16A retention/degradation signal, within the interface. Unbiased MD simulations revealed that the related Fc receptors FcεR1α and FcγR1 (CD64) likely form similar interfaces with the FcεR1γ dimer that include nearly identical interactions mediated by conserved FxxDT (FcεR1α) and FxxNT (CD64) TM sequences. We confirmed the importance of this sequence by examining the assembly and surface expression of FcεR1α in cells. These results indicate that the concepts identified here may serve as a useful guide to understand the assembly and cell biology of multiple activating immunoreceptor complexes where interactions between amino acids of complementary charge potential are not obviously relevant.

Results

CD16A Associates with Either FcεR1γ or CD247. It has previously been reported that cell surface expression of the CD16A receptor depends on a noncovalent association with the signaling dimers FcεR1γ and/or CD247 (2–4). Ex vivo analysis of CD16A cell surface expression on primary human NK cells deficient in either FcεR1γ or CD247 has suggested that CD16A does not discriminate between these adaptor molecules (15), and we confirmed these data in vitro when fibroblasts were transfected with CD16A alone or in combination with either FcεR1γ or CD247 adaptor molecules. Only small amounts of CD16A protein, which correspond to an immature (EndoH-sensitive) species, were detected in cells transfected with the receptor construct alone (Fig. 1*A*), and almost no surface expression of CD16A was observed (Fig. 1*B*). In contrast, when the CD16A construct was cotransfected with plasmids driving expression of the FcεR1γ or CD247 adaptor molecules, abundant glycosylated and EndoH-resistant CD16A protein was observed (Fig. 1*A*). These experiments showed that CD16A was retained in the ER and probably degraded, in the

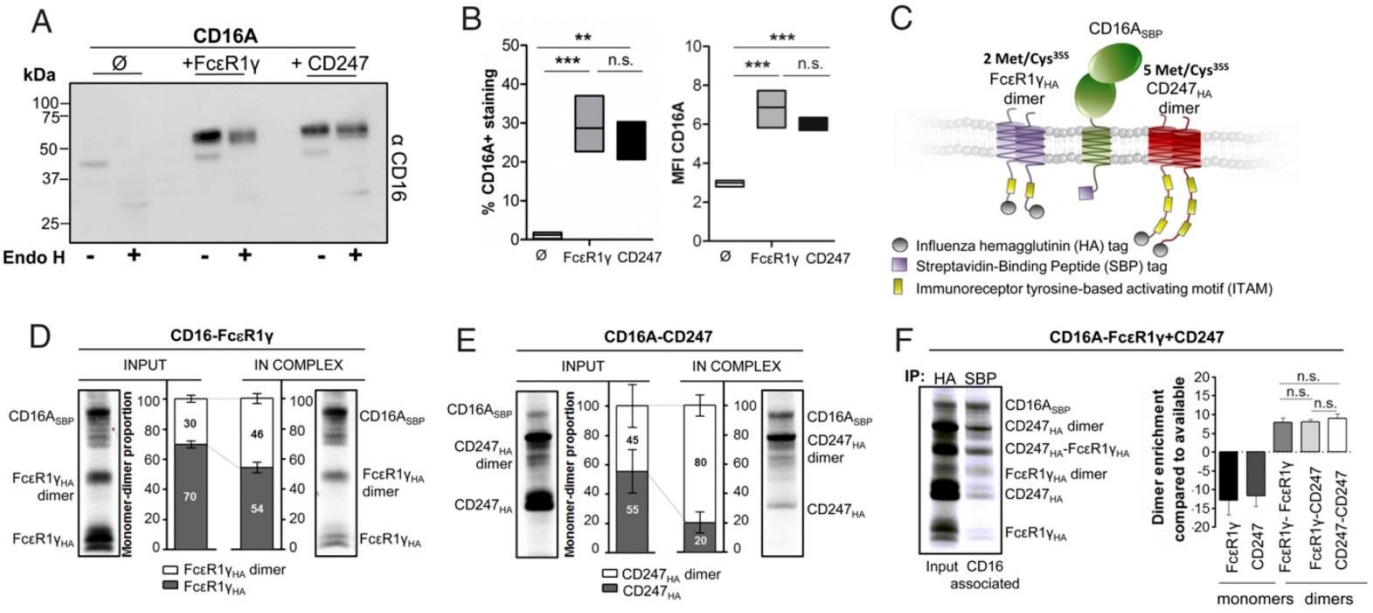

Fig. 1. CD16A requires association with adaptor modules for cell surface expression but shows no preference for assembly with either CD247 or FcεR1γ. An expression vector encoding CD16A was transfected, either alone or in combination with plasmids for CD247 or FcεR1γ, into 293T cells, and cell lysates were analyzed by Western blot (*A*). Aliquots of the same lysates were treated with EndoH endoglycosidase for determination of glycosylation state as a measure of maturation state (*A*). Representative image of three independent experiments is shown. Surface expression of CD16A was also analyzed by flow cytometry of transfected cells. (*B*) Percentage of cells expressing CD16 at the cell surface and mean fluorescence intensity (MFI) of CD16 staining was determined using Kaluza Flow Cytometry Analysis Software. Data represent mean of three experiments, and statistical significance was determined using the one-way ANOVA-Tukey's multiple comparison test (**$P < 0.01$; ***$P < 0.001$; n.s., not statistically significant $P > 0.05$). (*C*) Schematic showing CD16A-SBP and HA-tagged signaling dimers used for IVT assay. The different numbers of ^{35}S labeling positions are indicated. (*D–F*) CD16A mRNA was cotranslated with FcεR1γ (*D*), CD247 (*E*), or both FcεR1γ and CD247 (*F*) adaptor molecule mRNAs (in the presence of radioactively labeled ^{35}S methionine and cysteine). These reactions were done in ER-like conditions to allow assembly of the receptor complex. Each completed assembly reaction was then divided in two aliquots: one for HA immunoprecipitation, to quantify total full-length transcribed FcεR1γ$_{HA}$ and CD247$_{HA}$ protein and labeled "INPUT" control in our analysis and the other labeled "IN COMPLEX," where CD16-SBP was immunoprecipitated and associated HA-tagged adaptor molecules could be analyzed. The immunoprecipitates were analyzed in 12% SDS/PAGE gels in nonreducing conditions and transferred to PVDF membranes for phospho-imaging. Dimer and monomer species were quantified, normalized to the number of labeling positions, and plotted as mean ± SD. Statistical significance was calculated using one-way ANOVA. Images are representative of at least three independent experiments.

absence of adaptor (Fig. 1*A*). Cell-surface expression of CD16A seemed equivalent when either FcεR1γ or CD247 was present in the system (Fig. 1*B*). Therefore, these data confirm prior work demonstrating that association of the adaptor modules FcεR1γ or CD247 with CD16A not only is required for progression of this receptor through the secretory pathway and cell surface expression but also protects the CD16A protein from degradation (16).

Adaptor Modules FcεR1γ and CD247 Are Recruited Equally by CD16A. To address in detail how the CD16A receptor associates with the FcεR1γ or CD247 adaptors, we used an in vitro translation (IVT)-based experimental system that had previously been used to define the assembly of the TCRαβ/CD3εγδ/CD247 complex (11) and several NK receptor complexes (10). Streptavidin-binding peptide (SBP)-tagged CD16A was cotranslated with either HA-tagged FcεR1γ or HA-CD247 in the presence of ER-derived microsomes and ^{35}S-labeled methionine/cysteine, and then complex formation was quantitated in coimmunoprecipitation experiments (Fig. 1*C* and Fig. S1).

Inspection of the lanes corresponding to "INPUT" controls (Fig. 1 *D* and *E*) showed that HA-tagged FcεR1γ and CD247 species ran on nonreducing SDS/PAGE gels as dimers and monomers, but that, after immunoprecipitation of CD16A, the fraction of dimer species was clearly enriched (Fig. 1 *D* and *E*, "IN COMPLEX"). Quantitation of CD16A immunoprecipitates from these reactions confirmed that CD16A preferentially recruited adaptor molecule dimers rather than monomers (Fig. 1 *D* and *E*). Indeed, because dimerization of CD247 and FcεR1γ is driven by polar residues in the TM domain, we cannot exclude the possibility that a proportion of the monomeric species detected after SDS/PAGE were actually noncovalent dimeric species in which the disulphide bond had not yet formed. Experiments in which CD16A was cotranslated with both FcεR1γ and CD247 in the same reaction showed once again that dimeric species were highly enriched in CD16A immunoprecipitates, compared with monomeric adaptor molecules (Fig. 1*F*). Moreover, after integrating the radioactive signal in each band and correcting for the number of methionine/cysteine labeling positions in each dimeric species, no preference for FcεR1γ-FcεR1γ, FcεR1γ-CD247, or CD247-CD247 dimers was observed, suggesting that CD16A binds FcεR1γ and CD247 with similar affinity. This observation suggested that the association of CD16A with these adaptor molecules is mediated by similar protein interactions; this hypothesis was tested in the next set of experiments.

A Polar and Aromatic Interface Mediates the Association of CD16A with Adaptor Modules. To identify the TM residues involved in CD16A association with adaptor modules, a panel of mutants was prepared in three blocks of three mutations. Based on the documented roles of polar and aromatic residues in driving TM helix associations (17, 18), we mutated these amino acid types in the CD16A TM sequence (Fig. 2*A*) to alanine and evaluated the association of mutants with each signaling molecule using the IVT system described above. All three of the "triple" mutants ($S^{193}F^{194}C^{195}$ > A, $F^{202}D^{205}T^{206}$ > A, and $Y^{209}F^{210}S^{211}$ > A) showed marked defects in association with both FcεR1γ and CD247 (Fig. 2 *B* and *C*). To determine the contribution of specific residues to the defective association of the triple mutants with FcεR1γ, a panel of single mutants (Fig. S2*A*) was prepared and tested in quantitative analyses (Fig. 3*A*). This panel included a Q^{191} > A mutant that had not been tested in the block analysis but caused ∼40% reduction in CD16A association, identifying an additional polar amino acid involved in the assembly. The mutation of $S^{193}F^{194}C^{195}$ > A decreased CD16A association by more than 50%, and analysis of the individual substitutions showed that the single F^{194} > A mutation was sufficient to cause this decrease (Fig. 3*A*) whereas mutations at S^{193} and C^{195} had no significant effects. Dissection of the $F^{202}D^{205}T^{206}$ > A triple mutant revealed that single substitutions at either F^{202} or T^{206} provoked significant reductions in the association with FcεR1γ

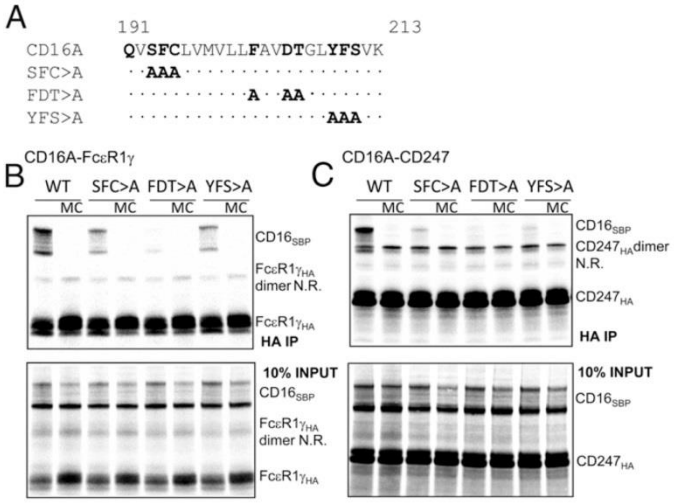

Fig. 2. The effects of CD16A triple block mutants on association with CD247 or FcεR1γ. Three triple mutants targeting groups of polar and aromatic residues along the length of the CD16A transmembrane domain were prepared (*A*), and the ability of these mutants to assemble with adaptor modules, FcεR1γ or CD247, was evaluated (*B* and *C*). After immunoprecipitation using anti-HA antibody, complex formation with FcεR1γ (*B*) and CD247 (*C*) was analyzed in 12% SDS/PAGE gels in reducing conditions. Then 10% of assembly reactions without immunoprecipitation were analyzed in parallel as loading controls. As can be observed in the gels, dimers of FcεR1γ, and especially CD247, were not completely reduced in these conditions. MC, mixing control in which CD16A and FcεR1γ/CD247 were translated in separate reactions and mixed just before detergent extraction; N.R., nonreduced.

whereas the substitution of alanine at D^{205} of the CD16A TM domain had a lesser effect (Fig. 3*A*). This result was surprising because of the prior observations on the crucial roles played by acidic and basic amino acids in the formation of other immunoreceptor complexes (10). To further explore the role of this acidic residue, substitutions of D^{205} with E, K, or N were tested for complex formation with FcεR1γ. Substitution with either E or K essentially abolished complex formation, suggesting that the size and charge at this position have an important impact on the association with FcεR1γ. Replacement with N (polar, nonionizable) also led to only a mild reduction in formation of the receptor complex, suggesting that the ionization of D^{205} is not critical for assembly. When single mutants of the $Y^{209}F^{210}S^{211}$ > Ala triple mutant were tested, alteration of the aromatic residues Y^{209} and F^{210} had the greatest effect on the CD16A–FcεR1γ complex formation whereas replacement of S^{211} with alanine produced only a mild defect (Fig. 3*A*). We tested the same CD16A TM mutants for their effects on association with CD247, and very similar results were obtained (Fig. 3*B*), consistent with the high sequence similarity between the TM domains of FcεR1γ and CD247 (Fig. 3*C*).

Mapping the amino acids that contributed most to the interactions of CD16A with FcεR1γ and CD247 onto a helical wheel projection (Fig. 3*D*), we observed that these residues are colocated on one face of the receptor TM domain whereas the only two polar residues located on the opposite side of the TM helix (S^{193} and S^{211}) had no effect on complex formation. The replacement of C^{195} with alanine on the interacting face also had no significant effect, indicating that disruption of the association with adaptor molecules is likely a specific effect of particular mutations rather than a generally disruptive effect of alanine substitution on the TM helix structure. This interpretation is consistent with the view that the helical structure of TM domains is driven primarily by backbone hydrogen bonds and the observation that alanine is, after leucine, the second most common α-helical TM residue (19). We therefore concluded that interactions between CD16A and its signaling adaptors FcεR1γ

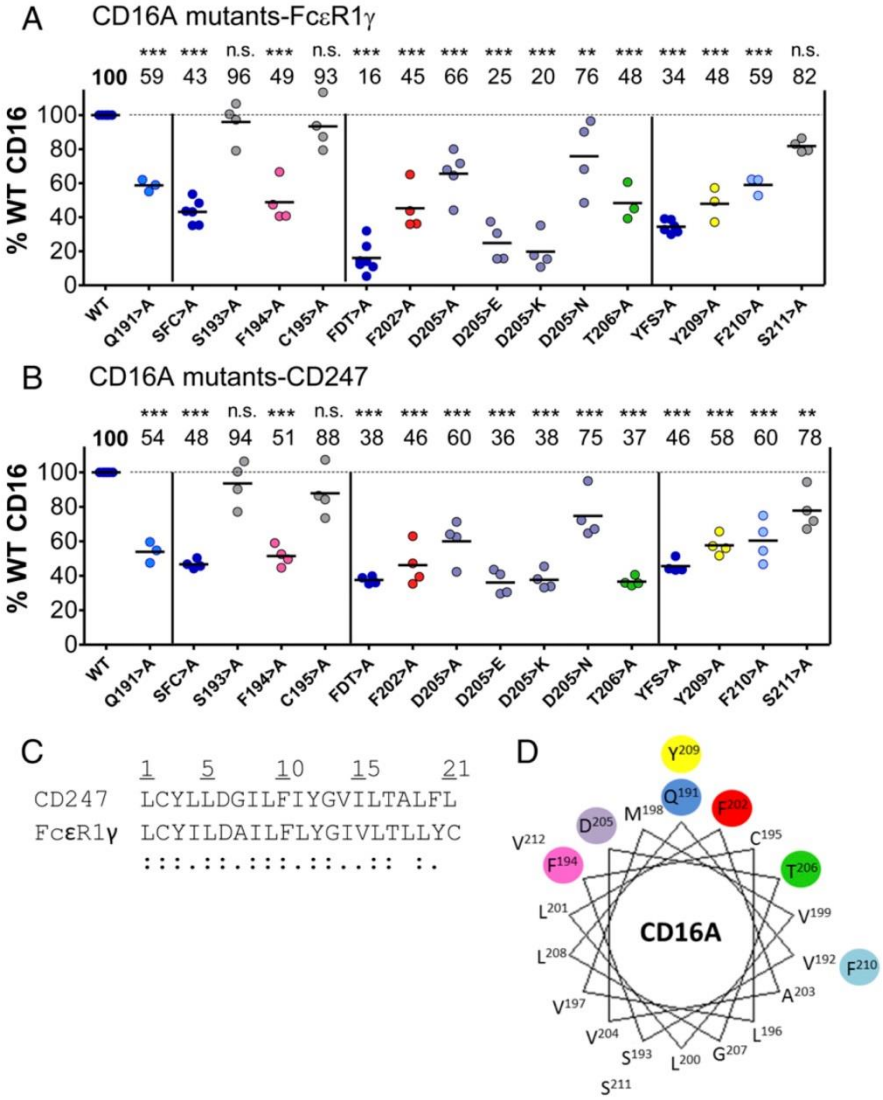

Fig. 3. The CD16A-FcεR1γ TM interface is dominated by polar and aromatic residues. Triple- and single-residue CD16A mutants were tested for association with FcεR1γ (*A*) or CD247 (*B*). Each dot represents an independent experiment where complex formation for WT or the indicated CD16A mutant was quantified. Statistical significance was calculated using one-way ANOVA-Dunnett posttest for multiple comparison (**$P < 0.01$; ***$P < 0.001$; n.s., not statistically significant $P > 0.05$). (*C*) Alignments of the predicted TM domains of FcεR1γ and CD247 showing the similarity between these adaptors. For ease of comparison between the two sequences, which have different extracellular lengths, the sequences have been numbered 1 to 21, beginning with the first TM residue. Double dot (:), fully conserved residue; single dot (.), weak similarity. (*D*) TM residues important for complex association (Q^{191}, F^{194}, F^{202}, D^{205}, T^{206}, Y^{209}, and F^{210}) were highlighted in a helical wheel representation of the predicted CD16A TM domain, showing their localization to the same aspect of CD16A-TM (residues are color-coded to their corresponding data points in *A* and *B*).

and CD247 are mediated by a specific helical face of the CD16A TM domain that is composed of mostly polar and aromatic amino acids.

Analysis of the Interactions Between CD16A and Signaling Adaptors in Live Cells. Although the IVT technique facilitates highly quantitative comparisons of mutants in receptor assembly, it has the drawback that the use of isolated ER microsomes means that only a fraction of the secretory pathway that membrane proteins must traverse to reach the cell surface is present in these experiments. Thus, it was important to analyze the CD16A-signaling adaptor association in live cells. To this end, 293T cells and two NK cell lines, NKL (20) and NK92-MI (21) (that express endogenous FcεR1γ and CD247) (Fig. S3), were transfected with selected TM mutants of CD16A. Flow cytometry analysis of 293T cells transfected with CD16A WT or selected mutants, in the presence of either FcεR1γ or CD247, confirmed that surface expression of the triple mutants $S^{193}F^{194}C^{195}$ > A and $Y^{209}F^{210}S^{211}$ > A was significantly reduced compared with WT receptor (Fig. 4*A*), consistent with the reduced ability of these mutants to associate with either FcεR1γ or CD247 in the IVT experiments (Fig. 3). Surprisingly, however, the $F^{202}D^{205}T^{206}$ > A mutant receptor reached the cell surface, despite being essentially unable to associate with the adaptor molecules in IVT experiments. Subsequent analysis of point mutants showed that substitution of any of the TM amino acids F^{194}, F^{202}, and T^{206} with alanine significantly impaired CD16A expression at the cell surface, supporting the conclusion that these residues contribute to the association with FcεR1γ and CD247. In contrast, the single change D^{205} > A sufficed to permit normal, or increased, levels of CD16A expression at the plasma membrane. Analysis of the NK cell lines NKL and NK92-MI transduced with the same panel of CD16A mutants confirmed these findings (Fig. 4 *B* and *C*) (representative FACS plots are shown in Fig. S3). These data strongly support the conclusion from IVT experiments that the CD16A TM residues F^{194}, F^{202}, and T^{206} mediate important contacts with the adaptor molecules and further indicate that D^{205} markedly influences intracellular retention of CD16A. In these experiments, the CD16A S^{193} > A mutant was also expressed at increased levels on the surface of the NKL and NK92-MI cell lines, but not on 293T cells. The IVT data showed that mutation of this amino acid had no effect on the interaction with signaling adaptor molecules, consistent with its predicted location on the opposite side of the TM helix from the residues that do participate directly in the interaction. It is possible that this increased expression simply reflects an increased ability to reach the cell surface due to the substitution of a nonpolar for a polar amino acid in the TM domain, but this hypothesis does not explain why this effect occurs in NK cell lines, but not 293T cells. Thus, we favor the idea that the S^{193} > A mutation leads to increased expression of CD16A at the cell surface by modulating the association of this receptor with some other molecule expressed in

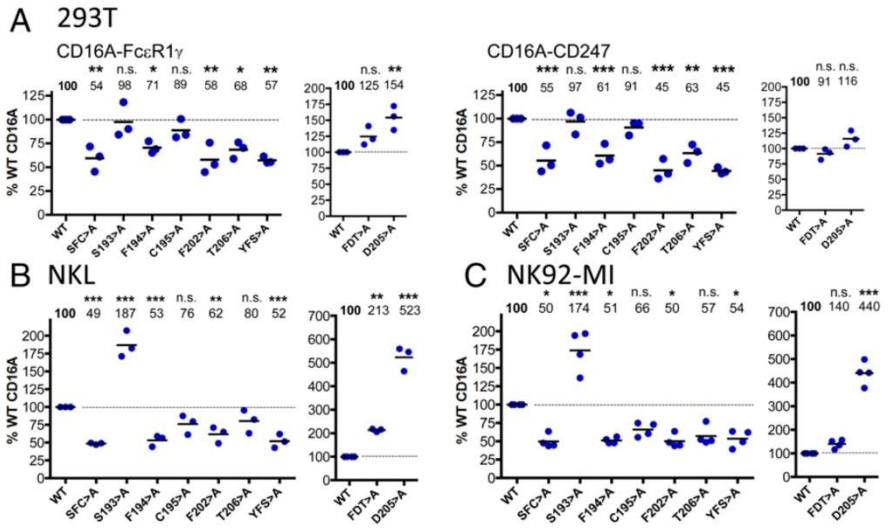

Fig. 4. Analysis of the surface expression of CD16A mutants in live cells. (*A*) The 293T cells were transfected with CD16A combined with either FcεR1γ or CD247. Surface expression of the different mutants was analyzed by flow cytometry, and the data are shown after normalization to WT CD16A. NK cell lines NKL (*B*) and NK92-MI (*C*) were transduced with lentivirus to express CD16A WT or selected mutants, and cell surface expression of these receptors was analyzed by flow cytometry. Representative dot plots of NK cell staining are shown (Fig. S3). Statistical significance was calculated using one-way ANOVA-Dunnett posttest for multiple comparison (*$P < 0.05$; **$P < 0.01$; ***$P < 0.001$; n.s., not statistically significant $P > 0.05$).

lymphoid cells (e.g., CD2) (22), but further experiments will be required to resolve this issue definitively.

The TM Amino Acid D^{205} Regulates Intracellular Trafficking of CD16A. Because CD16A is unable to reach the cell surface in the absence of adaptor modules and is instead degraded, it has been suggested that the association of CD16A with either FcεR1γ or CD247 masks a motif in the CD16A TM domain that might direct protein degradation (16) or retention (23). To test this hypothesis, 293T fibroblasts were transfected with different CD16A TM mutant proteins in the absence of adaptor proteins and analyzed by flow cytometry and Western blot. As previously shown (Fig. 1*A*), in the absence of signaling adaptors, WT CD16A accumulates in the ER, and little to no mature glycosylated species or cell surface expression can be detected (Fig. 5). In these experiments, the $S^{193}F^{194}C^{195}$ > A and $Y^{209}F^{210}S^{211}$ > A mutants behaved comparably with WT CD16A, showing no significant differences in cell surface expression (Fig. 5 *A* and *B*) or total cellular protein levels (Fig. 5 *C* and *D*). In contrast, cells transfected with the $F^{202}D^{205}T^{206}$ > A mutant in the absence of signaling adaptors showed a level of surface expression comparable with WT CD16A coexpressed with FcεR1γ (Fig. 5*A*), and a 3.5-fold increase in levels of both immature and fully glycosylated CD16A protein was detected by Western blot (Fig. 5 *C* and *D*). The CD16A D^{205} > A mutant was also expressed at very high levels on the cell surface, and, again, marked increases in the levels of total CD16A protein were obvious on Western blot analysis (Fig. 5 *E* and *F*). Together with the low surface expression and total cellular protein levels of the F^{202} > A and T^{206} > A mutants, these data confirm that D^{205} is the major TM residue controlling the intracellular retention before eventual degradation of CD16A and support the hypothesis that association with either FcεR1γ or CD247 masks this aspartic acid, facilitating export from the ER and expression at the plasma membrane.

The Influence of TM Residues on CD16A Function. The above data show clearly that the FxxDT sequence element not only critically influenced the association of CD16A with FcεR1γ, but also the intracellular traffic and expression of the receptor at the cell surface. Thus, it was important to address the ability of the $F^{202}D^{205}T^{206}$ > A and D^{205} > A mutants to trigger NK cell activation (degranulation measured by CD107a exposure) after stimulation via CD16A (Fig. 6). These experiments clearly showed that the $F^{202}D^{205}T^{206}$ > A mutant, which is expressed at higher than WT levels at the cell surface, was nonetheless unable to signal for activation, consistent with the impaired association of this receptor with the FcεR1γ and CD247 adaptor molecules observed in IVT experiments (Figs. 2 and 3). In contrast, the D^{205} > A mutant, which retained some ability to interact with adaptors in IVT experiments (Fig. 3), was able to trigger NK cell cytotoxicity. However, despite the roughly fivefold higher surface expression of this mutant compared with WT, NK cell activation via CD16A D^{205} > A was not increased, suggesting that, although the D^{205} > A mutant reaches the surface very efficiently, the association with FcεR1γ and/or CD247 is only partially intact. Overall, these observations strongly support our prior conclusions that the CD16A TM residues F^{202} and T^{206} mediate important contacts with the signaling adaptor molecules. Although D^{205} also contributes to these interactions, the major role of this amino acid seems to be to influence the intracellular trafficking of the receptor.

Structural Model of the Interface Between CD16A and Signaling Adaptors. To gain insight into how the residues identified in our mutagenesis experiments contribute to assembly with CD247 and FcεR1γ, we performed replica exchange molecular dynamics (REMD) simulations in an implicit bilayer model examining possible modes of association of the CD16A TM domain with dimeric signaling adaptors. A 30-aa CD16A fragment encompassing the predicted α-helical TM domain was tested in unrestrained assembly simulations with the previously reported CD247 TM dimer structure (24) (Fig. S4) and with an FcεR1γ dimer modeled on this structure (Fig. 7 *A* and D) (simulation parameters are described in *Materials and Methods*). Cluster analysis of the resulting trimeric models revealed a clearly favored conformation for each simulation in which the polar/aromatic face identified in our mutagenesis screen mediates extensive contacts to the composite surfaces formed by the CD247 (Fig. S4) and FcεR1γ dimers (Fig. 7 *A* and *D*). Of 1,000 structures randomly chosen for analysis from the CD16A-CD247 simulation (Fig. S4), 931 clustered together with only 1.21 Å average root mean square deviation (rmsd) compared with the centroid structure. For CD16A-FcεR1γ (Fig. 7 *A* and *D*), 800/1,000 structures clustered together with an average rmsd of 1.58 Å compared with the centroid structure. The two representative models from these independent simulations were essentially identical, with only 0.61 Å rmsd between the centroid structures.

In the trimeric complex structures, the $F^{202}D^{205}T^{206}$ trio that accounted for the most severe assembly defects in our screen of CD16A mutants forms the central core of the trimeric interface through highly favorable polar and van der Waals contacts. Comparison of the trimeric structures with the previously reported solution NMR structure of the CD247 dimer alone (Fig. S4) showed that one side of a symmetrical tyrosine-threonine hydrogen-bond pair that is essential for CD247 dimer formation (24)

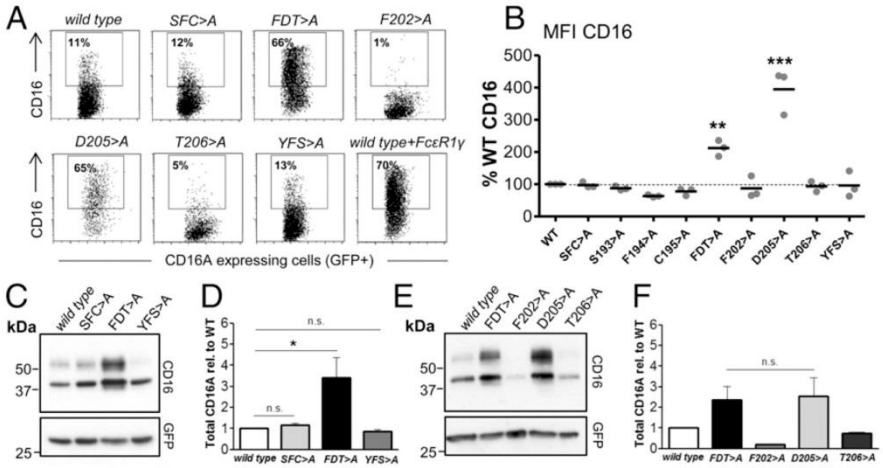

Fig. 5. Analysis of cell surface expression and stability of CD16A mutants in the absence of adaptor protein. The indicated CD16A TM mutants were transfected into 293T fibroblasts in the absence of adaptor protein. Representative dot plots of transfected cells are shown (*A*). Cells expressing CD16A at the cell surface are marked by a square. The mean fluorescence intensity (MFI) of cells expressing CD16A at the cell surface staining (*B*) was analyzed using Kaluza Flow Cytometry Analysis Software. Western blots analyzing total CD16A protein expression (*C* and *E*) was quantified using ImageJ and plotted after normalization to GFP as a control for transfection efficiency (*D* and *F*). Statistical significance was calculated using one-way ANOVA-Dunnett post test for multiple comparison (**P* < 0.05; ***P* < 0.01; ****P* < 0.001; n.s., not statistically significant *P* > 0.05).

rearranges to accommodate favorable contacts to CD16A. The receptor-facing side of the signaling dimer opens to establish two new hydrogen bonds to CD16A (CD247-FcεR1γ T^{17} with CD16A D^{205} and CD247-FcεR1γ Y^{12} with CD16A T^{206}) (Fig. S4 and Fig. 7*D*). CD16A F^{202} contributes to the surface complementarity in this region by occupying a cavity at G^{13} that is present in the interface of both signaling dimers (see surface representations in Fig. S4). Because the "rear" Y^{12}-T^{17} hydrogen bond in the signaling dimer is maintained, these new contacts to CD16A create a "belt" of hydrogen bonds in the lipid bilayer interior that constitutes a major stabilizing feature of the trimeric assembly. Although the relatively mild effect of alanine substitution at D^{205} suggests that loss of this hydrogen bond alone is not sufficient to abrogate assembly, its interior position in the closely packed interface explains why larger side-chains were not tolerated (Fig. 3).

The interactions near the outer (at the top of Fig. 7) and inner (at the bottom of Fig. 7) limits of the membrane also show interfacial contacts involving residues identified in our mutagenesis experiments. CD16A Q^{191} is positioned to make contacts to one of the aspartic acids in the signaling dimer whereas F^{194} also packs closely against the aspartic acid pair, where it may contribute favorable π-electronic interactions (25). Of the two aromatic residues at the bottom of the CD16A TM helix, only Y^{209} contacts the signaling dimer, fitting neatly into a groove between two aliphatic residues one helical turn apart in the signaling dimer (see surface representations in Fig. S4). The detrimental effects of mutations at F^{210}, which faces away from the interface, may be due to a role in stabilizing CD16A membrane insertion, a role commonly ascribed to aromatic residues near the inner leaflet of the lipid bilayer.

CD16A, FcεR1α, and FcγR1 (CD64) Form Similar Interfaces with FcεR1γ. Of the Fc receptors that require assembly with dimeric FcεR1γ (CD16A, FcεR1, FcγR1/CD64, and FcαR1/CD89), only CD89 contains a basic amino acid in its TM domain for assembly. Like CD16A, FcεR1α and CD64 both contain FxxDT-like sequences in their TM domains (FxxDT in FcεR1α and FxxNT in CD64). Given this sequence similarity and others (Fig. 8 *A* and *B*), we sought to determine whether these receptors could form comparable TM interfaces with the signaling adaptor. In independent and unrestrained REMD simulations of assembly with FcεR1γ dimers in a

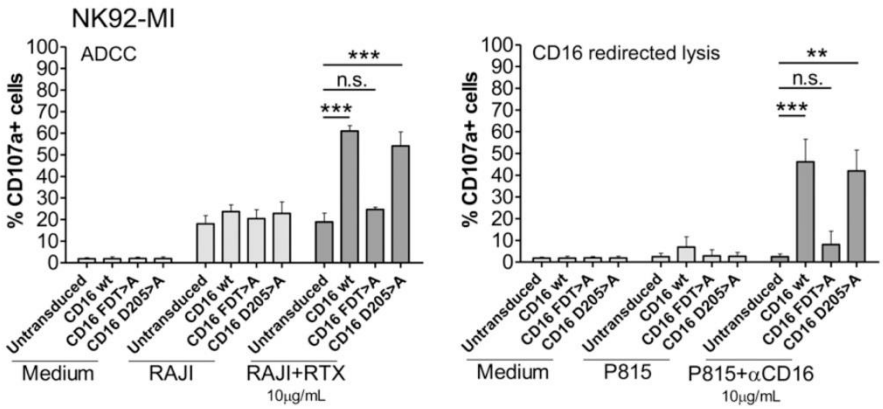

Fig. 6. Functional analysis of FDT > A and D^{205} > A NK92-MI transduced cell lines. NK92-MI cell lines transduced with CD16A WT, FDT > A, or D^{205} > A mutants were functionally tested in ADCC and redirected lysis experiments. NK cells were cultivated alone or in combination with Raji or P815 cell lines loaded, or not, with αCD20 (Rituximab) and CD16-specific mAb (3G8), respectively. After 2-h coculture, CD107a staining was measured by flow cytometry. Data represent mean of three experiments, and statistical significance was calculated using one-way ANOVA-Dunnett posttest for multiple comparison (***P* < 0.01; ****P* < 0.001; n.s., not statistically significant *P* > 0.05).

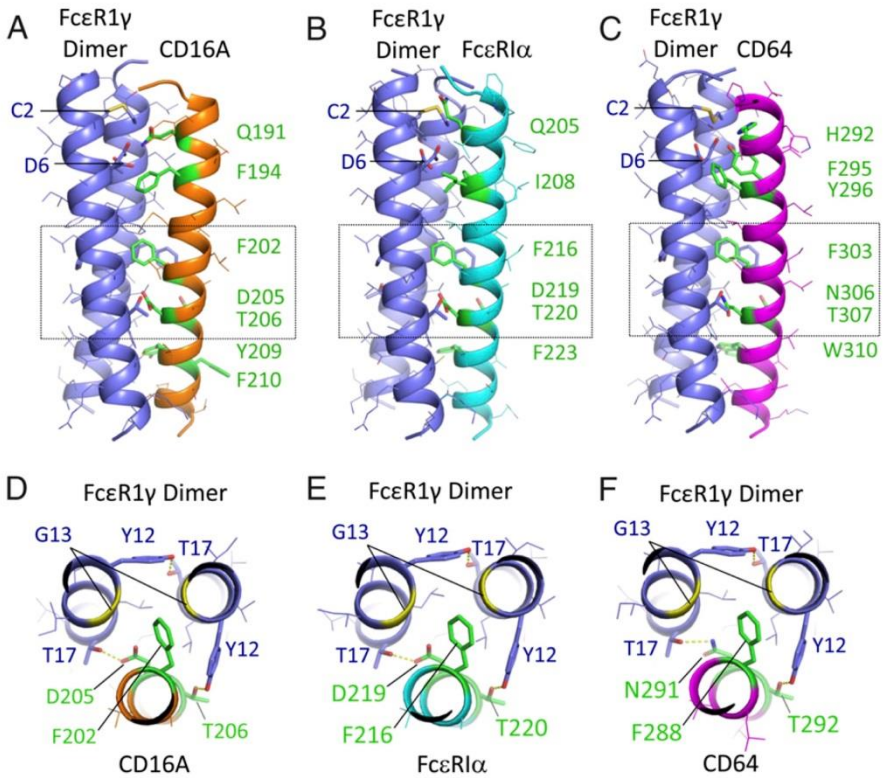

Fig. 7. Structural models of CD16A and related Fc receptors assembled with the FcεR1γ dimeric signaling adaptor. Centroid structures from the dominant cluster are shown for REMD assembly simulations of CD16A (*A* and *D*), FcεR1α (*B* and *E*), and CD64 (*C* and *F*) with FcεR1γ disulphide-linked dimers in model membranes (see *Materials and Methods* for simulation and cluster analysis procedures). FcεR1γ is shown in purple, and receptor TM domains are shown in orange (CD16A), cyan (FcεR1α), or magenta (CD64). Side views (*A*–*C*) are shown with key interface residues in stick representation and colored green in receptor TM domains. The FcεR1γ intermolecular disulphide bond (at C2) and aspartic acid pair (D6) are also indicated. For each model, the boxed region is also shown in a view down the long axis of the trimeric complex (*D*–*F*), highlighting the key features of the proposed core TM packing region. Hydrogen-bonding interactions discussed in the main text are represented by yellow dashed lines. A pair of glycine (G13) residues in FcεR1γ (yellow ribbons) create a cavity that accommodates the phenylalanine side-chain in the core packing motif. All figures were prepared in MacPyMol.

model membrane, both receptor TM domains indeed converged on very similar interfaces to that observed in the CD16A simulations. The models shown in Fig. 7 *B* and *C* represent the majority clusters in each assembly: 726/1,000 FcεR1α-FcεR1γ structures analyzed clustered together with an average rmsd of 1.40 Å compared with the centroid (Fig. 7*B*), and 839/1,000 CD64-FcεR1γ structures clustered together with average rmsd of only 1.10 Å compared with the centroid (Fig. 7*C*). Consistent with sequence differences in the N-terminal regions of the three TM domains, the major contacts to FcεR1γ at the outer membrane limit are variable. FcεR1α has a glutamine in the same position as CD16A Q^{191}, and, although it does not contact the aspartic acid pair in the centroid model shown (Fig. 7*B*), hydrogen bonds to the acidic side-chains are sampled in ~27% of structures in the majority cluster, suggesting that this polar residue may indeed play a similar role to Q^{191} in CD16A. In FcεR1α, an isoleucine (I) takes the place of CD16A F^{194}. In the CD64 model (Fig. 7*C*), the position of CD16A F^{194} is maintained, but neighboring histidine (H) and tyrosine (Y) residues provide the polar contacts to FcεR1γ aspartic acids. At the inner membrane limit (bottom), both receptors contain an aromatic residue in the position of CD16A Y^{209} (F in FcεR1α; W in CD64).

Remarkably, the FxxDT trio in FcεR1α and the FxxNT trio in CD64 established contacts to FcεR1γ dimers essentially identical to those we observed in the CD16A assembly models (Fig. 7 *D*–*F*). The similar role of aspartic acid and asparagine in these assembly models is fully consistent with the outcome of the D^{205} > N mutation in CD16A IVT experiments (Fig. 3), which we found was well-tolerated. These results indicate that Fc receptors without basic TM residues may all assemble based on core TM interactions similar to those we described for CD16A above.

We tested this hypothesis for one of the two additional receptors, FcεR1α, by examining the role of the FxxDT sequence in assembly and surface expression in cells (Fig. 8). Consistent with previous data (26), WT FcεR1α chain was not expressed at the cell surface unless cotransfected with FcεR1γ (Fig. 8 *C* and *D*). The FcεR1α $F^{216}D^{219}T^{220}$ > A triple mutant was unable to reach the cell surface regardless of whether FcεR1γ was coexpressed or not (compare Fig. 8 *C* and *E*). This observation confirms a role for this sequence in assembly but suggests that, unlike CD16A D^{205}, FcεR1α D^{219} does not play a dominant role in intracellular retention. This idea is consistent with previous data (27, 28). A Western blot analysis (Fig. 8*E*) shows that the $F^{216}D^{219}T^{220}$ > A mutant does accumulate intracellular protein to a much greater level than WT FcεR1α although it does not progress through the endocytic pathway and acquire mature glycosylation, suggesting that the D^{219} residue does play some role in regulating the turnover of FcεR1α protein. As in CD16A, substitution of either the F^{216} or T^{220} residues with alanine significantly reduced the ability of cotransfected FcεR1γ to promote receptor expression at the cell surface (Fig. 8*E*), and together these two mutations account for most of the expression defect observed in the triple mutant. These data show that FcεR1α assembles with its signaling adaptor through a similar core TM arrangement as CD16A.

Discussion

A key feature underlying the formation of activating immune receptor complexes is the formation of an interface between the TM

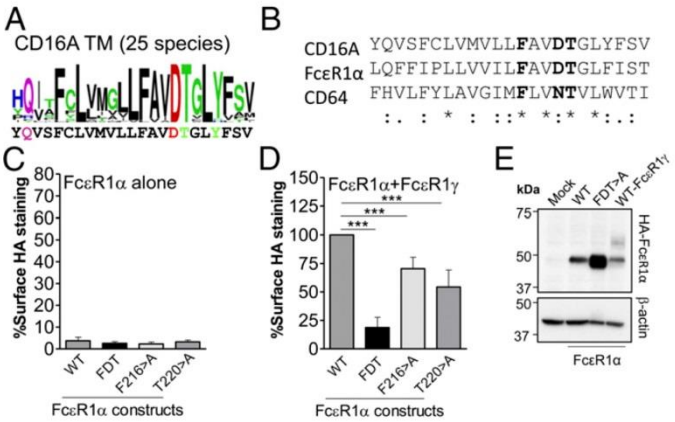

Fig. 8. The FxxDT element in FcεR1α significantly influences association with FcεR1γ and receptor degradation. (*A*) Sequence logo illustrating the degree of amino acid conservation within TM sequences of CD16A and FcεR1α from multiple mammalian species. The height of each letter stack indicates relative conservation at that position whereas the height of each individual letter indicates its relative prevalence at that position. The sequences of human CD16A and FcεR1α are shown below sequence logos for reference. Logo graphics were generated using the WEBLOGO application (weblogo.berkeley.edu). (*B*) Alignment of CD16A, FcεR1α, and CD64 TM sequences showing the conservation of the FxxD/NT sequence. *, conserved residue; double dot (:), strong similarity; single dot (.), weak similarity. WT FcεR1α or selected mutants were transfected into 293T cells alone (*C*) or in combination with FcεR1γ (*D*), and their expression at the cell surface was analyzed by flow cytometry. Data represent mean of three experiments, and statistical significance was calculated using one-way ANOVA-Dunnett posttest for multiple comparison (***$P < 0.001$; n.s., not statistically significant $P > 0.05$). The expression and maturation of FcεR1α WT or the FDT > A mutant in the absence of adaptor molecule was studied using lysates of transfected 293T cells and analyzed by Western blot (*E*).

helix of the ligand-binding receptor subunit and the paired TM helices of the dimeric adaptor module that is crucial for intracellular signaling. In this paper, we have characterized how TM helices can associate to form an activating immunoreceptor complex in the absence of complementary charge potential and have gone on to show that a subset of the residues in the receptor TM domain that mediate association with the adaptor molecules also have a marked influence on the cell biology of the receptor.

Many activating immunoreceptors associate with signaling adaptor molecules via the interaction of a basic amino acid in the TM domain of the receptor with a pair of acidic residues in the TM region of the dimeric signaling module (10). However, our studies of the complex formed between CD16A and the signaling adaptor molecules FcεR1γ and CD247 have revealed that this three-helix interface can also form via interactions between polar and aromatic residues extending over the whole length of the TM domain. In this mode of association, multiple residues located on a single aspect of the receptor TM helix contribute to the interaction with the signaling dimer. These data contrast markedly with receptor complexes such as KIR2DS2–DAP12 and NKG2D–DAP10, wherein a single, properly placed lysine or arginine residue within a polyvaline or polyleucine TM sequence is sufficient for interaction with a pair of aspartic acid residues in the signaling adaptor module and cell surface expression (14). It has been argued that focusing the interaction of signaling adaptor molecules on a single charged residue facilitates the interaction of these adaptors with multiple receptor TM domains with widely varying sequences (14), but our data demonstrate that CD247 and FcεR1γ can also enlarge the repertoire of receptors with which they interact by associating with TM domains in more than one way. Indeed, it could be argued that the mode of interaction of FcεR1γ or CD247 with CD16A might, in evolutionary terms, be more robust because there is no one pair of interacting residues that is absolutely critical and so multiple mutations would have to occur to ablate this association.

Our independent and unbiased REMD simulations are in excellent agreement with the mutagenesis analysis, identifying the polar/aromatic face of the CD16A TM domain as the key assembly surface and reaching nearly identical conformations for assembled CD16A–CD247 and CD16A–FcεR1γ complexes. Similar to the previously published solution NMR structure of the NKG2C–DAP12 trimeric TM complex (29), the receptor TM helix is predicted to bind along an extended groove formed by the interface of the two signaling module α-helices. However, where NKG2C assembly is governed by a single, centrally located lysine residue binding to the paired DxxxT motifs in DAP12, CD16A establishes a more extensive interface, dependent on polar and aromatic residues, with CD247/FcεR1γ that is anchored around the central $F^{202}D^{205}T^{206}$ trio but also has significant contributions at both ends of the helices. Thus, the modeling data strongly support the suggestion from the experimental data that interactions involving specific polar and aromatic residues of CD16A are critical for the association between the receptor and adaptor molecules.

The rearrangement of the previously described CD247 interface (24) to accommodate the new contacts to CD16A is striking in view of the recent report suggesting that CD247 also undergoes a significant structural alteration upon incorporation into the TCR–CD3 complex (30), and this flexibility may be particularly important for the demonstrated ability of both CD247 and FcεR1γ to form stable assemblies with many different receptor TM sequences. Interestingly, despite the apparent interchangeability of human FcεR1γ and CD247, murine CD247 is essentially unable to function in the assembly of either human or mouse CD16A so that, in murine NK cells, only FcεR1γ participates in the assembly of this receptor complex (4). This phenotype has been mapped to an isoleucine for leucine change in murine CD247 (16) at a position that is buried within the trimeric interface formed with the CD16A $F^{202}D^{205}T^{206}$ sequence in our models (Fig. S5). This positioning suggests that the β-branched structure of isoleucine is disruptive to the central intermolecular packing motif, providing a molecular explanation for the inability of murine CD247 to associate with CD16A and additional support for our assembly model.

The observation that CD16A associates equally well with human CD247 and FcεR1γ homodimers, as well as the heterodimer (Fig. 1), is consistent with the convergence of the modeling results. It therefore seems likely that the major factors influencing whether CD16A associates with CD247 or FcεR1γ are related to the relative levels of expression of the different adaptors and possible competition from other receptors that also bind CD247 and FcεR1γ. For example, a population of terminally differentiated human NK cells lose expression of FcεR1γ (31), and, in these cells, CD16A associates exclusively with CD247 (15). In contrast, the majority of circulating human NK cells express both FcεR1γ and CD247, but they also express multiple NK receptors that associate with these adaptor molecules. These receptors show little sequence similarity between their TM domains, and it is possible that they recruit CD247 and FcεR1γ unequally from the pool of available adaptors because an interaction between amino acids of complementary charge in the hydrophobic core of the lipid bilayer could differ in "affinity" from one that depends on interactions involving polar and aromatic residues. It is also possible that the specificity of the interaction could be modulated by steric hindrance between domains of the receptors flanking the TM region (13, 14).

Apart from the mechanism of association of CD16A with FcεR1γ and CD247, the other striking observation emerging from these experiments is that D^{205} within the CD16A TM, unless sequestered within the three-helix interface upon assembly with either FcεR1γ or CD247, promotes intracellular retention of the receptor. It has long been appreciated that the formation of specific polar contacts between TM domain amino acids is a key mechanism to ensure the accurate assembly of multicomponent protein

complexes to be expressed on the cell surface (9, 10) and that, in the absence of these contacts, unassembled subunits and partially formed complexes are retained intracellularly and eventually degraded (32). In the case of the TCR, it is the same charged residues providing the core assembly contacts that mediate this quality-control function. In contrast, we found that CD16A D^{205} makes only a limited contribution to the receptor/adaptor interaction, but its sequestration within the assembly interface seems to act as a quality control mechanism to ensure that only complete receptor complexes can traffic to the cell surface. Thus, in CD16A, the quality-control function has been separated, at least partially, from the assembly function although both are still located in the TM domain. This FxxDT sequence is highly conserved among the predicted TM sequences of CD16A from multiple mammalian species (Fig. 8*A*) and is also present in FcεR1α and CD64 (as FxxNT) (Fig. 8*B*), both of which formed trimeric complexes with FcεR1γ in our assembly simulations that used CD16A-like interfaces (Fig. 7). Indeed, mutation of these residues in FcεR1α caused loss of surface expression and intracellular retention of the receptor, indicating that this sequence also regulates cell-surface expression of FcεR1α, most likely through assembly with FcεR1γ. In contrast to our observations with CD16A, the FDT triple mutant of FcεR1α was not expressed at the cell surface in the absence of adaptor molecules, but the large accumulation of intracellular protein detected by Western blot suggests that mutation of the aspartic acid did indeed protect unassembled FcεR1α protein from degradation. The lack of cell surface expression of this mutant likely reflects the action of ER retention motifs present in the cytoplasmic tail of this receptor that have previously been identified as key elements regulating the trafficking of FcεR1α to the plasma membrane (27, 28).

Overall, these data strongly suggest that the Fxx(D/N)T sequences found in three different Fc receptor TM domains form the core membrane-embedded interaction motifs that drive assembly with signaling adaptor molecules and, at least in a subset of these receptor complexes, regulate receptor protein turnover. Thus, at least two completely different solutions for TM-mediated receptor assembly with CD247/FcεR1γ signaling modules have arisen during evolution, one driven by a single basic TM residue and another based on the more complex polar/aromatic interface described here. These findings may provide more broadly useful insights into the biology of other immune receptors that do not contain charged residues in their TM domains and how they assemble into complexes with signaling adaptor molecules.

Materials and Methods

Transmembrane Domain Mutagenesis. A WT human FcγRIIIA (CD16A) sequence was amplified by PCR and cloned into a modified pSP64 vector (11) for coupling to a streptavidin binding protein (SBP) tag. FcεR1γ was amplified and cloned into a vector bearing an HA tag. The CD247 construct has been described previously (11). Multiple and single amino acid substitutions in CD16A were generated by QuikChange PCR-based mutagenesis. The sequences of the oligonucleotides used for cloning and mutagenesis are shown in Table S1. The integrity of all WT and mutant CD16A, FcεR1γ, and CD247 constructs was verified by sequencing (GATC-Biotech). In some cases, CD16A WT and mutant cDNAs were then subcloned into the lentiviral vector pHRSIN-C56W-UbEM (a gift of Paul Lehner, Cambridge Institute for Medical Research, Cambridge, United Kingdom) to simultaneously express CD16A under the SFFV promoter and the GFP derivative protein, Emerald, under a ubiquitin promoter. A cDNA clone encoding the mature FcεR1α cDNA was amplified by PCR and cloned into the pMX-HA puro vector (a gift of Chiwen Chang, Department of Pathology, University of Cambridge, Cambridge, UK) for expression as an N-terminally HA-tagged protein.

In Vitro Translation Assay. In vitro-transcribed mRNAs encoding all full-length receptor subunits and mutants were pretested for matched translation and ER microsome import. CD16A, FcεR1γ, and CD247 were then cotranslated in the presence of ER microsomes for 30 min at 30 °C before addition of oxidized glutathione (4 mM final concentration) to initiate oxidative folding and assembly. After a further 2-h incubation at 30 °C, the completed assembly reactions were stopped by dilution in 0.5 mL of ice-cold Tris-buffered saline (TBS) (pH 8) containing 10 mM iodoacetamide. The membrane fraction was collected by centrifugation and washed with cold TBS before extraction with 1% digitonin in TBS containing 10 mM iodoacetamide to block disulphide bond formation after extraction and during handling. Lysates were cleared by centrifugation and immunoprecipitated with antibody-coupled agarose beads (4 °C for 2 h). Final products were eluted in SDS, separated on 12% NuPAGE gels (Life Technologies) under nonreducing conditions and transferred to PVDF membranes for phospho-imaging.

Cell Lines. Cells were maintained at 37 °C and 5% CO_2 in a humidified incubator and split as necessary. The 293T cell line was cultivated in Dulbecco's modified Eagle's medium (DMEM) with 10% FCS. NKL and NK92-MI cells were grown in RPMI with 5% FCS, 5% human serum, and 50 U/mL IL-2 (Peprotech). Media were supplemented with 2 mM L-glutamine, 0.1 mM sodium pyruvate, 100 U/mL penicillin, 100 U/mL streptomycin, and 50 μM β-mercaptoethanol. The 293T cells were transfected with plasmids bearing CD16A WT or mutant constructs using the jetPEI transfection reagent. Twenty-four hours after transfection, cells were either lysed or recovered for flow cytometry analysis. Lentiviral transduction was used to express CD16A and mutants in NKL and NK92-MI cell lines.

Lentiviral Gene Transduction. Lentiviruses were generated by transfection of 293T cells with the indicated lentivector together with the plasmids pCMVR8.91 and pMD2G. Two days after transfection, the culture media containing the lentiviruses were harvested, filtered, and stored at −80 °C. For each lentiviral transduction, 0.1×10^6 cells were mixed with 0.75 mL of virus supernatant in the presence of either 1 μM TBK1 inhibitor BX795 (InvivoGen), 8 μg/mL protamine sulfate (Sigma-Aldrich), and 50 U/mL IL-2 (NKL and NK92-MI cells) and seeded in five wells of a 96-well plate (BD Biosciences). The plates were then centrifuged at 120 × *g* for 1 h at 33 °C. After centrifugation, without removing viral supernatants, the plates were incubated at 37 °C, 5% CO_2 for 4 to 6 h and then spun again at 120 × *g* for 1 h at 33 °C. The supernatants were then removed from the wells, and fresh growth medium was added.

Flow Cytometry. Cells were washed and incubated in PBS/0.5% (wt/vol) BSA/1% (vol/vol) FBS/0.1% sodium azide buffer (PBA buffer) and stained using purified CD16A-specific mAb (3G8) or the HA-specific mAb 12CA5, followed by anti-mouse–Ig coupled to PE (phyco-erythrin) (Dako Cytomation) for 30 min at 4 °C. Cells were analyzed using FACSCalibur (BD Biosciences) and Gallios (Beckman Coulter) cytometers. Data were analyzed with FlowJo and Kaluza Flow Cytometry Analysis programs.

Degranulation Assay. For degranulation assays quantifying cell surface CD107a expression, 1×10^5 resting NK92MI cells were washed twice in PBS and added to 2×10^5 target cells in 200 μL of complete medium. Two target cells were used in these antibody-dependent cell-mediated cytotoxicity (ADCC) and redirected cytotoxicity experiments; Raji cells and P815 cells sensitized, or not, with Rituximab or the CD16-specific mAb 3G8, respectively (33). Cells were spun down for 3 min at 100 × *g* and incubated for 2 h at 37 °C in 5% CO_2. The cells were then washed once in ice-cold PBS/2% BSA/2mM EDTA/0.05% sodium azide (PBA) and stained with PE-conjugated anti-CD94 for NK cell gating and APC-conjugated anti-CD107a mAbs for 30 min at 4 °C. The cells were washed, resuspended in PBA, and analyzed by flow cytometry.

Western Blot. Cells were collected, washed once with ice-cold PBS, and lysed in radioimmunoprecipitation assay (RIPA) lysis buffer [50 mM Tris, pH 7.4, 150 mM NaCl, 1% Triton X-100, 1% sodium deoxycholate, and 0.1% SDS with protease inhibitors (1 μM pepstatin A, 1 μM leupeptin)] and 0.5 mM iodoacetamide for at least 30 min on ice. Lysates were centrifuged to pellet insoluble material for 15 min at 4 °C and then quantified; 25 to 30 μg of protein were loaded onto 8 to 12% SDS reducing polyacrylamide gels and electrophoresed, followed by transfer to PVDF (Immobilon-P; Millipore). Membranes were blocked in 5% dried skimmed milk (1 h, 25 °C), washed three times in 0.05% Tween/TBS, and incubated (overnight, 4 °C) in primary antibodies: mouse monoclonal anti-CD16A (clone DJ130c), rabbit polyclonal anti-GFP (both from Santa Cruz Biotechnology), mouse monoclonal anti-β actin (Sigma Aldrich), or 3F10 (HA-specific; Roche) in 0.05% Tween/TBS. Membranes were then washed in 0.05% Tween/TBS (5 min, 2×), and bound antibodies were visualized using goat anti-mouse or goat anti-rabbit secondary reagents (Dako Cytomation) and the ECL-Western Blot Detection Reagent (GE Healthcare). For EndoH treatment, a 25-μg sample was denatured for 10 min at 100 °C and treated with 0.25 units of EndoH enzyme (New England Biolabs) for 1 h at 37 °C and visualized as mentioned before. Western quantification was carried out using ImageJ and normalized against GFP as reporter of transfection efficiency.

TM Assembly Modeling. To model complex structures of CD247-CD16A, FcεR1γ-CD16A, FcεR1γ-FcεR1α, and FcεR1γ-CD64 TM domains, we used the replica exchange molecular dynamics (REMD) simulation method (34). The TM sequences used in this study were DPKLCYLL**D**GILFIYGVILTALFLRVKFS (CD247), EPQLCYIL-**D**AILFLYGIVLTLLYCRLKIQ (FcεR1γ), SPPGYQVSFCLVMVLLFAV**D**TGLYFSVKTN (CD16A), EKYWLQFFIPLLVVILFAV**D**TGLFISTQQQ (FcεR1α), and TPVWF**H**VLFY-LAVGIMFLV**N**TVLWVTIRKE (CD64). We assigned the aspartic acid residues (bold) in CD16A and FcεR1α to the protonated state based on our observation that mutation to asparagine was tolerated and the results of test simulations indicating that the deprotonated state destabilizes CD16A TM in the membrane. The histidine residue in CD64 was protonated at both N atoms based on preliminary simulations where conformations of the complex based on neutral histidine in CD64 did not converge. The CD247 and FcεR1γ homodimers were modeled with one protonated and one deprotonated aspartic acid based on previous simulations indicating that a mixed ionization state is likely in signaling adaptor dimers (35, 36). The solution NMR structure of CD247 TM homodimer (PDB ID code 2HAC) (24) was used to model the initial structure of the FcεR1γ TM homodimer, and an α-helical secondary structure was assumed for the initial state of CD16A TM. The initial configurations were generated by first placing the adaptor TM dimer's *xy*-center of mass (*xy*-COM) at $x = y = 0$ on the *xy*-plane (perpendicular to the membrane normal) and then positioning the CD16A *xy*-COM along a circle of radius 25 Å (every 11.25° for 32 complex systems, each with random rotation along the membrane normal). The initial configurations of FcεR1γ-FcεR1α and FcεR1γ-CD64 TM helices were generated in the same manner.

Using these initial configurations, 60-ns (CD247-CD16A and FcεR1γ-CD16A), 70-ns (FcεR1γ-CD64), and 110-ns (FcεR1γ-FcεR1α) REMD simulations with 32 replicas each in a temperature range of 300 to 750 K were carried out using CHARMM (37). The membrane environment was mimicked by a generalized Born with a simple switching (GBSW) implicit membrane model (38), where we used the default options provided in *Implicit Solvent Modeler* in CHARMM-GUI (39), except with an empirical surface tension coefficient (0.03 kcal·mol^{-1}·Å^{-2}) for the nonpolar solvation contribution. A time-step of 2 fs was used with the SHAKE algorithm (40), and the collision frequency was set as $\gamma = 5$ ps^{-1} for the Langevin dynamics simulation. Weak dihedral restraints ($k = 50$ kcal·mol^{-1}·rad^{-2}) were applied to each TM domain to hold α-helical structure at high-*T* replicas. Replica exchanges were controlled by the REPDSTR module (41) in CHARMM, with exchange attempts at every 1 ps. Conformations during the last 20-ns trajectory at 300 K were sampled every 20 ps (1,000 conformations) and clustered based on (pairwise) rmsd of Cα atoms with a cutoff value of 3.0 Å, where the time interval 20 ps was chosen to balance the number of samples and computational cost.

ACKNOWLEDGMENTS. We thank Dr. Cesar Santiago for helpful advice on design of the mutagenesis strategy; Dr. Mar Valés Gómez for critical reading of the manuscript; Ruth López-Caro, Dr. Mario Mellado, Pilar Lucas, Dr. Laura Martínez-Muñoz, and Dr. Blanca Soler-Palacios for constructive advice and help; and Dr. Gloria Esteso for daily encouragement and support. This work was supported by Ministerio de Economia y Competitividad (MINECO) Grant SAF2014-58752-R (to H.T.R.), MINECO PhD Studentship SVP-2014-068263 (to A.B.-M.), Australian Research Council Future Fellowship FT120100145 (to M.J.C.), Extreme Science and Engineering Discovery Environment Grant MCB070009 (to W.I.), National Science Foundation Grant MCB-1727508 (to W.I.), and National Institutes of Health Grant R01-GM092950 (to W.I.).

1. Ravetch JV, Perussia B (1989) Alternative membrane forms of Fc gamma RIII(CD16) on human natural killer cells and neutrophils: Cell type-specific expression of two genes that differ in single nucleotide substitutions. *J Exp Med* 170:481–497.
2. Hibbs ML, et al. (1989) Mechanisms for regulating expression of membrane isoforms of Fc gamma RIII (CD16). *Science* 246:1608–1611.
3. Lanier LL, Yu G, Phillips JH (1989) Co-association of CD3 zeta with a receptor (CD16) for IgG Fc on human natural killer cells. *Nature* 342:803–805.
4. Kurosaki T, Ravetch JV (1989) A single amino acid in the glycosyl phosphatidylinositol attachment domain determines the membrane topology of Fc gamma RIII. *Nature* 342:805–807.
5. Samelson LE, Patel MD, Weissman AM, Harford JB, Klausner RD (1986) Antigen activation of murine T cells induces tyrosine phosphorylation of a polypeptide associated with the T cell antigen receptor. *Cell* 46:1083–1090.
6. Weissman AM, Samelson LE, Klausner RD (1986) A new subunit of the human T-cell antigen receptor complex. *Nature* 324:480–482.
7. Perez-Montfort R, Kinet JP, Metzger H (1983) A previously unrecognized subunit of the receptor for immunoglobulin E. *Biochemistry* 22:5722–5728.
8. Li X, et al. (2012) The unique cytoplasmic domain of human FcγRIIIA regulates receptor-mediated function. *J Immunol* 189:4284–4294.
9. Ashwell JD, Klusner RD (1990) Genetic and mutational analysis of the T-cell antigen receptor. *Annu Rev Immunol* 8:139–167.
10. Call ME, Wucherpfennig KW (2007) Common themes in the assembly and architecture of activating immune receptors. *Nat Rev Immunol* 7:841–850.
11. Call ME, Pyrdol J, Wiedmann M, Wucherpfennig KW (2002) The organizing principle in the formation of the T cell receptor-CD3 complex. *Cell* 111:967–979.
12. Garrity D, Call ME, Feng J, Wucherpfennig KW (2005) The activating NKG2D receptor assembles in the membrane with two signaling dimers into a hexameric structure. *Proc Natl Acad Sci USA* 102:7641–7646.
13. Feng J, Garrity D, Call ME, Moffett H, Wucherpfennig KW (2005) Convergence on a distinctive assembly mechanism by unrelated families of activating immune receptors. *Immunity* 22:427–438.
14. Feng J, Call ME, Wucherpfennig KW (2006) The assembly of diverse immune receptors is focused on a polar membrane-embedded interaction site. *PLoS Biol* 4:e142.
15. Vales-Gomez M, et al. (2016) Natural killer cell hyporesponsiveness and impaired development in a CD247-deficient patient. *J Allergy Clin Immunol* 137:942–945 e944.
16. Kurosaki T, Gander I, Ravetch JV (1991) A subunit common to an IgG Fc receptor and the T-cell receptor mediates assembly through different interactions. *Proc Natl Acad Sci USA* 88:3837–3841.
17. Johnson RM, Hecht K, Deber CM (2007) Aromatic and cation-pi interactions enhance helix-helix association in a membrane environment. *Biochemistry* 46:9208–9214.
18. Moore DT, Berger BW, DeGrado WF (2008) Protein-protein interactions in the membrane: Sequence, structural, and biological motifs. *Structure* 16:991–1001.
19. Ulmschneider MB, Sansom MS (2001) Amino acid distributions in integral membrane protein structures. *Biochim Biophys Acta* 1512:1–14.
20. Robertson MJ, et al. (1996) Characterization of a cell line, NKL, derived from an aggressive human natural killer cell leukemia. *Exp Hematol* 24:406–415.
21. Tam YK, et al. (1999) Characterization of genetically altered, interleukin 2-independent natural killer cell lines suitable for adoptive cellular immunotherapy. *Hum Gene Ther* 10:1359–1373.
22. Grier JT, et al. (2012) Human immunodeficiency-causing mutation defines CD16 in spontaneous NK cell cytotoxicity. *J Clin Invest* 122:3769–3780.
23. Kim MK, et al. (2003) Fcgamma receptor transmembrane domains: Role in cell surface expression, gamma chain interaction, and phagocytosis. *Blood* 101:4479–4484.
24. Call ME, et al. (2006) The structure of the zetazeta transmembrane dimer reveals features essential for its assembly with the T cell receptor. *Cell* 127:355–368.
25. Philip V, et al. (2011) A survey of aspartate-phenylalanine and glutamate-phenylalanine interactions in the protein data bank: Searching for anion-π pairs. *Biochemistry* 50: 2939–2950.
26. Albrecht B, Woisetschläger M, Robertson MW (2000) Export of the high affinity IgE receptor from the endoplasmic reticulum depends on a glycosylation-mediated quality control mechanism. *J Immunol* 165:5686–5694.
27. Letourneur F, Hennecke S, Démollière C, Cosson P (1995) Steric masking of a dilysine endoplasmic reticulum retention motif during assembly of the human high affinity receptor for immunoglobulin E. *J Cell Biol* 129:971–978.
28. Cauvi DM, Tian X, von Loehneysen K, Robertson MW (2006) Transport of the IgE receptor alpha-chain is controlled by a multicomponent intracellular retention signal. *J Biol Chem* 281:10448–10460.
29. Call ME, Wucherpfennig KW, Chou JJ (2010) The structural basis for intramembrane assembly of an activating immunoreceptor complex. *Nat Immunol* 11:1023–1029.
30. Lee MS, et al. (2015) A mechanical switch couples t cell receptor triggering to the cytoplasmic juxtamembrane regions of CD3ζζ. *Immunity* 43:227–239.
31. Hwang I, et al. (2012) Identification of human NK cells that are deficient for signaling adaptor FcRγ and specialized for antibody-dependent immune functions. *Int Immunol* 24:793–802.
32. Bonifacino JS, Cosson P, Klausner RD (1990) Colocalized transmembrane determinants for ER degradation and subunit assembly explain the intracellular fate of TCR chains. *Cell* 63:503–513.
33. Perussia B, Loza MJ (2000) Assays for antibody-dependent cell-mediated cytotoxicity (ADCC) and reverse ADCC (redirected cytotoxicity) in human natural killer cells. *Methods Mol Biol* 121:179–192.
34. Sugita Y, Okamoto Y (2000) Replica-exchange molecular dynamics method for protein folding. *Chem Phys Lett* 314:141–151.
35. Petruk AA, et al. (2013) The structure of the CD3 ζζ transmembrane dimer in POPC and raft-like lipid bilayer: A molecular dynamics study. *Biochim Biophys Acta* 1828:2637–2645.
36. Knoblich K, et al. (2015) Transmembrane complexes of DAP12 crystallized in lipid membranes provide insights into control of oligomerization in immunoreceptor assembly. *Cell Reports* 11:1184–1192.
37. Brooks BR, et al. (2009) CHARMM: The biomolecular simulation program. *J Comput Chem* 30:1545–1614.
38. Im W, Feig M, Brooks CL, 3rd (2003) An implicit membrane generalized born theory for the study of structure, stability, and interactions of membrane proteins. *Biophys J* 85:2900–2918.
39. Jo S, Kim T, Iyer VG, Im W (2008) CHARMM-GUI: A web-based graphical user interface for CHARMM. *J Comput Chem* 29:1859–1865.
40. Ryckaert J-P, Ciccotti G, Berendsen JC (1977) Numerical integration of the cartesian equations of motion of a system with constraints: Molecular dynamics of n-alkanes. *J Comput Phys* 23:327–341.
41. Woodcock HL, 3rd, et al. (2007) Interfacing Q-Chem and CHARMM to perform QM/MM reaction path calculations. *J Comput Chem* 28:1485–1502.

Supporting Information

Blázquez-Moreno et al. 10.1073/pnas.1706483114

A

CD247 sequence (NM_198053.2)= 6 labelling residues/5 (if signal peptide cleaved)

MKWKALFTAAILQAQLPITEAQSFGLLDPKLCYLLDGILFIYGVILTALFLRVKFSRSADAPAYQQGQNQLYNELN
LGRREEYDVLDKRRGRDPEMGGKPQRRKNPQEGLYNELQKDKMAEAYSEIGMKGERRRGKGHDGLYQGLS
TATKDTYDALHMQALPPR

FcεRIγ (NM_004106.1)= 3 labelling residues/2 (if signal peptide cleaved)

MIPAVVLLLLLVEQAAALGEPQLCYILDAILFLYGIVLTLLYCRLKIQVRKAAITSYEKSDGVYTGLSTRNQETYETL
KHEKPPQ

B

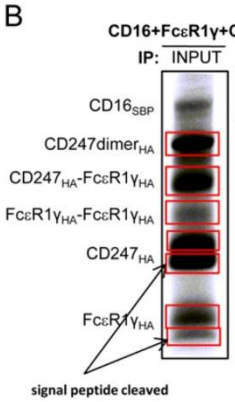

	Signal acquired	Labelled residues	Relative amount	Percentage of total
CD247dimer$_{HA}$	24018368	5	4803673	17
CD247$_{HA}$-FcεR1γ$_{HA}$	15070841	3,5	4305954	16 (8+8)
FcεR1γ$_{HA}$-FcεR1γ$_{HA}$	8939598	2	4469799	16
CD247$_{HA}$	16365740	6	2931022	12
	17585134	5	3273148	12
FcεR1γ$_{HA}$	13806205	3	4602068	17
	5103042	2	2551521	10
		Total	26937185	51% FcεRIγ 49% CD247

Fig. S1. Quantitation of in vitro translations. In vitro-transcribed mRNAs were translated using a methionine- and cysteine-free amino acid mixture supplemented with ^{35}S-labeled amino acids. (*A*) Each protein is labeled to a different level, depending on the protein sequence. In some cases, the signal peptide (underlined) is only partially cleaved, and then an extra Met residue is present in some bands. (*B*) For quantitation, the signal from each band (shown boxed in red) is normalized by dividing the signal acquired by the number of labeled residues (shown in red in *A*) from each protein to obtain the relative amounts of protein. Because the HA and SBP epitope tags are located at the C termini of the proteins, HA immunoprecipitation was used as "INPUT" control to only pull down and quantify full-length translated molecules of FcεR1γ and CD247.

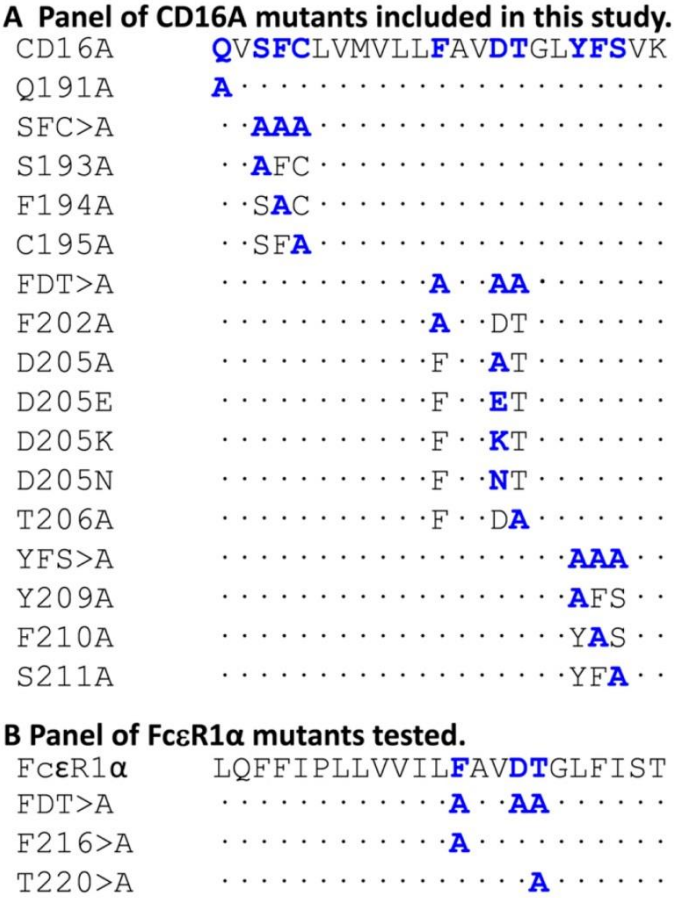

Fig. S2. Panels of CD16A and FcεR1α mutants used in these studies. Shown are alignments of the transmembrane domains of (*A*) CD16A and (*B*) FcεR1α indicating the mutants studied in these experiments. Mutated residues are shown in blue.

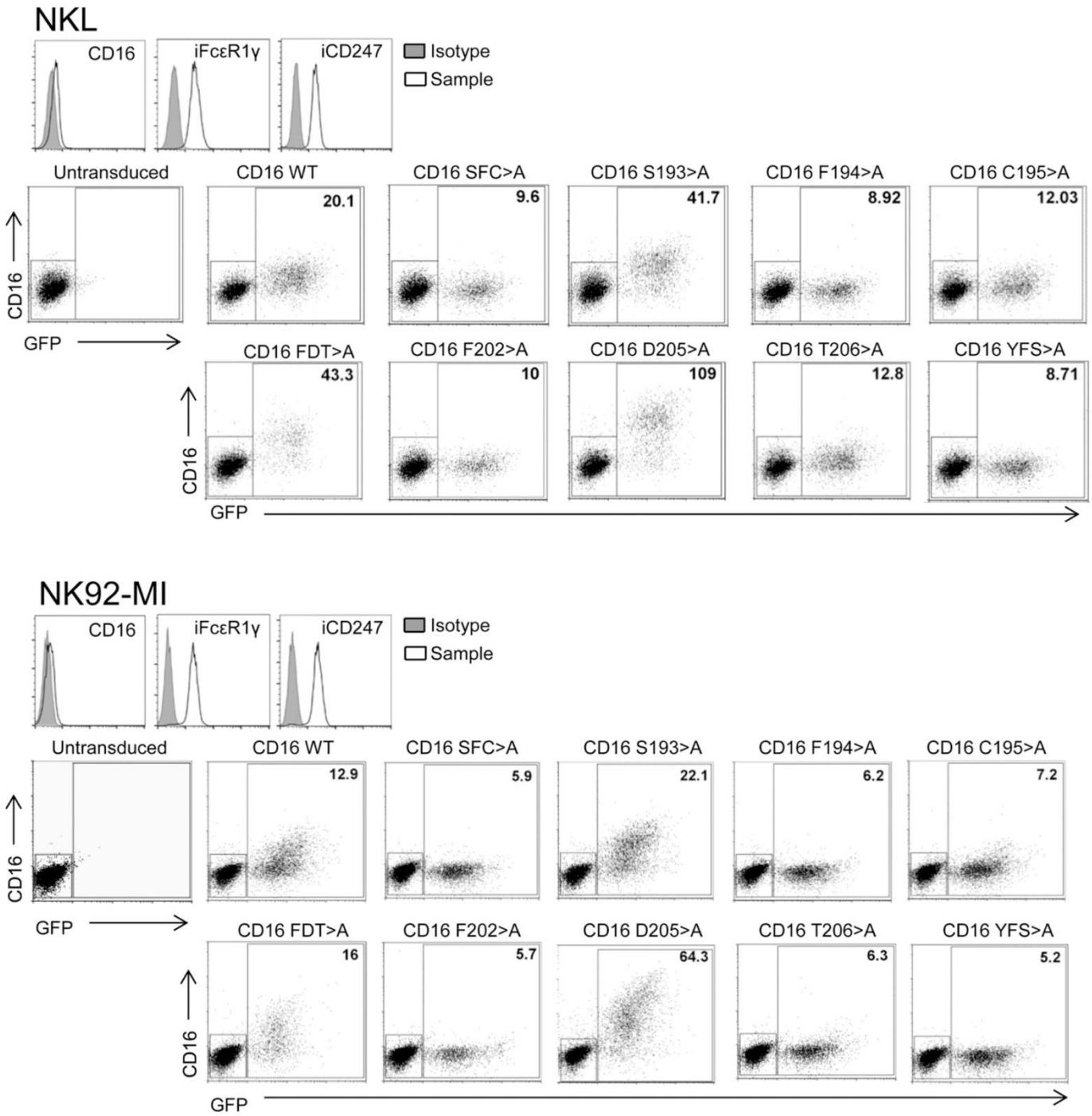

Fig. S3. Representative flow cytometry analyses of the NK cell lines NKL and NK92-MI. Histograms show that FcεR1γ and CD247 are expressed in unmanipulated NK92-MI and NKL cell lines, but CD16A is only present at very low levels on the cell surface. Dot plots show CD16A expression at the cell surface of the NK92-MI and NKL cell lines transduced with either WT CD16A or the indicated mutants. Transduced cells were gated using GFP as marker of the lentiviral-based vector used. The number indicates the MFI of CD16A surface staining in the GFP-positive gate for each transduced cell line.

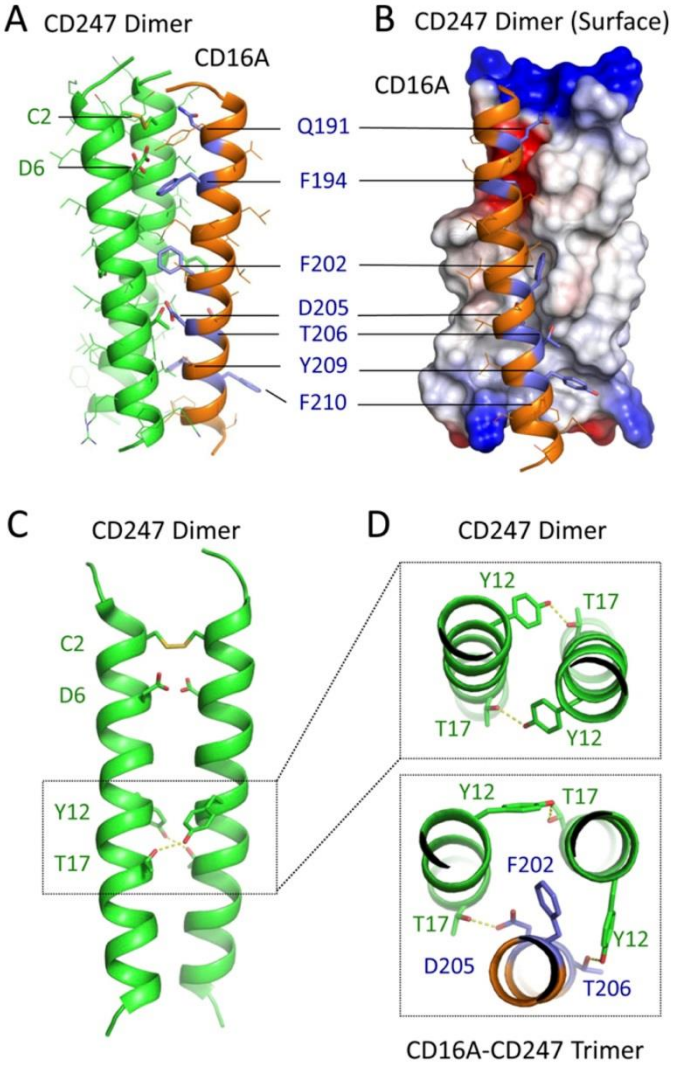

Fig. S4. Model of CD16A assembled with CD247 dimer. The previously reported solution NMR structure of human CD247 dimer (PDB ID code 2HAC) was assembled with a helical model of the human CD16A TM sequence in a 60-ns REMD simulation in a model lipid bilayer as described in *Materials and Methods*. The major cluster contained 800/1,000 randomly chosen models with an average rmsd of 1.58 Å compared with the centroid structure shown here. In the ribbon diagram shown in *A*, CD247 is colored green, and CD16A is colored orange. Key residues are shown as sticks, with residue type and number labeled. Interface residues also identified in the CD16A mutagenesis are colored purple. (*B*) Rotated view of the structure in *A*, with CD247 shown as an electrostatic surface. (*C*) "Front" view of the solution NMR structure of CD247 dimer alone for comparison. Key residues are shown as sticks. (*D*) A view down the long axis of the CD247 dimer (*Top*) and CD247-CD16A trimer (*Bottom*) highlighting the rearrangement of the Y12-T17 hydrogen-bond network to accommodate new contact to CD16A. Colored as in *A*.

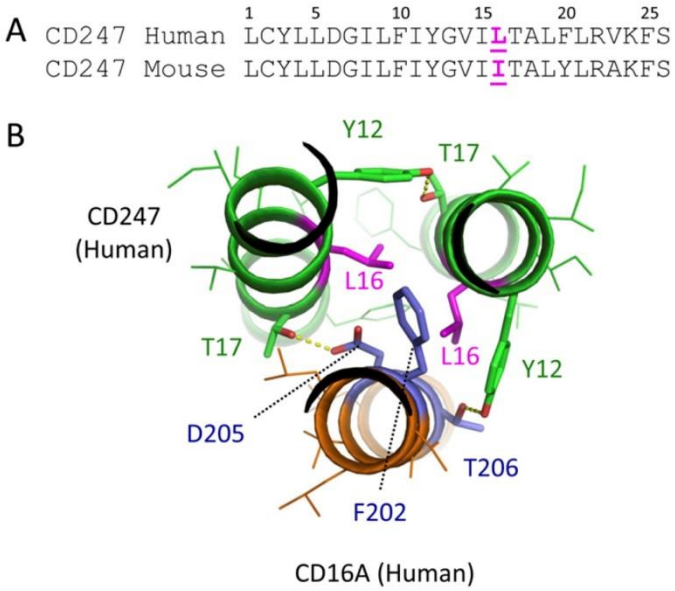

Fig. S5. A single isoleucine residue in the mouse CD247 TM sequence that prevents assembly with CD16A is located in the core TM packing interface. (*A*) Alignment of human and mouse CD247 TM sequence highlighting the position of the variation identified in ref. 16 as blocking association with CD16A (magenta). (*B*) A view down the long axis of the human CD247-CD16A trimer model showing the internal position of L^{16} in the $F^{202}D^{205}T^{206}$ interface. We hypothesize that substitution of leucine with the β-branched side-chain of isoleucine is not well accommodated in the tightly packed interface, leading to defective assembly.

Table S1. Primers used in the preparation of WT and mutant constructs of CD16A, FcεR1γ, and FcεR1α

Primer name	Sequence 5′–3′
CD16A WT cloning For	GCCAAGCTTGCCACCATGTGGCAGCTGCTCCTCCC
CD16A WT cloning Rev	GCCGGATCCTTTGTCTTGAGGGTCCTTTCTC
CD16ATM Q191 > A For	CCTGGGTACGCAGTCTCTTTC
CD16ATM Q191 > A Rev	GAAAGAGACTGCGTACCCAGG
CD16ATM S193 > A For	GTACCAAGTCGCTTTCTGCTT
CD16ATM S193 > A Rev	AAGCAGAAAGCGACTTGGTAC
CD16ATM F194 > A For	CCAAGTCTCTGCCTGCTTGGTG
CD16ATM F194 > A Rev	CACCAAGCAGGCAGAGACTTGG
CD16ATM C195 > A For	AGTCTCTTTCGCCTTGGTGATG
CD16ATM C195 > A Rev	CATCACCAAGGCGAAAGAGACT
CD16ATM F202 > A For	GGTACTCCTTGCTGCAGTGGAC
CD16ATM F202 > A Rev	GTCCACTGCAGCAAGGAGTACC
CD16ATM D205 > A For	TTTGCAGTGGCCACAGGACTA
CD16ATM D205 > A Rev	TAGTCCTGTGGCCACTGCAAA
CD16ATM D205 > E For	TTGCAGTGGAAACAGGACTAT
CD16ATM D205 > E Rev	ATAGTCCTGTTTCCACTGCAA
CD16ATM D205 > K For	TTTTGCAGTGAAGACAGGACTAT
CD16ATM D205 > K Rev	ATAGTCCTGTCTTCACTGCAAAA
CD16ATM D205 > N For	TTTTGCAGTGAACACAGGACT
CD16ATM D205 > N Rev	AGTCCTGTGTTCACTGCAAAA
CD16ATM T206 > A For	CCTTTTTGCAGTGGACGCAGGACTATATTTC
CD16ATM T206 > A Rev	GAAATATAGTCCTGCGTCCACTGCAAAAAGG
CD16ATM Y209 > A For	CACAGGACTAGCTTTCTCTGTG
CD16ATM Y209 > A Rev	CACAGAGAAAGCTAGTCCTGTG
CD16ATM F210 > A For	AGGACTATATGCCTCTGTGAAG
CD16ATM F210 > A Rev	CTTCACAGAGGCATATAGTCCT
CD16ATM S211 > A For	ACTATATTTCGCTGTGAAGAC
CD16ATM S211 > A Rev	GTCTTCACAGCGAAATATAGT
CD16ATM S193F194C195 > A For	CCTGGGTACCAAGTCGCTGCCGCCTTGGTGATGGTACT
CD16ATM S193F194C195 > A Rev	AGTACCATCACCAAGGCGGCAGCGACTTGGTACCCAGG
CD16ATM Y209F210S211 > A For	GTGGACACAGGACTAGCTGCCGCTGTGAAGACAAACA
CD16ATM Y209F210S211 > A Rev	TGTTTGTCTTCACAGCGGCAGCTAGTCCTGTGTCCAC
CD16ATM D205T206 > A For	CTCCTTGCTGCAGTGAAGGCAGGACTATATTTCT
CD16ATM D205T206 > A Rev	AGAAATATAGTCCTGCCTTCACTGCAGCAAGGAG
FcεR1γ WT cloning For	GCCAAFCTTGCCACCATGATTCCAGCAGTGGTCTTGC
FcεR1γ WT cloning Rev	GCCGGATCCCTGTGGTGGTTTCTCATGCTTC
FcεR1α WT cloning For	GCGAATTCGTCCCTCAGAAACCTAAGGTC
FcεR1α WT cloning Rev	GCTGCGGCCGCTAGTTGTTTTTGGGGTTTGGCTTAG
FcεR1αTM F216 > A For	GTGATTCTGGCTGCTGTGGACACAG
FcεR1αTM F216 > A Rev	CTGTGTCCACAGCAGCCAGAATCAC
FcεR1αTM T220 > A For	GCTGTGGACGCAGGATTATTTATC
FcεR1αTM T220 > A Rev	GATAAATAATCCTGCGTCCACAGC
FcεR1αTM D219T220 > A For	CTGCTGTGGCCGCAGGATTATTTATC
FcεR1αTM D219T220 > A Rev	GATAAATAATCCTGCGGCCACAGCAG

For, forward; Rev, reverse.

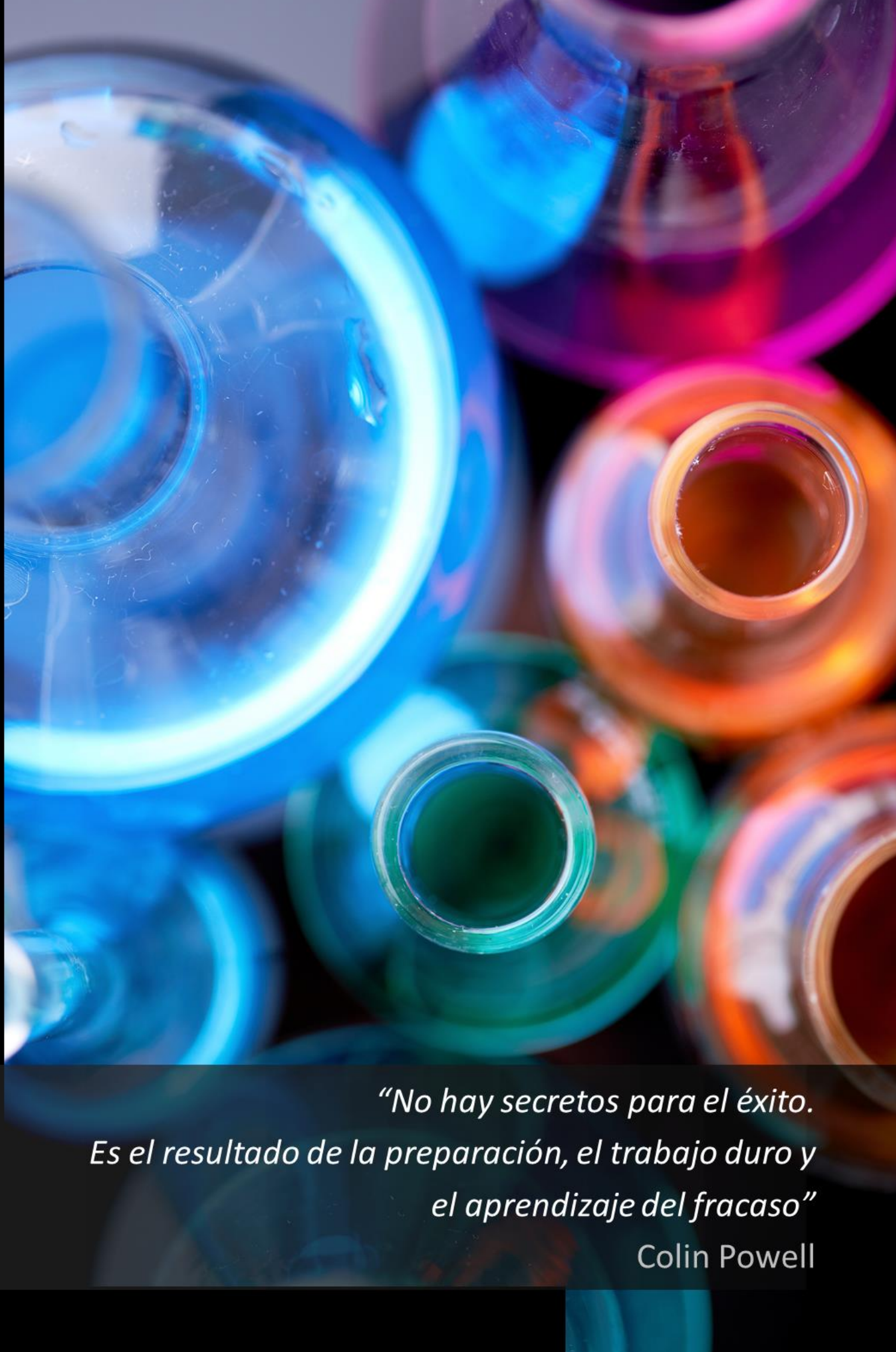

“No hay secretos para el éxito.
Es el resultado de la preparación, el trabajo duro y
el aprendizaje del fracaso”
Colin Powell

UNPUBLISHED DATA

RESULTS

NKp46 AND NKp30 SPLICE VARIANTS PLASMA MEMBRANE EXPRESSION

Given the observations regarding surface expression of the NKp30 and NKp46 NK cell receptors in the CD247 deficient patient; we further investigated the requirements for both receptors to associate with adaptor molecules to reach the plasma membrane in a controlled transfection system *in vitro*.

NKp30 expression was significantly decreased in the CD247 deficient patient and relatives, even in individuals heterozygous for the CD247 inactivating mutation. This observation was surprising since this receptor would be expected to associate with the Fcε1Rγ adaptor molecule to maintain some level of surface expression [222]. Therefore, the levels of NKp30 mRNA expression were assessed. Total levels of NKp30 mRNA were normal (data not shown).

Due to alternative splicing, three isoforms of the NKp30 gene with differences in the cytoplasmic tails are expressed in healthy individuals. Analysis of the expressed repertoire of these variants by RT-qPCR showed that the splice variant NKp30 II/b was the dominant isoform expressed in this family (data not shown). This observation is consistent with previous data showing that the NKp30 II/b isoform is the most frequently expressed in healthy individuals [133].

Transfection of NKp30 isoforms constructs alone showed that the NKp30 I/c and NKp30 III/a isoforms can be stably expressed at the plasma membrane themselves despite the presence of an arginine residue at their transmembrane domain. NKp30 staining was increased when NKp30 III/a was co-transfected with CD247, while no variation was observed for NKp30 I/c when signaling adaptor molecules were co-expressed. In contrast, NKp30 II/b was barely expressed at the cell surface when transfected alone (Figure 4A).

Strikingly, in transient transfection experiments co-expression of the “b” isoform with CD247 led to significantly enhanced levels of cell surface NKp30 compared to co-expression with FcεRγ (Figure 4A). This marked preference of the NKp30 II/b isoform to associate with CD247 rather than Fcε1Rγ explains the marked loss of NKp30 expression by the NK cells of family members with either partial or complete loss of CD247 expression.

In contrast to the observations made for the isoform I/c and III/a, where the presence of arginine residue at the plasma membrane did not seem to affect stable expression at the cell surface; the NKp30 II/b transmembrane arginine residues was important since a leucine for arginine substitution allowed receptor surface expression (Figure 4B), indicating that the exposure of this charged residue at NKp30 II/b interfered with membrane localization.

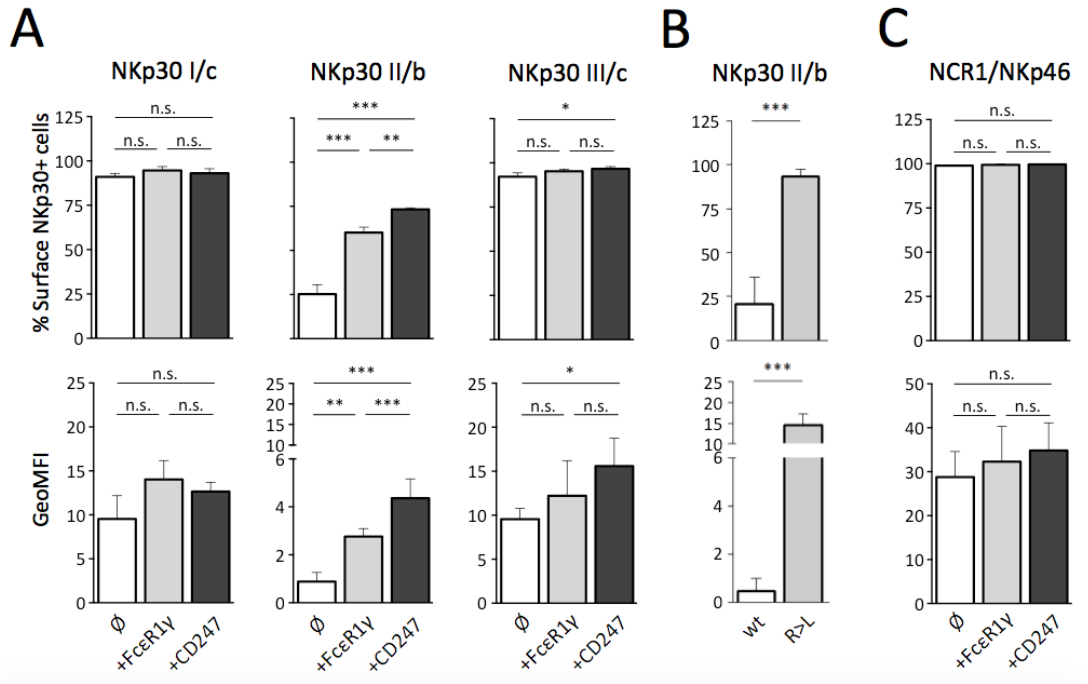

Figure 4: NKp46 and NKp30 splice variants association with signaling adaptor molecules: 293T cells were transiently transfected with the indicated combination of plasmids and then analysed by flow cytometry for receptor cell surface expression. The percentage of cells expressing NKp30 or NKp46 on cell surface and the geometric mean fluorescence intensity of staining are shown. Data represent the mean ± SD of at least three independent experiments. Statistical significance was determined using one-way ANOVA-Tukey´s multiple comparison test (*, P<0.05; **, P<0.01; ***, P<0.001).

NKp46 expression on NK cells was comparable in all the patients, independent of their genotypes; suggesting that CD247 was not required for surface expression of NKp46. In agreement with this observation, transfection of 293T cells also showed that NKp46 was able to reach the plasma membrane alone, independently of either signaling adaptor molecule (Figure 4C), and no increase was observed when co-transfected with either Fcε1Rγ or CD247. This result is consistent with the observation that transfection of an NKp46 cDNA, in the absence of any adaptor molecule, was sufficient for surface expression of the NKp46 protein [223], even though NKp46, like CD16A, has been reported to associate with both CD247 and Fcε1Rγ [223].

MATERIALS AND METHODS

Cell lines

The 293T cell line was maintained at 37°C and 5% CO2 in a humidified incubator and split as necessary and cultivated in Dulbecco´s Modified Eagle medium (DMEM) with 10% foetal calf serum (FCS). Media were supplemented with 2 mM L-Glutamine, 0.1 mM sodium pyruvate, 100 U/mL penicillin, 100 U/mL streptomycin.

Construct generation

cDNA clones corresponding to each NKp30 isoform as well as NKp46 were amplified by PCR using specific pairs of primers and cloned into the pEGFPN1 vector (Clontech) to be expressed as a fusion with EGFP. Full length cDNA clones of CD247 and FcεR1γ were amplified by PCR and then cloned into the pHRSin expression vector [219]. The integrity of all plasmids was verified by sequence analysis. The arginine to leucine mutation at NKp30 II/b transmembrane domain was generated by PCR.

Table 2: List of primers used for construct generation.

Gene	Primer 5´→ 3´
NKp30 I/c	F: TTTCCTCCATGACCACCGG R: TTCCCATGTGACAGTGGCATT
NKp30 II/b	F: TTTCCTCCATGACCACCGG R: CGGAGAGAGTAGATTTGGCATATT
NKp30 II/b R>L mutant	F: GTCCTCCTCCTTCTGGCTGGATTCTATG R: CATAGAATCCAGCCAGAAGGAGGAGGAC
NKp30 III/a	F: TTTCCTCCATGACCACCGG R: GGACCTTTCCAGGTCAGACATT
NKp46	F: GCCAAGCTTGCCACCATGTCTTC R: GCGGTACCCCAAGAGTCTGTGTG
CD247	F: GCCAAGCTTGCCACCATGAAGTGGAAGGCGCTTTTC R: GCGGTACCCGAGGGGGCAGGGCCTG
FcεR1γ	F: GGGGATCCAGAACGGCCCGATCTCCAG R: GATCGCGGCCGCGAGTCCAGTCCATGGCAGTT

Transient transfection

10^5 293T cells were transfected with a plasmid driving receptor expression in the presence or absence of plasmids encoding the Fcε1Rγ or CD247 signaling adaptor molecules using the jetPEI® transfection reagent. 24 hours after transfection, cells were harvested and cell surface receptor expression was evaluated by flow cytometry.

Flow cytometry

293T cells were harvested, washed and incubated in PBS/0.5% (w/v) bovine serum albumin/1% (v/v) foetal bovine serum/0.1% sodium azide buffer (PBA buffer) and stained using purified NKp30 (R&D, MAB1849) or NKp46 (R&D, MAB1850) specific mAbs, followed by anti-mouse-Ig coupled to PE (Dako Cytomation) for 30 min at 4ºC. Cells were analysed using FACSCalibur (BD Biosciences) cytometer. Data were analysed with FlowJo and Kaluza Flow Cytometry Analysis programs.

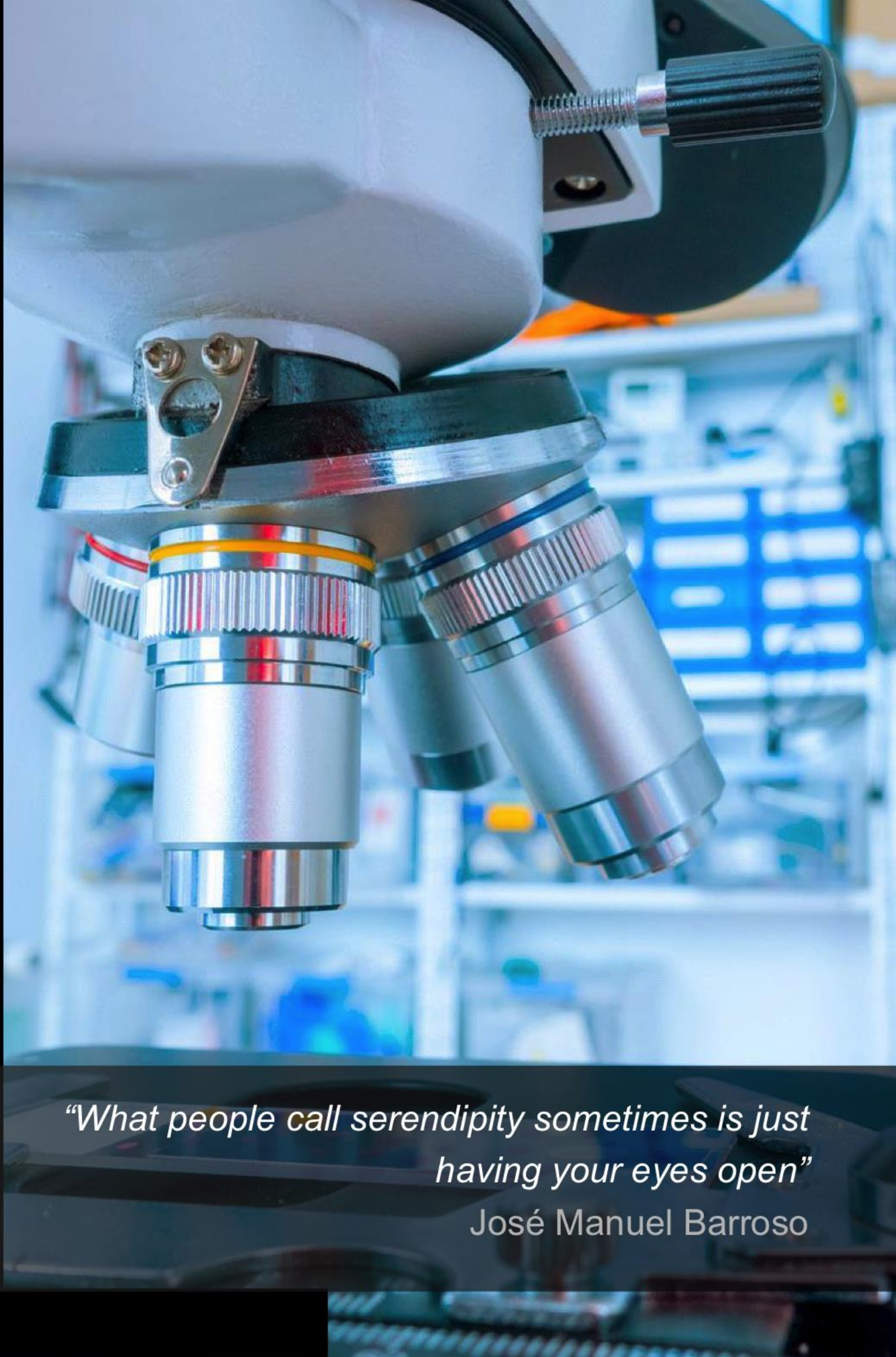

“What people call serendipity sometimes is just having your eyes open”

José Manuel Barroso

DISCUSSION

Primary immunodeficiencies are a diverse group of rare diseases affecting the immune system. They are generally single gene disorders, either inherited or due to *de novo* mutations during embryogenesis, that affect specific components of the immune system. Detailed analysis of samples from these patients provides a unique opportunity to study the consequences of the lack of a single protein in human immune biology [6]. In particular, CD247 deficiency is an extremely rare disease and the identification and characterisation of this new case has stimulated detailed evaluation, and re-evaluation, of several aspects of the biology of this key signaling adaptor molecule in the human immune system.

CD247 DEFICIENCY: IMMUNE SYSTEM ALTERATIONS

To date, three patients with mutations affecting the function of CD247 have been described. In the first two patients, T cell alterations were analysed in detail, but little work was done on the NK cells from these patients. Therefore, the key objective of the experiments done on the third patient was to analyse in detail the effects of the lack of CD247 on NK cells.

Analyses of **surface expression of a panel of NK cell receptors** revealed dramatic decreases in CD16A and NKp30 expression at the cell surface. This observation was expected because these receptors are known to associate with CD247 [56, 222, 224]. Interestingly, however, surface expression of another CD247-associated receptor, NKp46 [223], did not vary in the absence of this signaling molecule. Subsequent *in vitro* experiments revealed that this surprising result was because NKp46 is able to reach the cell surface even in the absence of signaling adapter molecules despite the presence of an exposed arginine residue. As expected, membrane expression of the 2B4 receptor that does not associate with CD247 did not differ between patient and controls. Several splice variants of NKp30 have been described [132] and qPCR analysis of NKp30 isoform expression in the CD247-deficient patient showed that NKp30b was the dominant isoform expressed *in vivo* in this individual. *In vitro* experiments involving transfection of specific NK cell receptors, alone or in combination with adaptor molecules, corroborated that NKp30b and CD16A have to complex with the signaling modules to be stably expressed at the cell surface. In contrast, NKp46, NKp30a and NKp30c did not require association with

adaptor molecules to be expressed at the plasma membrane.

NKp30 splice variants are highly similar and only differ in their cytoplasmic tail sequence. Further experiments studying cytoplasmic tail mutants of each NKp30 isoform showed that these sequences limit or favour membrane expression (data not shown, in preparation). In the case of NKp30 II/b, an arginine to leucine mutation in the transmembrane domain made this receptor independent of adaptor molecule association for cell surface expression, indicating that this charged residue also controls membrane stability and has to be shielded for expression at the cell surface. Therefore, *in vitro* experiments and analyses of CD247 deficient NK cells indicate that membrane targeting and localization of NK cell receptors are tightly regulated by transmembrane and cytosolic determinants specific for each particular receptor.

In functional experiments, **NK cell function** after ligation of specific receptors was also evaluated and showed that CD247-partner receptors driven function was compromised in a genotype-dependent manner. Surprisingly, the response of the NK cell receptor 2B4 that does not signal through CD247 was also impaired, suggesting that patient NK cells are hyporesponsive, likely due to alterations in maturation process.

Since the *in vitro* transfection and IVT experiments showed that CD16A had no clear **signaling module preference**, associating equally well with either FcεR1γ or CD247 [218], it was expected that membrane expression should be maintained with FcεR1γ even in the absence of CD247, but that was not the case. This result may indicate that FcεR1γ is preferentially recruited by other receptors or simply that FcεR1γ expression is insufficient to sustain membrane expression of CD16, NKp30 II/b and NKp46. It has previously been shown that FcεR1γ protein abundance, even in NK cells from healthy individuals, is limited compared to CD247 [225].

Similarly, in all of the CD247 deficient patients reported, the absence of such a key adaptor molecule also caused **severe defects in T cell receptor expression** at the cell surface. Indeed, T cell receptor stimulated responses, analysed in either primary or immortalised T cells, such as proliferation, signaling cascade protein phosphorylation, activation markers, etc., were markedly impaired [26-28], even though the CD3γδε subunits still provide four ITAM motifs to the TCR complex. Thus the functional impairment is due to the key role of CD247 in TCR assembly, essential for membrane

expression, and not to the partial loss of ITAM signaling within the complex.

Hematopoietic lineages and cellular differentiation have been widely studied in mice. However, for obvious reasons, much less is known about cellular development and differentiation in humans. CD247 has been shown to play a key role in T cell development and education in thymus [41], thus the opportunity to analyse NK cells from a CD247 deficient patient provided an opportunity to study the **effect of the absence of CD247 on NK cell development.** The analysis of peripheral blood NK cells in the CD247 deficient patient revealed an alteration in the normal distribution of circulating $CD56^{bright}$ and $CD56^{dim}$ NK cell populations so that the proportion of $CD56^{bright}$ NK cells was increased. However, this increase in circulating $CD56^{bright}$ NK cells was noted not only in the CD247 deficient patient, but also in all the CD3 deficient patients examined, and was statistically significant even after removal of an outlier sample. Thus these data suggest that the increased frequency of $CD56^{bright}$ NK cells circulating in the peripheral blood of these immunodeficient patients is related to the absence of fully functional T cells in these individuals rather than a specific defect in CD247 function. Interestingly, a marked increase in the frequency of $CD56^{bright}$ NK cells was also reported to be a feature of a case of X-linked severe combined immunodeficiency, secondary to a γc defect, with Omenn syndrome-like symptoms [226].

It is fascinating how a T cell compartment defect [28] has an indirect effect on NK cells. Indeed, it seems probable that all immunodeficiencies causing TCR defects will affect the **contribution of T cells to NK cell growth, maturation and development**. IL2 has been reported to be produced mainly by CD4 T cells, allowing lymphocyte proliferation [227]. The addition of recombinant IL2 to mixed lymphocyte cultures for NK cell expansion rescues NK cell growth and expansion [57], which corroborates the importance of a fully functional T cell compartment able to secrete IL2 for proper NK cell development, maturation and responsiveness.

Finally, alterations in CD247 protein expression have been reported in other, different contexts. Populations of T cells that have lost CD247 expression can be found in systemic lupus erythematosus (SLE), rheumatoid arthritis, cancer, and infectious diseases [228-231]. In contrast, it has been recently described that CD247 protein is upregulated in leukaemia patients [232, 233] with increased T cell response and

cytokine production by T cells, that lead to inflammation [234]. However, the consequences of the somatic appearance of a population that lack CD247 are completely different compared to an inherited CD247 defect that inhibits T cell repertoire formation and enhances susceptibility to infection since birth.

SPONTANEOUS REVERSION OF PATIENT CD247 MUTATION

It has been known for many years that the mutation rate varies across the genome [235]. Variation in mutation rate has not only clear implications for evolutionary biology, but also underexplored implications for our understanding of hereditary diseases and cancer.

***De novo* mutations** have been widely shown to be a major cause of severe early-onset genetic disorders such as intellectual disability, autism spectrum disorder, and other developmental diseases. However, when genetic defects are inherited, *de novo* mutation phenomena can also, albeit infrequently, provoke the opposite effect; *ie.* spontaneous mutations can generate a nucleotide change at the same position as the genetic defect and so revert the inherited mutation.

The occurrence of *de novo* mutations can be related to cell-specific properties. Mutational hotspots for genomic rearrangements are largely determined by the underlying genomic architecture associated with chromatin state, transcriptional status, and gene expression levels. Briefly, areas with open chromatin, high replication transitions, and high frequencies of CpG dinucleotides have been shown to be more likely to display elevated mutability. Thus, it can be expected that the higher the intrinsic mutation rate, the more likely a locus is to have a genetic defect, but also reversion.

The **molecular bases and factors influencing *de novo* mutations** have been widely studied by different approaches and models. Some of the explanations of variation patterns have clear mechanistic bases, but much of the rate variation remains unexplained.

The analysis of non-coding DNA, such as the CpG islands, has been shown to affect genetic variation rates in mammals, with up to 15 fold increase over normal variation rate [236-239], mainly because of uncorrected C to T transitions after the deamination of methylated cytosine bases (which are unstable) to thymidine [240]. Indeed, we observed a higher frequency of these dinucleotides in genes where

individuals with defect reversion have been reported.

Genome transcription levels and packaging have also been described to affect mutation rate since DNA becomes more exposed as it becomes unwound from the nucleosomes and as it becomes single stranded [241]. However, this area is somewhat controversial. Some studies support the idea that transcriptionally active DNA will be more prone to nucleotide mistakes during DNA replication so giving rise to *de novo* mutations as a result of the erroneous incorporation of nucleotides by DNA polymerases [242], and escape of proofreading function of polymerase subunit or either restoration by the mismatch repair pathway (MMR) [243]. Transcriptionally active DNA can be also more exposed to potential mutagens. On the other hand, transcriptionally active regions may be repaired at higher rates than inactive parts of the genome, and proliferating cells may display higher repair activities than quiescent cells. This might arise from a tight coupling of the repair process with both transcription and replication, all these processes taking place on the nuclear matrix. Repair activities differ greatly among species, and there is a good correlation between life span and repair among mammals. It is predicted that genes that are transcriptionally active in germ-cell lineages have a lower mutation rate than bulk DNA, a circumstance that is expected to be reflected in evolution [244]. It is not clear whether CD247 transcription levels during T and NK cell differentiation may have an effect on mutation rate affecting our particular case of CD247 deficiency. Synthesis of CD247 is known to be the rate-limiting component of T cell receptor complex assembly, but how this relates to transcription of CD247 in T cells is unclear. When CD247 transcripts from healthy controls were cloned and sequenced, a high variation compared to consensus sequence and other genes localized in the same chromosome was observed. Moreover, this phenomenon seemed specific to CD247, as such variation was not a feature of other CD3 gene transcripts even in patients suffering deficiencies affecting these CD3 genes.

Although the molecular basis of the putative mutability of CD247 is unknown it is interesting to note that the CD247 gene has been reported to display a particular pattern of polymorphism so that while most SNPs in the human genome are biallelic; some genes, including CD247, have triallelic SNPs. The factors underlying this phenomenon are not clear, but it has been suggested that in these genes the

occurrence of one mutation can induce the simultaneous production of two new mutations within the same individual on the same genetic background [245], which support the idea of a high mutational state for CD247 and so an elevated possibility of CD247 deficient patients to revert their gene defects.

The process by which **newly synthesized proteins** are efficiently targeted to the translocation machinery of the endoplasmic reticulum (ER) is presumed to begin with the emergence from the ribosome of a signal sequence. Typically, signal sequences are cleaved from the protein during or immediately after translocation to the ER lumen. Therefore, changes such as additions or deletions that may affect the signal cleavage site can influence the interaction of newly transcribed molecules with various components of the ER translocation system [246]. Actually, that mRNAs possess sequences that alter protein translation was postulated some time ago [247].

In eukaryotic cells, the synthesis of membrane proteins destined for the plasma membrane, ER or any other membrane-bound compartment begins on cytosolic ribosomes. After a short segment of protein has been synthesized, the ribosome, mRNA and nascent protein chain associate with the ER, where the rest of the protein is made and simultaneously inserted into the membrane. This phenomenon was first characterised by Günter Blobel, David Sabatini and Bernhard Dobberstein in the 1970s. These scientists proposed that there is a binding factor, lately called N terminal signal sequence, that recognizes the emerging protein chain and can dock the ribosome at the ER membrane [247].

Analysis of the **most frequent somatic mutation found in revertant T cells** from this new patient showed that this variant compensated for the loss of the normal initiation codon by a point mutation 3 codons upstream that created a new ATG codon and lengthened the signal peptide by three amino acids (Asp-Lys-Thr). Some signal peptide-prediction programs (SOSUIsignal) indicated that this new sequence would function as a signal peptide, while others (SignalP-4.1) suggested that this longer sequence would not be an efficient signal peptide. Transfection of Ma5.8 cells with wild-type CD247 and the mutant showed that the mutant could restore surface TCR expression, but less efficiently than wild-type CD247 (Figure 5), consistent with a possible lower efficiency of mutant CD247 protein translocation into the ER. Here it is interesting to note that previous analyses of revertant T cells in CD247 deficient

patients had shown that although these T cells had recovered TCR expression, they were still not fully functional in that phosphorylation of ZAP70 after TCR stimulation was defective [26]. Interestingly, analysis of Ma5.8 cells transduced to express the essentially TM-only domain of CD247 described by Rieux-Laucat *et al*, also led to restoration of cell surface TCR expression (data not shown), but again at lower levels than those achieved by expression of the wild-type CD247 molecule. This observation is striking, because the patient in whom this mutation was identified suffered a marked T-lymphopaenia [26], thus these data suggest that the failure to detect circulating CD3 positive T cells in this patient is due to a defect in signaling, possibly at thymus selection state, rather than simply a defect in assembly and expression of the TCR complex.

These data also emphasise that mutations in different locations of CD247 can produce very different consequences depending on the role and function of the specific protein segment affected. In fact, it has been previously reported that there are functional differences even between closely related regions of the CD247 molecule [248].

Finally, it is important to highlight that **the possibilities of detecting genetic reversion events that repair gene defects depends on the selective advantage** of the gain of function after reconstitution in revertant cells (Figure 5). This determines *in vivo* expansion, that, in turn, depends on the magnitude and importance of the particular gene function affected initially, but in some cases (eg WAS) can lead to disease “cure”.

In fact, a closer look at the genes where reversion has been described, showed that many genes within this group are key for immune development and host defence, such as IL2RG, CD247, RAG, etc. It is possible that there may be more PID in which reversion events take place but that these have not been detected due to their particular effect on cell surveillance, proliferation or function and thus clinical detection. For example, the CD40 ligand gene affected in Hyper-IgM syndrome shows a high mutation rate, but no reversion events have been described even though more than one hundred patients have been described. However for this reversion to be visible it would have to occur in a follicular dendritic cell that interacts with a B cell

that makes an antibody that is potently selected for *in vivo*, despite the IVIG treatment that is generally given to these patients. It's obvious that it's much more unlikely that any such reversion event would be detected compared to a mutation that directly affects the ability of a given lymphocyte to expand.

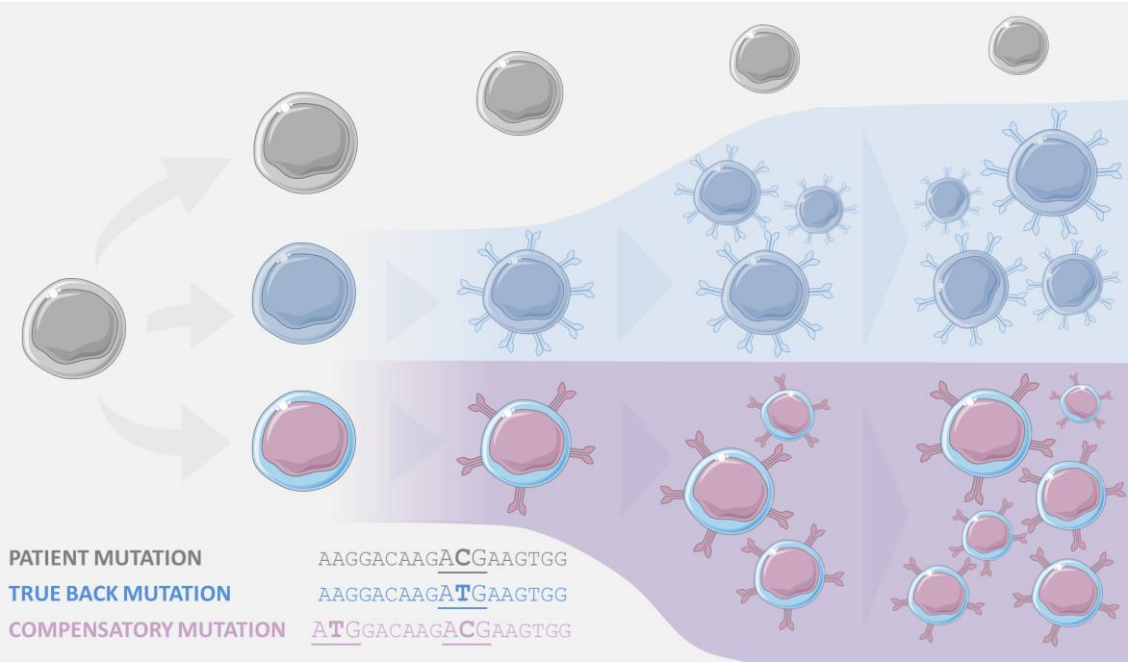

Figure 5: Illustration of the proliferation and gain of functionality of revertant T cells: Schematic representation of the consequences of the different CD247 gene reversion in contrast to mutant cells fate. Cells are colour-matched with CD247 sequences. Patient mutation affects CD247 initiation codon and avoids protein expression. Patient CD247 gene reverts due to a true back mutation and a compensatory mutation; both of which allow TCR assembly and surface expression, though compensatory mutant cells had lower levels of TCR at the cell surface. Revertants selective advantage triggers an expansion of these cells in patient T cell cultures containing revertants. Transcripts initiation codons are underlined and patient mutation and revertant mutations are highlighted in bold.

INSIGHTS INTO THE BIOCHEMISTRY OF MODULAR RECEPTORS

Between 20% and 30% of the proteome of eukaryotic organisms is predicted to comprise integral membrane proteins [249]. These are typically synthesised at the endoplasmic reticulum (ER), where transmembrane domains (TMDs) are integrated into the lipid bilayer and cytoplasmic/luminal domains undergo the folding steps and post-translational modifications necessary to achieve their native structure [250]. From the ER, correctly folded proteins are incorporated intro transport vesicles from delivery to the cis-Golgi and subsequently to the trans-Golgi network, from where they are sorted to their site of function [251]. In contrast, proteins that fail to attain the

correct conformation are prevented from moving along the secretory pathway by a series of quality control checkpoints, including those at the ER, Golgi apparatus and plasma membrane [252-255].

Unlike sorting signals in cytosolic domains, transmembrane domain sorting determinants are not conserved amino acid sequences but rather depend on physical properties such as the length and hydrophicity of the transmembrane span.

A helical bundle of **completely hydrophobic residues is a very limited structure** with which to accomplish transmembrane functions, so it is not surprising that more polar groups are found, including Q, N, H, D, E, R, and K. Many of these have been implicated in proton or electron transport or in binding prosthetic groups. When these groups are placed in a low dielectric environment, they are likely to be in their uncharged forms, but will nonetheless remain strongly polar [195].

Close inspection of the NMR CD247 dimer structure [256], showed that in this situation, the aspartic acid side chains from each CD247 molecules face one another, and are not exposed to the hydrophobic environment of the bilayer. In this scenario the CD247 TM domains are in a state of partial ionization [257]. Results obtained in dimerization experiments using CD247 TM mutants suggest that dimerization only requires a combination of at least one acidic residue and a polar residue at position 6 in the two strands, and there may be one charged residue and the other one protonated [256].

In fact, when molecular modelling studies **assembling the CD247 dimer together with the CD16A** receptor were carried out, only the condition in which one aspartic acid of the CD247 dimer pair was charged enabled the association with CD16A, strongly suggesting that one charged and one protonated and so with polar behaviour aspartic acids may be the most probable situation in the low dielectric environment of the inside of the membrane bilayer.

Another observation from these studies modelling the interaction of CD16A with the CD247 dimer was that the dimer structure changes its organization and orientation, opening to accommodate the CD16A receptor. In this situation, CD247 aspartic acids are now exposed and interact with receptor interface. This supports the idea that the presence of charged or polar residues in the transmembrane domain is unfavourable and these amino-acids have to be shielded either by dimerization or by

association with another molecule. Otherwise, exposed, unshielded charged residues mark unsuccessful or unassembled complexes to be recognized and shunted to degradation [258].

Furthermore, these observations also show that dimer structures are diverse and adaptable depending on the molecular context. Disulphide bonded molecules are not such restricted structures as previously reported [259] and allow at least some limited rotation and exposure of different residues to adjust to different scenarios.

The data on how CD16A associates with the FcεR1γ and CD247 signaling adaptor molecules also show how there are **different roles of charged residues within the lipid bilayer** for each receptor. While it was widely accepted that charged residues were key for interactions, these data now show that the presence of charged residues in particular receptors is involved in quality control so that only fully assembled complexes exit ER/Golgi and reach the plasma membrane. Strikingly, NKp30 I/c and III/a were able to reach the plasma membrane in the absence of adaptor molecules, despite the presence of charged TM residues. The biochemical basis of this capacity is unclear, but the length and composition of the cytoplasmic tails of these receptors were important for this effect. It is interesting that even though NKp30 I/c and III/a could be expressed at the cell surface, receptor functionality still depended on being coupled to signaling modules (data not shown).

The presence of a nonpolar, fluid hydrocarbon interior is one of the defining **features of a lipid bilayer**. However, many proteins possess charged or polar amino acid residues within their transmembrane domain. The incorporation of a charged amino acid side chain such as arginine from water to the interior of a membrane is expected to be unfavourable, primarily because of the high energetic cost of dehydrating the charge. Indeed, continuum electrostatics calculations that model the membrane as a slab of low dielectric material (e.g., oil) sandwiched by a high dielectric material (e.g., water) predict that the energetic penalty of moving a charge from water into a membrane is on the order of tens of kcal mol-1 [260].

To begin to understand how charged side chains can be accommodated in membranes, it is necessary to take a more detailed look at the membrane. The complete structure of a lipid bilayer, determined by joint refinement of X-ray and neutron scattering data, revealed that only roughly half of the bilayer, the innermost 3

nm or so, is occupied exclusively by hydrocarbon, while the remainder is a chemically heterogeneous mixture of lipid polar groups and water molecules [261]. Consequently, the bilayer–water interface is not an abrupt boundary between low and high dielectric media, but rather is a roughly 1.5nm region over which the polarity smoothly decreases from the high polarity of water to the low polarity of liquid hydrocarbon [261].

Thus, it is conceivable that the **energetic cost of placing a charged side chain into a membrane** could be greatly reduced if the side chain is located in a region of the membrane where it is solvated by water and lipid polar groups. In fact, the proximity of the charged residue to the outer leaflet of the plasma membrane seems also to be crucial. Interestingly, these effects of potentially charged residues appear to correlate with the high levels of free energy required to partition their potentially charged side chains from water into a lipid bilayer. Indeed, it has been previously confirmed that the placement of charged residues closer to the end or the upper part of the bilayer has a lesser effect on degradation and membrane targeting alterations than a more central location where a higher energy has to be overcome [258].

Regarding the observation that the CD16A receptor is shunted to degradation while a D^{205}>A mutant accumulated in the ER and did not undergo degradation. It is known that charged residues in the TM of different proteins control their fate and degradation. Bonifacino and colleagues observed that incorporation of a charged residue, either R or D (in central positions, near the outer membrane leaflet it has little or no effect, which support that charged residues at TM has to be either shielded or this protein will be degraded), into a transmembrane protein renders it unable to reach cell surface and targets it for degradation.

The analysis reported here demonstrates that placement of a single potentially charged residue within the transmembrane domain of a typical integral membrane protein can result in its retention and rapid degradation in the ER [258]. This is different to previous studies of the TCR subunits [39, 40], where these charged residues directly influence both protein-protein association and protein control. In the case of CD16A, the TM aspartic acid was controlling only turnover/ degradation/ ER exit, since no alteration in CD16A driven functions was noted in the CD16A D^{205}>A mutant.

The precise position of charged residue in the lipid bilayer has not only implications for energetic cost, but also in **determining the specific complex partner selected**. For example, the FcεR1γ and DAP12 signaling modules are expressed by a variety of different cell types of hematopoietic origin and serve as signaling subunits for many different receptors. FcεR1γ and DAP12 exhibit a preference for particular basic side chain, FcεR1γ for arginine and DAP12 for lysine. However, the location of the ionizable TM residues also contributes to specificity of assembly, an aspect that is important because FcεR1γ and DAP12 are co-expressed by a number of different cell types. Genetic variation that allows binding to an incorrect signaling molecule could lead to novel responses with unpredictable consequences (Figure 6).

One important question about this newly described mode of association is how different it is compared to the established widely known model for two component complexes one residue is involved per subunit and mutation of the interacting residues will totally abolish complex formation. For CD16A several TM residues are involved and the IVT and cellular experiments show that no single mutation abolishes receptor complex assembly totally, thus mutations or polymorphisms in single residues will have less effect so this novel model of receptor complex may then reflect a more evolutionarily robust interaction (Figure 7A, B).

However, it is also true that apparently minor amino acid changes, at positions that don't participate directly in the interaction, can alter the proximity of the complex subunits and thus modulate complex formation. For example, close inspection of the interacting interfaces reveals a plausible explanation for how an apparently subtle difference between human and mouse CD247 TM sequences (a single isoleucine/leucine change) prevents the mouse version from

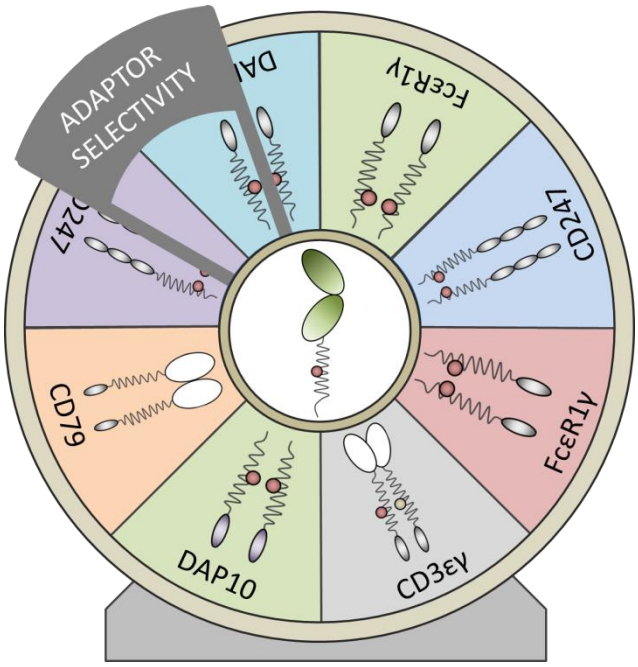

Figure 6: Signaling adaptor molecule selectivity: CD16A receptor selectivity for adaptor molecules is not a random process. Precisely positioned charged residues within transmembrane domain restrict adaptor association to each receptor.

assembling with CD16A [218].

In the cell, receptors and signaling adaptor molecules are translated simultaneously. In the particular case of NK cells where there are many receptors that associate with either CD247 or FcεR1γ, these receptors may have to compete for adaptor molecules binding and the **association mechanism may have an impact on association efficiency or speed**. In this context, how single residue interactions compare to multiple residue interactions for the recruitment of adaptor molecules is not clear (Figure 7C). One way to test this hypothesis would be to use the IVT technique. In the proposed experiment, two mRNAs encoding different receptors (that bind a single adaptor molecule through the different interacting modes, e.g CD16A and IgA binding to FcεR1γ) could be simultaneously expressed together with the adaptor molecule in a competition assay. If an excess of one receptor complex forms, compared to the other, this will reflect a stronger interaction. In cells, interpretation of such an experiment is more complex due to simultaneous occurring processes such as degradation, which will not be a problem in the IVT system.

The role of TMD based signals in the quality control of misfolded membrane proteins in mammalian cells is also not fully understood. Novel approaches are being developed in order to characterize how membrane proteins are embedded into the plasma membranes and properly fold [262]. In these experiments, proteins are extracted from the bilayer using atomic force microscopy (AFM) based single-molecule force spectroscopy (SMFS) and its transfer into a new bilayer (which can already contain another, different protein) visualised. It would be also interesting to elucidate if the association between receptor complexes that involve **multiple interactions follow an ordered sequence of events, or not,** between the different residues involved in the association (Figure 7C). Perhaps the previously described experimental approach could be applied to fully characterize how multicomponent receptors are assembled in the ER/Golgi membrane. For example, CD16A receptors could be extracted from a bilayer and placed into a new one with a high density of the desired adaptor molecule to test if a controlled, orderly sequence of residue interactions exists.

Lastly, it is interesting to point out that generally receptors have positively charged residues and the adaptors negative ones. This might, in part, reflect that some of the signaling adaptor molecules are evolutionarily related, but it's probably also relevant that the dielectric constant of the internal part of the membrane bilayer is such that arginine and lysine will likely be fully charged while aspartic and glutamic acids will often be protonated. Perhaps this explains why two acidic residues (from the adaptor dimer) are needed to offset a single basic amino-acid in the receptor.

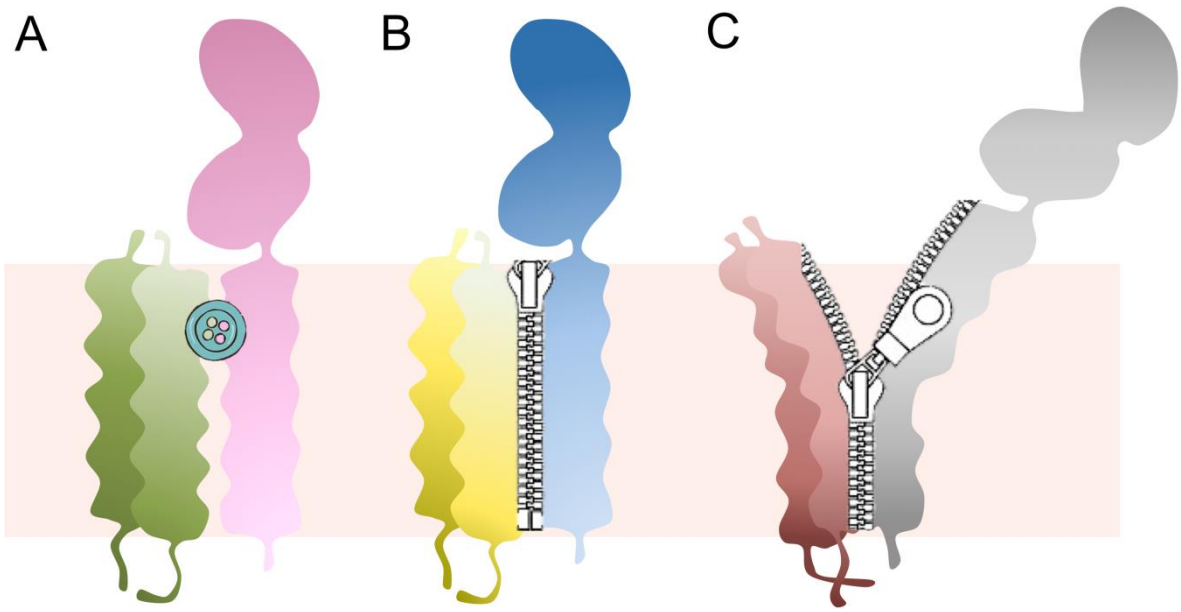

Figure 7: Receptor complexes association models: Schematic representation of different receptor based association models. Most immunoreceptors association rely on single residue interaction (A) meanwhile our novel model of receptor association for Fc receptors is based on multiple polar and aromatic interactions that extend the length of the transmembrane domain (B). Graphic representation of the possible ordered association for receptor complexes that interact by multiple interactions (C). Pink rectangle represents lipid bilayer in which receptor and signaling dimers are embedded.

Over time, immune receptors have evolved differently so that some possess both recognition and intrinsic signaling modules, while others rely on a second element for signaling capacity. A fundamental issue is therefore to discuss what the possible reasons or advantages, if any, might justify the separation of **ligand binding and signaling in two different elements.** One possibility is that the separation of these functions adds a new point of control during receptor biogenesis, assembly and extracellular exposure. Only properly assembled complexes can reach the cell surface to signal. Another possibility is that for modular receptor complexes, changes in

extracellular sequence may modulate ligand recognition while maintaining signaling capacity, whereas alterations in the transmembrane domain can change the signaling molecule a receptor binds to and in consequence, link ligand recognition to a different cellular signaling network and so alter the functional consequences of receptor ligation.

Generally, the novelty of these findings lies in the description of a completely new mode of assembly for immune receptors that can be applied more generally to other key receptors of the immune system. Only one of the four Fc receptors that require association with signaling adaptor proteins has the familiar basic TM residue that guides assembly of most modular activating immune receptors. These new data provide a plausible structural explanation for how the remaining three Fc receptors assemble with FcεRIγ and/or CD247 and show that at least two very distinct assembly mechanisms have arisen during evolution for the association of different receptors with the same set of signaling adaptors. Moreover, these data also provide a new view of the possible role of charged residues within a multicomponent modular receptor.

CONCLUSIONS

1. Cell surface expression of Natural Killer receptors CD16A and NKp30 is reduced in CD247 deficiency in a genotype-dependent manner, while NKp46 and 2B4 expression remain normal.

2. In the absence of the CD247 signaling molecule, the function of various NK cell receptors, including some that do and others that do not associate with CD247, is compromised, indicating that CD247 deficient patient NK cells are hyporesponsive.

3. Patient T cell defects, together with the absence of CD247 protein correlate with impaired NK cell development and maturation, as shown by a dramatic decrease in KIR2D expression and elevated proportions of $CD56^{bright}$ and NKG2A/CD94+ cells.

4. Detailed flow cytometric analysis of CD247 patient PBMCs revealed a minimal population of revertant T and NK cells with normal levels of TCR and CD247 protein expression, respectively.

5. Genetic analysis of patient cell cultures containing revertant cells showed extensive sequence variation in CD247 cDNAs and also identified genetic reversion due to a true back mutation and an upstream compensatory mutation, both compatible with CD247 expression allowing TCR reconstitution.

6. Analysis of the patterns of sequence variability in control genes and PID genes where reversion events have or have not been described revealed that the propensity of genes to mutate influences the probability of spontaneous reversion of genetic defects in PID.

7. The CD16A receptor interacts with CD247 and FcεR1γ signaling dimers via multiple aromatic and polar interactions between the transmembrane domains. This mode of transmembrane interaction is novel. Moreover, CD16A receptor showed no preference in signaling dimer recruitment, either CD247 or FcεR1γ.

8. Analysis of CD16A membrane expression and function in different cell lines expressing wild-type receptor and mutants identified a dual function of the $F^{202}D^{205}T^{206}$ transmembrane element: while F^{202} and T^{206} residues support complex association, D^{205} controls receptor quality control.

9. Modeling studies indicate that similar features underlie the association of CD64 and FcεR1α Fc receptors that also bind FcεR1γ and this was confirmed biochemically for the FcεR1α association with FcεR1γ.

CONCLUSIONES

1. En la deficiencia de CD247, la expresión en superficie de los receptores CD16A y NKp30 de las células NK disminuye en función del genotipo, mientras que la expresión de los receptores NKp46 y 2B4 es normal.

2. En ausencia de la molécula de señalización CD247, la respuesta NK a través de distintos receptores está comprometida, formen o no complejo con CD247, lo que indica un defecto funcional de las células NK del paciente deficiente en CD247.

3. Las células NK del paciente deficiente en CD247 muestran una gran disminución de la expresión de KIR2D, altos niveles de $CD56^{bright}$ y $NKG2A/CD94^{+}$, lo que indica un desarrollo y maduración incorrectos de las NK. Este defecto se atribuye a la ausencia de células T funcionales junto a la carencia de proteína CD247 del paciente.

4. El análisis detallado de los PBMCs del paciente deficiente en CD247 reveló la existencia de una pequeña población de células T y NK revertientes con niveles normales de TCR y CD247, respectivamente.

5. El análisis genético de cultivos celulares del paciente, que contenían células revertientes, mostró una alta tasa de variación en el ADN codificante de CD247. Además, identificamos que dicha reversión tenía lugar por una retromutación y una mutación compensatoria, ambas compatibles con la expresión de CD247 y la reconstitución del TCR.

6. Las diferencias entre los patrones de variabilidad de genes afectados en inmunodeficiencias primarias, con y sin eventos de reversión, respecto a genes control, indicaron que la propensión de un gen a mutar influye sobre la probabilidad de revertir de manera espontánea los defectos genéticos presentes en dicha patología.

7. El receptor CD16A interacciona con los módulos de señalización CD247 y FcεR1γ a través de un nuevo modelo de asociación, basado en múltiples interacciones aromáticas y polares entre sus dominios transmembrana. Además, el receptor CD16A no muestra preferencia al reclutar y asociarse a uno de ambos módulos de señalización.

8. El análisis en células NK de la expresión en superficie y la respuesta funcional de las diferentes construcciones de CD16A, permitió identificar una función dual del elemento transmembrana $F^{202}D^{205}T^{206}$; mientras F^{202} y T^{206} median la formación del complejo, D^{205} regula el control de calidad del receptor.

9. El modelo informático de los receptores de Fc, CD64 y FcεR1α, en asociación con FcεR1γ mostró que la formación de sus complejos se rige por características similares. Este hallazgo fue confirmado experimentalmente para la asociación de FcεR1α con FcεR1γ.

“La ignorancia es el peor enemigo de un pueblo que quiere ser libre”

Jonathan Hennessey

REFERENCES

1. Bonilla, F.A., et al., *Practice parameter for the diagnosis and management of primary immunodeficiency.* J Allergy Clin Immunol, 2015. **136**(5): p. 1186-205 e1-78.
2. Morgan, G. and R.J. Levinsky, *Clinical significance of IgA deficiency.* Arch Dis Child, 1988. **63**(6): p. 579-81.
3. Geha, R.S., et al., *Primary immunodeficiency diseases: an update from the International Union of Immunological Societies Primary Immunodeficiency Diseases Classification Committee.* J Allergy Clin Immunol, 2007. **120**(4): p. 776-94.
4. Picard, C., et al., *Primary Immunodeficiency Diseases: an Update on the Classification from the International Union of Immunological Societies Expert Committee for Primary Immunodeficiency 2015.* J Clin Immunol, 2015. **35**(8): p. 696-726.
5. Notarangelo, L.D., *Primary immunodeficiencies.* J Allergy Clin Immunol, 2010. **125**(2 Suppl 2): p. S182-94.
6. Casanova, J.L., et al., *Guidelines for genetic studies in single patients: lessons from primary immunodeficiencies.* J Exp Med, 2014. **211**(11): p. 2137-49.
7. Al-Herz, W., et al., *Consanguinity and primary immunodeficiencies.* Hum Hered, 2014. **77**(1-4): p. 138-43.
8. Acuna-Hidalgo, R., J.A. Veltman, and A. Hoischen, *New insights into the generation and role of de novo mutations in health and disease.* Genome Biol, 2016. **17**(1): p. 241.
9. Hirschhorn, R., *In vivo reversion to normal of inherited mutations in humans.* J Med Genet, 2003. **40**(10): p. 721-8.
10. Jonkman, M.F., *Revertant mosaicism in human genetic disorders.* Am J Med Genet, 1999. **85**(4): p. 361-4.
11. Youssoufian, H. and R.E. Pyeritz, *Mechanisms and consequences of somatic mosaicism in humans.* Nat Rev Genet, 2002. **3**(10): p. 748-58.
12. Youssoufian, H., *Natural gene therapy and the Darwinian legacy.* Nat Genet, 1996. **13**(3): p. 255-6.
13. Moncada-Velez, M., et al., *Somatic mosaicism caused by monoallelic reversion of a mutation in T cells of a patient with ADA-SCID and the effects of enzyme replacement therapy on the revertant phenotype.* Scand J Immunol, 2011. **74**(5): p. 471-81.
14. Kuijpers, T.W., et al., *A reversion of an IL2RG mutation in combined immunodeficiency providing competitive advantage to the majority of CD8+ T cells.* Haematologica, 2013. **98**(7): p. 1030-8.
15. Wada, T., et al., *Oligoclonal expansion of T lymphocytes with multiple second-site mutations leads to Omenn syndrome in a patient with RAG1-deficient severe combined immunodeficiency.* Blood, 2005. **106**(6): p. 2099-101.
16. Davis, B.R., et al., *Somatic mosaicism in the Wiskott-Aldrich syndrome: molecular and functional characterization of genotypic revertants.* Clin Immunol, 2010. **135**(1): p. 72-83.
17. Jing, H., et al., *Somatic reversion in dedicator of cytokinesis 8 immunodeficiency modulates disease phenotype.* J Allergy Clin Immunol, 2014. **133**(6): p. 1667-75.
18. Nishikomori, R., et al., *X-linked ectodermal dysplasia and immunodeficiency caused by reversion mosaicism of NEMO reveals a critical role for NEMO in human T-cell development and/or survival.* Blood, 2004. **103**(12): p. 4565-72.
19. Jondeau, G., et al., *International Registry of Patients Carrying TGFBR1 or TGFBR2 Mutations: Results of the MAC (Montalcino Aortic Consortium).* Circ Cardiovasc Genet, 2016. **9**(6): p. 548-558.
20. Hull, S., et al., *Somatic mosaicism of a novel IKBKG mutation in a male patient with incontinentia pigmenti.* Am J Med Genet A, 2015. **167**(7): p. 1601-4.
21. Palendira, U., et al., *Expansion of somatically reverted memory CD8+ T cells in patients with X-linked lymphoproliferative disease caused by selective pressure from Epstein-Barr virus.* J Exp Med, 2012. **209**(5): p. 913-24.

22. Uzel, G., et al., *Reversion mutations in patients with leukocyte adhesion deficiency type-1 (LAD-1).* Blood, 2008. **111**(1): p. 209-18.
23. Gregory, J.J., Jr., et al., *Somatic mosaicism in Fanconi anemia: evidence of genotypic reversion in lymphohematopoietic stem cells.* Proc Natl Acad Sci U S A, 2001. **98**(5): p. 2532-7.
24. Gross, M., et al., *Reverse mosaicism in Fanconi anemia: natural gene therapy via molecular self-correction.* Cytogenet Genome Res, 2002. **98**(2-3): p. 126-35.
25. Waisfisz, Q., et al., *Spontaneous functional correction of homozygous fanconi anaemia alleles reveals novel mechanistic basis for reverse mosaicism.* Nat Genet, 1999. **22**(4): p. 379-83.
26. Rieux-Laucat, F., et al., *Inherited and somatic CD3zeta mutations in a patient with T-cell deficiency.* N Engl J Med, 2006. **354**(18): p. 1913-21.
27. Roberts, J.L., et al., *T-B+NK+ severe combined immunodeficiency caused by complete deficiency of the CD3zeta subunit of the T-cell antigen receptor complex.* Blood, 2007. **109**(8): p. 3198-206.
28. Marin, A.V., et al., *Primary T-cell immunodeficiency with functional revertant somatic mosaicism in CD247.* J Allergy Clin Immunol, 2017. **139**(1): p. 347-349 e8.
29. Blazquez-Moreno, A., et al., *Analysis of the recovery of CD247 expression in a PID patient: insights into the spontaneous repair of defective genes.* Blood, 2017. **130**(10): p. 1205-1208.
30. Davis, M.M. and P.J. Bjorkman, *T-cell antigen receptor genes and T-cell recognition.* Nature, 1988. **334**(6181): p. 395-402.
31. Call, M.E. and K.W. Wucherpfennig, *Common themes in the assembly and architecture of activating immune receptors.* Nat Rev Immunol, 2007. **7**(11): p. 841-50.
32. Krogsgaard, M. and M.M. Davis, *How T cells 'see' antigen.* Nat Immunol, 2005. **6**(3): p. 239-45.
33. Weiss, A., *T cell antigen receptor signal transduction: a tale of tails and cytoplasmic protein-tyrosine kinases.* Cell, 1993. **73**(2): p. 209-12.
34. Call, M.E., et al., *The organizing principle in the formation of the T cell receptor-CD3 complex.* Cell, 2002. **111**(7): p. 967-79.
35. Orloff, D.G., et al., *Biochemical characterization of the eta chain of the T-cell receptor. A unique subunit related to zeta.* J Biol Chem, 1989. **264**(25): p. 14812-7.
36. Bonifacino, J.S., et al., *Subunit interactions within the T-cell antigen receptor: clues from the study of partial complexes.* Proc Natl Acad Sci U S A, 1988. **85**(18): p. 6929-33.
37. Koning, F., et al., *The biosynthesis and assembly of T cell receptor alpha- and beta-chains with the CD3 complex.* J Immunol, 1988. **140**(9): p. 3126-34.
38. Alarcon, B., et al., *Assembly of the human T cell receptor-CD3 complex takes place in the endoplasmic reticulum and involves intermediary complexes between the CD3-gamma.delta.epsilon core and single T cell receptor alpha or beta chains.* J Biol Chem, 1988. **263**(6): p. 2953-61.
39. Minami, Y., et al., *Building a multichain receptor: synthesis, degradation, and assembly of the T-cell antigen receptor.* Proc Natl Acad Sci U S A, 1987. **84**(9): p. 2688-92.
40. Ashwell, J.D. and R.D. Klusner, *Genetic and mutational analysis of the T-cell antigen receptor.* Annu Rev Immunol, 1990. **8**: p. 139-67.
41. Malissen, B., et al., *Function of the CD3 subunits of the pre-TCR and TCR complexes during T cell development.* Adv Immunol, 1999. **72**: p. 103-48.
42. Alarcon, B., et al., *Congenital T-cell receptor immunodeficiencies in man.* Immunodefic Rev, 1990. **2**(1): p. 1-16.
43. Morgan, N.V., et al., *Mutation in the TCRalpha subunit constant gene (TRAC) leads to a human immunodeficiency disorder characterized by a lack of TCRalphabeta+ T cells.* J Clin Invest, 2011. **121**(2): p. 695-702.

44. Arnaiz-Villena, A., et al., *Brief report: primary immunodeficiency caused by mutations in the gene encoding the CD3-gamma subunit of the T-lymphocyte receptor.* N Engl J Med, 1992. **327**(8): p. 529-33.
45. Sanal, O., et al., *Low expression of T-cell receptor-CD3 complex: a case with a clinical presentation resembling humoral immunodeficiency.* Turk J Pediatr, 1996. **38**(1): p. 81-4.
46. Allende, L.M., et al., *Fourteen years' follow-up of an autoimmune patient lacking the CD3 gamma subunit of the T-lymphocyte receptor.* Blood, 2000. **96**(12): p. 4007-8.
47. Recio, M.J., et al., *Differential biological role of CD3 chains revealed by human immunodeficiencies.* J Immunol, 2007. **178**(4): p. 2556-64.
48. Dadi, H.K., A.J. Simon, and C.M. Roifman, *Effect of CD3delta deficiency on maturation of alpha/beta and gamma/delta T-cell lineages in severe combined immunodeficiency.* N Engl J Med, 2003. **349**(19): p. 1821-8.
49. de Saint Basile, G., et al., *Severe combined immunodeficiency caused by deficiency in either the delta or the epsilon subunit of CD3.* J Clin Invest, 2004. **114**(10): p. 1512-7.
50. Takada, H., et al., *Severe combined immunodeficiency caused by a splicing abnormality of the CD3delta gene.* Eur J Pediatr, 2005. **164**(5): p. 311-4.
51. Marcus, N., et al., *Hematopoietic stem cell transplantation for CD3delta deficiency.* J Allergy Clin Immunol, 2011. **128**(5): p. 1050-7.
52. Gil, J., et al., *A leaky mutation in CD3D differentially affects alphabeta and gammadelta T cells and leads to a Talphabeta-Tgammadelta+B+NK+ human SCID.* J Clin Invest, 2011. **121**(10): p. 3872-6.
53. Soudais, C., et al., *Independent mutations of the human CD3-epsilon gene resulting in a T cell receptor/CD3 complex immunodeficiency.* Nat Genet, 1993. **3**(1): p. 77-81.
54. Regueiro JR, R.M., *T-Cell Receptor Complex Deficiency*. 3rd ed. Primary Immunodeficiency Diseases: A Molecular and Genetic Approach. 2013: Oxford University Press.
55. Anderson, P., et al., *CD3-negative natural killer cells express zeta TCR as part of a novel molecular complex.* Nature, 1989. **341**(6238): p. 159-62.
56. Lanier, L.L., G. Yu, and J.H. Phillips, *Co-association of CD3 zeta with a receptor (CD16) for IgG Fc on human natural killer cells.* Nature, 1989. **342**(6251): p. 803-5.
57. Vales-Gomez, M., et al., *Natural killer cell hyporesponsiveness and impaired development in a CD247-deficient patient.* J Allergy Clin Immunol, 2016. **137**(3): p. 942-5 e4.
58. Kiessling, R., E. Klein, and H. Wigzell, *"Natural" killer cells in the mouse. I. Cytotoxic cells with specificity for mouse Moloney leukemia cells. Specificity and distribution according to genotype.* Eur J Immunol, 1975. **5**(2): p. 112-7.
59. Herberman, R.B., M.E. Nunn, and D.H. Lavrin, *Natural cytotoxic reactivity of mouse lymphoid cells against syngeneic acid allogeneic tumors. I. Distribution of reactivity and specificity.* Int J Cancer, 1975. **16**(2): p. 216-29.
60. Angelo, L.S., et al., *Practical NK cell phenotyping and variability in healthy adults.* Immunol Res, 2015. **62**(3): p. 341-56.
61. Westermann, J. and R. Pabst, *Distribution of lymphocyte subsets and natural killer cells in the human body.* Clin Investig, 1992. **70**(7): p. 539-44.
62. Melsen, J.E., et al., *Human Circulating and Tissue-Resident CD56(bright) Natural Killer Cell Populations.* Front Immunol, 2016. **7**: p. 262.
63. Yu, J., A.G. Freud, and M.A. Caligiuri, *Location and cellular stages of natural killer cell development.* Trends Immunol, 2013. **34**(12): p. 573-82.
64. Carrega, P. and G. Ferlazzo, *Natural killer cell distribution and trafficking in human tissues.* Front Immunol, 2012. **3**: p. 347.
65. Lodoen, M.B. and L.L. Lanier, *Natural killer cells as an initial defense against pathogens.* Curr Opin Immunol, 2006. **18**(4): p. 391-8.

66. Vivier, E., et al., *Functions of natural killer cells.* Nat Immunol, 2008. **9**(5): p. 503-10.
67. Cooper, M.A., T.A. Fehniger, and M.A. Caligiuri, *The biology of human natural killer-cell subsets.* Trends Immunol, 2001. **22**(11): p. 633-40.
68. Robertson, M.J., *Role of chemokines in the biology of natural killer cells.* J Leukoc Biol, 2002. **71**(2): p. 173-83.
69. Miller, J.S., K.A. Alley, and P. McGlave, *Differentiation of natural killer (NK) cells from human primitive marrow progenitors in a stroma-based long-term culture system: identification of a CD34+7+ NK progenitor.* Blood, 1994. **83**(9): p. 2594-601.
70. Galy, A., et al., *Human T, B, natural killer, and dendritic cells arise from a common bone marrow progenitor cell subset.* Immunity, 1995. **3**(4): p. 459-73.
71. Grzywacz, B., et al., *Natural killer-cell differentiation by myeloid progenitors.* Blood, 2011. **117**(13): p. 3548-58.
72. Haller, O., et al., *Generation of natural killer cells: an autonomous function of the bone marrow.* J Exp Med, 1977. **145**(5): p. 1411-6.
73. Freud, A.G., et al., *A human CD34(+) subset resides in lymph nodes and differentiates into CD56bright natural killer cells.* Immunity, 2005. **22**(3): p. 295-304.
74. Di Santo, J.P. and C.A. Vosshenrich, *Bone marrow versus thymic pathways of natural killer cell development.* Immunol Rev, 2006. **214**: p. 35-46.
75. Chinen, H., et al., *Lamina propria c-kit+ immune precursors reside in human adult intestine and differentiate into natural killer cells.* Gastroenterology, 2007. **133**(2): p. 559-73.
76. Wu, X., et al., *Development of murine hepatic NK cells during ontogeny: comparison with spleen NK cells.* Clin Dev Immunol, 2012. **2012**: p. 759765.
77. Freud, A.G., et al., *Evidence for discrete stages of human natural killer cell differentiation in vivo.* J Exp Med, 2006. **203**(4): p. 1033-43.
78. Spits, H., et al., *Innate lymphoid cells--a proposal for uniform nomenclature.* Nat Rev Immunol, 2013. **13**(2): p. 145-9.
79. Romagnani, C., et al., *CD56brightCD16- killer Ig-like receptor- NK cells display longer telomeres and acquire features of CD56dim NK cells upon activation.* J Immunol, 2007. **178**(8): p. 4947-55.
80. Carson, W.E., T.A. Fehniger, and M.A. Caligiuri, *CD56bright natural killer cell subsets: characterization of distinct functional responses to interleukin-2 and the c-kit ligand.* Eur J Immunol, 1997. **27**(2): p. 354-60.
81. Lanier, L.L., et al., *The relationship of CD16 (Leu-11) and Leu-19 (NKH-1) antigen expression on human peripheral blood NK cells and cytotoxic T lymphocytes.* J Immunol, 1986. **136**(12): p. 4480-6.
82. Freud, A.G., J. Yu, and M.A. Caligiuri, *Human natural killer cell development in secondary lymphoid tissues.* Semin Immunol, 2014. **26**(2): p. 132-7.
83. Wu, C., et al., *Clonal tracking of rhesus macaque hematopoiesis highlights a distinct lineage origin for natural killer cells.* Cell Stem Cell, 2014. **14**(4): p. 486-499.
84. Yu, J., et al., *CD94 surface density identifies a functional intermediary between the CD56bright and CD56dim human NK-cell subsets.* Blood, 2010. **115**(2): p. 274-81.
85. Juelke, K., et al., *CD62L expression identifies a unique subset of polyfunctional CD56dim NK cells.* Blood, 2010. **116**(8): p. 1299-307.
86. Cichocki, F., et al., *Epigenetic regulation of NK cell differentiation and effector functions.* Front Immunol, 2013. **4**: p. 55.
87. Eller, M.A. and J.R. Currier, *OMIP-007: phenotypic analysis of human natural killer cells.* Cytometry A, 2012. **81**(6): p. 447-9.
88. Horowitz, A., et al., *Genetic and environmental determinants of human NK cell diversity revealed by mass cytometry.* Sci Transl Med, 2013. **5**(208): p. 208ra145.

89. Strauss-Albee, D.M., et al., *Human NK cell repertoire diversity reflects immune experience and correlates with viral susceptibility.* Sci Transl Med, 2015. **7**(297): p. 297ra115.
90. Hwang, I., et al., *Identification of human NK cells that are deficient for signaling adaptor FcRgamma and specialized for antibody-dependent immune functions.* Int Immunol, 2012. **24**(12): p. 793-802.
91. Lee, J., et al., *Epigenetic modification and antibody-dependent expansion of memory-like NK cells in human cytomegalovirus-infected individuals.* Immunity, 2015. **42**(3): p. 431-42.
92. Vivier, E., et al., *Innate or adaptive immunity? The example of natural killer cells.* Science, 2011. **331**(6013): p. 44-9.
93. Zhang, T., et al., *Cutting edge: antibody-dependent memory-like NK cells distinguished by FcRgamma deficiency.* J Immunol, 2013. **190**(4): p. 1402-6.
94. Nabekura, T. and L.L. Lanier, *Antigen-specific expansion and differentiation of natural killer cells by alloantigen stimulation.* J Exp Med, 2014. **211**(12): p. 2455-65.
95. Reeves, R.K., et al., *Antigen-specific NK cell memory in rhesus macaques.* Nat Immunol, 2015. **16**(9): p. 927-32.
96. O'Leary, J.G., et al., *T cell- and B cell-independent adaptive immunity mediated by natural killer cells.* Nat Immunol, 2006. **7**(5): p. 507-16.
97. Cooper, M.A., et al., *Cytokine-induced memory-like natural killer cells.* Proc Natl Acad Sci U S A, 2009. **106**(6): p. 1915-9.
98. Sun, J.C., J.N. Beilke, and L.L. Lanier, *Adaptive immune features of natural killer cells.* Nature, 2009. **457**(7229): p. 557-61.
99. Paust, S., et al., *Critical role for the chemokine receptor CXCR6 in NK cell-mediated antigen-specific memory of haptens and viruses.* Nat Immunol, 2010. **11**(12): p. 1127-35.
100. Min-Oo, G., et al., *Natural killer cells: walking three paths down memory lane.* Trends Immunol, 2013. **34**(6): p. 251-8.
101. Arase, H., et al., *Direct recognition of cytomegalovirus by activating and inhibitory NK cell receptors.* Science, 2002. **296**(5571): p. 1323-6.
102. Smith, H.R., et al., *Recognition of a virus-encoded ligand by a natural killer cell activation receptor.* Proc Natl Acad Sci U S A, 2002. **99**(13): p. 8826-31.
103. Sun, J.C., J.N. Beilke, and L.L. Lanier, *Immune memory redefined: characterizing the longevity of natural killer cells.* Immunol Rev, 2010. **236**: p. 83-94.
104. Guma, M., et al., *Imprint of human cytomegalovirus infection on the NK cell receptor repertoire.* Blood, 2004. **104**(12): p. 3664-71.
105. Lopez-Verges, S., et al., *Expansion of a unique CD57(+)NKG2Chi natural killer cell subset during acute human cytomegalovirus infection.* Proc Natl Acad Sci U S A, 2011. **108**(36): p. 14725-32.
106. Foley, B., et al., *Human cytomegalovirus (CMV)-induced memory-like NKG2C(+) NK cells are transplantable and expand in vivo in response to recipient CMV antigen.* J Immunol, 2012. **189**(10): p. 5082-8.
107. Foley, B., et al., *Cytomegalovirus reactivation after allogeneic transplantation promotes a lasting increase in educated NKG2C+ natural killer cells with potent function.* Blood, 2012. **119**(11): p. 2665-74.
108. Mombaerts, P., et al., *RAG-1-deficient mice have no mature B and T lymphocytes.* Cell, 1992. **68**(5): p. 869-77.
109. Shinkai, Y., et al., *RAG-2-deficient mice lack mature lymphocytes owing to inability to initiate V(D)J rearrangement.* Cell, 1992. **68**(5): p. 855-67.
110. Long, E.O., et al., *Controlling natural killer cell responses: integration of signals for activation and inhibition.* Annu Rev Immunol, 2013. **31**: p. 227-58.

111. Vivier, E., J.A. Nunes, and F. Vely, *Natural killer cell signaling pathways.* Science, 2004. **306**(5701): p. 1517-9.
112. Elliott, J.M. and W.M. Yokoyama, *Unifying concepts of MHC-dependent natural killer cell education.* Trends Immunol, 2011. **32**(8): p. 364-72.
113. Shifrin, N., D.H. Raulet, and M. Ardolino, *NK cell self tolerance, responsiveness and missing self recognition.* Semin Immunol, 2014. **26**(2): p. 138-44.
114. Joncker, N.T., et al., *Mature natural killer cells reset their responsiveness when exposed to an altered MHC environment.* J Exp Med, 2010. **207**(10): p. 2065-72.
115. Elliott, J.M., J.A. Wahle, and W.M. Yokoyama, *MHC class I-deficient natural killer cells acquire a licensed phenotype after transfer into an MHC class I-sufficient environment.* J Exp Med, 2010. **207**(10): p. 2073-9.
116. Orr, M.T., W.J. Murphy, and L.L. Lanier, *'Unlicensed' natural killer cells dominate the response to cytomegalovirus infection.* Nat Immunol, 2010. **11**(4): p. 321-7.
117. Tu, M.M., A.B. Mahmoud, and A.P. Makrigiannis, *Licensed and Unlicensed NK Cells: Differential Roles in Cancer and Viral Control.* Front Immunol, 2016. **7**: p. 166.
118. Mahmoud, A.B., et al., *Influenza Virus Targets Class I MHC-Educated NK Cells for Immunoevasion.* PLoS Pathog, 2016. **12**(2): p. e1005446.
119. Boudreau, J.E., et al., *KIR3DL1 and HLA-B Density and Binding Calibrate NK Education and Response to HIV.* J Immunol, 2016. **196**(8): p. 3398-410.
120. Tarek, N., et al., *Unlicensed NK cells target neuroblastoma following anti-GD2 antibody treatment.* J Clin Invest, 2012. **122**(9): p. 3260-70.
121. Valiante, N.M., et al., *Functionally and structurally distinct NK cell receptor repertoires in the peripheral blood of two human donors.* Immunity, 1997. **7**(6): p. 739-51.
122. Suto, Y., et al., *Gene arrangement of the killer cell inhibitory receptor family on human chromosome 19q13.4 detected by fiber-FISH.* Immunogenetics, 1998. **48**(4): p. 235-41.
123. Parham, P., *MHC class I molecules and KIRs in human history, health and survival.* Nat Rev Immunol, 2005. **5**(3): p. 201-14.
124. Borrego, F., et al., *Recognition of human histocompatibility leukocyte antigen (HLA)-E complexed with HLA class I signal sequence-derived peptides by CD94/NKG2 confers protection from natural killer cell-mediated lysis.* J Exp Med, 1998. **187**(5): p. 813-8.
125. Braud, V.M., et al., *HLA-E binds to natural killer cell receptors CD94/NKG2A, B and C.* Nature, 1998. **391**(6669): p. 795-9.
126. Lee, N., et al., *HLA-E is a major ligand for the natural killer inhibitory receptor CD94/NKG2A.* Proc Natl Acad Sci U S A, 1998. **95**(9): p. 5199-204.
127. Ljunggren, H.G. and K. Karre, *In search of the 'missing self': MHC molecules and NK cell recognition.* Immunol Today, 1990. **11**(7): p. 237-44.
128. Sivori, S., et al., *p46, a novel natural killer cell-specific surface molecule that mediates cell activation.* J Exp Med, 1997. **186**(7): p. 1129-36.
129. Vitale, M., et al., *NKp44, a novel triggering surface molecule specifically expressed by activated natural killer cells, is involved in non-major histocompatibility complex-restricted tumor cell lysis.* J Exp Med, 1998. **187**(12): p. 2065-72.
130. Pende, D., et al., *Identification and molecular characterization of NKp30, a novel triggering receptor involved in natural cytotoxicity mediated by human natural killer cells.* J Exp Med, 1999. **190**(10): p. 1505-16.
131. Moretta, L., et al., *Surface NK receptors and their ligands on tumor cells.* Semin Immunol, 2006. **18**(3): p. 151-8.
132. Neville, M.J. and R.D. Campbell, *A new member of the Ig superfamily and a V-ATPase G subunit are among the predicted products of novel genes close to the TNF locus in the human MHC.* J Immunol, 1999. **162**(8): p. 4745-54.
133. Delahaye, N.F., et al., *Alternatively spliced NKp30 isoforms affect the prognosis of gastrointestinal stromal tumors.* Nat Med, 2011. **17**(6): p. 700-7.

134. Rusakiewicz, S., et al., *NCR3/NKp30 contributes to pathogenesis in primary Sjogren's syndrome.* Sci Transl Med, 2013. **5**(195): p. 195ra96.
135. Semeraro, M., et al., *Clinical impact of the NKp30/B7-H6 axis in high-risk neuroblastoma patients.* Sci Transl Med, 2015. **7**(283): p. 283ra55.
136. Messaoudene, M., et al., *NKp30 isoforms and NKp46 transcripts in metastatic melanoma patients: Unique NKp30 pattern in rare melanoma patients with favorable evolution.* Oncoimmunology, 2016. **5**(12): p. e1154251.
137. Rusakiewicz, S., et al., *NKp30 isoforms and NKp30 ligands are predictive biomarkers of response to imatinib mesylate in metastatic GIST patients.* Oncoimmunology, 2017. **6**(1): p. e1137418.
138. Shemesh, A., et al., *First Trimester Pregnancy Loss and the Expression of Alternatively Spliced NKp30 Isoforms in Maternal Blood and Placental Tissue.* Front Immunol, 2015. **6**: p. 189.
139. Cantoni, C., et al., *NKp44, a triggering receptor involved in tumor cell lysis by activated human natural killer cells, is a novel member of the immunoglobulin superfamily.* J Exp Med, 1999. **189**(5): p. 787-96.
140. Allcock, R.J., et al., *The human TREM gene cluster at 6p21.1 encodes both activating and inhibitory single IgV domain receptors and includes NKp44.* Eur J Immunol, 2003. **33**(2): p. 567-77.
141. Campbell, K.S., et al., *NKp44 triggers NK cell activation through DAP12 association that is not influenced by a putative cytoplasmic inhibitory sequence.* J Immunol, 2004. **172**(2): p. 899-906.
142. Rosental, B., et al., *Proliferating cell nuclear antigen is a novel inhibitory ligand for the natural cytotoxicity receptor NKp44.* J Immunol, 2011. **187**(11): p. 5693-702.
143. Ravetch, J.V. and J.P. Kinet, *Fc receptors.* Annu Rev Immunol, 1991. **9**: p. 457-92.
144. Kinet, J.P., *Antibody-cell interactions: Fc receptors.* Cell, 1989. **57**(3): p. 351-4.
145. Owen J, P.J., Stranford S, Jones P *Immunology*. 7th ed. 2009, New York: W.H. Freeman and Company. 423.
146. Otten, M.A. and M. van Egmond, *The Fc receptor for IgA (FcalphaRI, CD89).* Immunol Lett, 2004. **92**(1-2): p. 23-31.
147. Fridman, W.H., *Fc receptors and immunoglobulin binding factors.* FASEB J, 1991. **5**(12): p. 2684-90.
148. Shibuya, A. and S. Honda, *Molecular and functional characteristics of the Fcalpha/muR, a novel Fc receptor for IgM and IgA.* Springer Semin Immunopathol, 2006. **28**(4): p. 377-82.
149. Cho, Y., et al., *Molecular characteristics of IgA and IgM Fc binding to the Fcalpha/muR.* Biochem Biophys Res Commun, 2006. **345**(1): p. 474-8.
150. Ochiai, K., et al., *A review on Fc epsilon RI on human epidermal Langerhans cells.* Int Arch Allergy Immunol, 1994. **104 Suppl 1**(1): p. 63-4.
151. Prussin, C. and D.D. Metcalfe, *5. IgE, mast cells, basophils, and eosinophils.* J Allergy Clin Immunol, 2006. **117**(2 Suppl Mini-Primer): p. S450-6.
152. von Bubnoff, D., et al., *The central role of FcepsilonRI in allergy.* Clin Exp Dermatol, 2003. **28**(2): p. 184-7.
153. Kikutani, H., et al., *Structure and function of Fc epsilon receptor II (Fc epsilon RII/CD23): a point of contact between the effector phase of allergy and B cell differentiation.* Ciba Found Symp, 1989. **147**: p. 23-31; discussion 31-5.
154. Perussia, B., et al., *Immune interferon induces the receptor for monomeric IgG1 on human monocytic and myeloid cells.* J Exp Med, 1983. **158**(4): p. 1092-113.
155. Looney, R.J., G.N. Abraham, and C.L. Anderson, *Human monocytes and U937 cells bear two distinct Fc receptors for IgG.* J Immunol, 1986. **136**(5): p. 1641-7.
156. Qiu, W.Q., et al., *Organization of the human and mouse low-affinity Fc gamma R genes: duplication and recombination.* Science, 1990. **248**(4956): p. 732-5.

157. Sammartino, L., et al., *Assignment of the gene coding for human FcRII (CD32) to bands q23q24 on chromosome 1.* Immunogenetics, 1988. **28**(5): p. 380-1.
158. Grundy, H.O., et al., *The polymorphic Fc gamma receptor II gene maps to human chromosome 1q.* Immunogenetics, 1989. **29**(5): p. 331-9.
159. Bredius, R.G., et al., *Role of neutrophil Fc gamma RIIa (CD32) and Fc gamma RIIIb (CD16) polymorphic forms in phagocytosis of human IgG1- and IgG3-opsonized bacteria and erythrocytes.* Immunology, 1994. **83**(4): p. 624-30.
160. Koene, H.R., et al., *Fc gammaRIIIa-158V/F polymorphism influences the binding of IgG by natural killer cell Fc gammaRIIIa, independently of the Fc gammaRIIIa-48L/R/H phenotype.* Blood, 1997. **90**(3): p. 1109-14.
161. Franke, L., et al., *Association analysis of copy numbers of FC-gamma receptor genes for rheumatoid arthritis and other immune-mediated phenotypes.* Eur J Hum Genet, 2016. **24**(2): p. 263-70.
162. Li, X., A.W. Gibson, and R.P. Kimberly, *Human FcR polymorphism and disease.* Curr Top Microbiol Immunol, 2014. **382**: p. 275-302.
163. Wu, J., et al., *A novel polymorphism of FcgammaRIIIa (CD16) alters receptor function and predisposes to autoimmune disease.* J Clin Invest, 1997. **100**(5): p. 1059-70.
164. Andren, M., et al., *IgG Fc receptor polymorphisms and association with autoimmune disease.* Eur J Immunol, 2005. **35**(10): p. 3020-9.
165. Indik, Z.K., et al., *The molecular dissection of Fc gamma receptor mediated phagocytosis.* Blood, 1995. **86**(12): p. 4389-99.
166. Harrison, P.T., et al., *Binding of monomeric immunoglobulin G triggers Fc gamma RI-mediated endocytosis.* J Biol Chem, 1994. **269**(39): p. 24396-402.
167. Maverakis, E., et al., *Glycans in the immune system and The Altered Glycan Theory of Autoimmunity: a critical review.* J Autoimmun, 2015. **57**: p. 1-13.
168. Zhu, X., et al., *MHC class I-related neonatal Fc receptor for IgG is functionally expressed in monocytes, intestinal macrophages, and dendritic cells.* J Immunol, 2001. **166**(5): p. 3266-76.
169. Firan, M., et al., *The MHC class I-related receptor, FcRn, plays an essential role in the maternofetal transfer of gamma-globulin in humans.* Int Immunol, 2001. **13**(8): p. 993-1002.
170. Simister, N.E., et al., *New functions of the MHC class I-related Fc receptor, FcRn.* Biochem Soc Trans, 1997. **25**(2): p. 481-6.
171. Anderson, P., et al., *Fc gamma receptor type III (CD16) is included in the zeta NK receptor complex expressed by human natural killer cells.* Proc Natl Acad Sci U S A, 1990. **87**(6): p. 2274-8.
172. Lanier, L.L., J.H. Phillips, and R. Testi, *Membrane anchoring and spontaneous release of CD16 (FcR III) by natural killer cells and granulocytes.* Eur J Immunol, 1989. **19**(4): p. 775-8.
173. Vivier, E., et al., *Structural similarity between Fc receptors and T cell receptors. Expression of the gamma-subunit of Fc epsilon RI in human T cells, natural killer cells and thymocytes.* J Immunol, 1991. **147**(12): p. 4263-70.
174. Letourneur, O., et al., *Characterization of the family of dimers associated with Fc receptors (Fc epsilon RI and Fc gamma RIII).* J Immunol, 1991. **147**(8): p. 2652-6.
175. Cassatella, M.A., et al., *Fc gamma R(CD16) interaction with ligand induces Ca2+ mobilization and phosphoinositide turnover in human natural killer cells. Role of Ca2+ in Fc gamma R(CD16)-induced transcription and expression of lymphokine genes.* J Exp Med, 1989. **169**(2): p. 549-67.
176. Anegon, I., et al., *Interaction of Fc receptor (CD16) ligands induces transcription of interleukin 2 receptor (CD25) and lymphokine genes and expression of their products in human natural killer cells.* J Exp Med, 1988. **167**(2): p. 452-72.

177. Li, T., et al., *Modulating IgG effector function by Fc glycan engineering.* Proc Natl Acad Sci U S A, 2017. **114**(13): p. 3485-3490.
178. Chen, T.F., et al., *Engineering Aglycosylated IgG Variants with Wild-Type or Improved Binding Affinity to Human Fc Gamma RIIA and Fc Gamma RIIIAs.* J Mol Biol, 2017. **429**(16): p. 2528-2541.
179. Okazaki, A., et al., *Fucose depletion from human IgG1 oligosaccharide enhances binding enthalpy and association rate between IgG1 and FcgammaRIIIa.* J Mol Biol, 2004. **336**(5): p. 1239-49.
180. Yamane-Ohnuki, N. and M. Satoh, *Production of therapeutic antibodies with controlled fucosylation.* MAbs, 2009. **1**(3): p. 230-6.
181. Wang, T.T., et al., *IgG antibodies to dengue enhanced for FcgammaRIIIA binding determine disease severity.* Science, 2017. **355**(6323): p. 395-398.
182. Ochoa, M.C., et al., *Antibody-dependent cell cytotoxicity: immunotherapy strategies enhancing effector NK cells.* Immunol Cell Biol, 2017. **95**(4): p. 347-355.
183. Shields, R.L., et al., *High resolution mapping of the binding site on human IgG1 for Fc gamma RI, Fc gamma RII, Fc gamma RIII, and FcRn and design of IgG1 variants with improved binding to the Fc gamma R.* J Biol Chem, 2001. **276**(9): p. 6591-604.
184. Lazar, G.A., et al., *Engineered antibody Fc variants with enhanced effector function.* Proc Natl Acad Sci U S A, 2006. **103**(11): p. 4005-10.
185. Garni-Wagner, B.A., et al., *A novel function-associated molecule related to non-MHC-restricted cytotoxicity mediated by activated natural killer cells and T cells.* J Immunol, 1993. **151**(1): p. 60-70.
186. Mathew, P.A., et al., *Cloning and characterization of the 2B4 gene encoding a molecule associated with non-MHC-restricted killing mediated by activated natural killer cells and T cells.* J Immunol, 1993. **151**(10): p. 5328-37.
187. Nakajima, H. and M. Colonna, *2B4: an NK cell activating receptor with unique specificity and signal transduction mechanism.* Hum Immunol, 2000. **61**(1): p. 39-43.
188. Lee, K.M., et al., *2B4 acts as a non-major histocompatibility complex binding inhibitory receptor on mouse natural killer cells.* J Exp Med, 2004. **199**(9): p. 1245-54.
189. Ma, C.S., K.E. Nichols, and S.G. Tangye, *Regulation of cellular and humoral immune responses by the SLAM and SAP families of molecules.* Annu Rev Immunol, 2007. **25**: p. 337-79.
190. Watzl, C., C.C. Stebbins, and E.O. Long, *NK cell inhibitory receptors prevent tyrosine phosphorylation of the activation receptor 2B4 (CD244).* J Immunol, 2000. **165**(7): p. 3545-8.
191. Chen, R., et al., *Molecular dissection of 2B4 signaling: implications for signal transduction by SLAM-related receptors.* Mol Cell Biol, 2004. **24**(12): p. 5144-56.
192. Meinke, S. and C. Watzl, *NK cell cytotoxicity mediated by 2B4 and NTB-A is dependent on SAP acting downstream of receptor phosphorylation.* Front Immunol, 2013. **4**: p. 3.
193. Watson, H., *Biological membranes*. Essays in Biochemistry ed. Vol. 59. 2015.
194. Tusnady, G.E. and I. Simon, *Principles governing amino acid composition of integral membrane proteins: application to topology prediction.* J Mol Biol, 1998. **283**(2): p. 489-506.
195. Popot, J.L. and D.M. Engelman, *Helical membrane protein folding, stability, and evolution.* Annu Rev Biochem, 2000. **69**: p. 881-922.
196. Berry, R. and M.E. Call, *Modular Activating Receptors in Innate and Adaptive Immunity.* Biochemistry, 2017. **56**(10): p. 1383-1402.
197. Natarajan, A., et al., *Structural Model of the Extracellular Assembly of the TCR-CD3 Complex.* Cell Rep, 2016. **14**(12): p. 2833-45.
198. Martinez-Martin, N., et al., *Cooperativity between T cell receptor complexes revealed by conformational mutants of CD3epsilon.* Sci Signal, 2009. **2**(83): p. ra43.

199. Kuhns, M.S. and M.M. Davis, *Disruption of extracellular interactions impairs T cell receptor-CD3 complex stability and signaling.* Immunity, 2007. **26**(3): p. 357-69.
200. Beddoe, T., et al., *Antigen ligation triggers a conformational change within the constant domain of the alphabeta T cell receptor.* Immunity, 2009. **30**(6): p. 777-88.
201. Ghendler, Y., et al., *One of the CD3epsilon subunits within a T cell receptor complex lies in close proximity to the Cbeta FG loop.* J Exp Med, 1998. **187**(9): p. 1529-36.
202. Kuhns, M.S. and M.M. Davis, *TCR Signaling Emerges from the Sum of Many Parts.* Front Immunol, 2012. **3**: p. 159.
203. Kim, S.T., et al., *Distinctive CD3 heterodimeric ectodomain topologies maximize antigen-triggered activation of alpha beta T cell receptors.* J Immunol, 2010. **185**(5): p. 2951-9.
204. Samelson, L.E., et al., *A 20-kDa protein associated with the murine T-cell antigen receptor is phosphorylated in response to activation by antigen or concanavalin A.* Proc Natl Acad Sci U S A, 1985. **82**(7): p. 1969-73.
205. Weissman, A.M., et al., *Molecular cloning of the zeta chain of the T cell antigen receptor.* Science, 1988. **239**(4843): p. 1018-21.
206. Kuster, H., H. Thompson, and J.P. Kinet, *Characterization and expression of the gene for the human Fc receptor gamma subunit. Definition of a new gene family.* J Biol Chem, 1990. **265**(11): p. 6448-52.
207. Weissman, A.M., et al., *Molecular cloning and chromosomal localization of the human T-cell receptor zeta chain: distinction from the molecular CD3 complex.* Proc Natl Acad Sci U S A, 1988. **85**(24): p. 9709-13.
208. Baniyash, M., et al., *The isolation and characterization of the murine T cell antigen receptor zeta chain gene.* J Biol Chem, 1989. **264**(22): p. 13252-7.
209. Orloff, D.G., et al., *Family of disulphide-linked dimers containing the zeta and eta chains of the T-cell receptor and the gamma chain of Fc receptors.* Nature, 1990. **347**(6289): p. 189-91.
210. Weissman, A.M., et al., *Tyrosine phosphorylation of the human T cell antigen receptor zeta-chain: activation via CD3 but not CD2.* J Immunol, 1988. **141**(10): p. 3532-6.
211. Lanier, L.L., *Up on the tightrope: natural killer cell activation and inhibition.* Nat Immunol, 2008. **9**(5): p. 495-502.
212. Sigalov, A.B., *Multichain immune recognition receptor signaling from spatiotemporal organization to human disease. Preface.* Adv Exp Med Biol, 2008. **640**: p. ix-xi.
213. Metzger, H., *Transmembrane signaling: the joy of aggregation.* J Immunol, 1992. **149**(5): p. 1477-87.
214. Eriksson, M., et al., *Inhibitory receptors alter natural killer cell interactions with target cells yet allow simultaneous killing of susceptible targets.* J Exp Med, 1999. **190**(7): p. 1005-12.
215. Garrity, D., et al., *The activating NKG2D receptor assembles in the membrane with two signaling dimers into a hexameric structure.* Proc Natl Acad Sci U S A, 2005. **102**(21): p. 7641-6.
216. Feng, J., et al., *Convergence on a distinctive assembly mechanism by unrelated families of activating immune receptors.* Immunity, 2005. **22**(4): p. 427-38.
217. Feng, J., M.E. Call, and K.W. Wucherpfennig, *The assembly of diverse immune receptors is focused on a polar membrane-embedded interaction site.* PLoS Biol, 2006. **4**(5): p. e142.
218. Blazquez-Moreno, A., et al., *Transmembrane features governing Fc receptor CD16A assembly with CD16A signaling adaptor molecules.* Proc Natl Acad Sci U S A, 2017. **114**(28): p. E5645-E5654.
219. Demaison, C., et al., *High-level transduction and gene expression in hematopoietic repopulating cells using a human immunodeficiency [correction of imunodeficiency]*

virus type 1-based lentiviral vector containing an internal spleen focus forming virus promoter. Hum Gene Ther, 2002. **13**(7): p. 803-13.
220. Sussman, J.J., et al., *Failure to synthesize the T cell CD3-zeta chain: structure and function of a partial T cell receptor complex.* Cell, 1988. **52**(1): p. 85-95.
221. Itan, Y., et al., *The human gene damage index as a gene-level approach to prioritizing exome variants.* Proc Natl Acad Sci U S A, 2015. **112**(44): p. 13615-20.
222. Moretta, L. and A. Moretta, *Unravelling natural killer cell function: triggering and inhibitory human NK receptors.* EMBO J, 2004. **23**(2): p. 255-9.
223. Pessino, A., et al., *Molecular cloning of NKp46: a novel member of the immunoglobulin superfamily involved in triggering of natural cytotoxicity.* J Exp Med, 1998. **188**(5): p. 953-60.
224. Hibbs, M.L., et al., *Mechanisms for regulating expression of membrane isoforms of Fc gamma RIII (CD16).* Science, 1989. **246**(4937): p. 1608-11.
225. Schlums, H., et al., *Cytomegalovirus infection drives adaptive epigenetic diversification of NK cells with altered signaling and effector function.* Immunity, 2015. **42**(3): p. 443-56.
226. Shibata, F., et al., *Skin infiltration of CD56(bright) CD16(-) natural killer cells in a case of X-SCID with Omenn syndrome-like manifestations.* Eur J Haematol, 2007. **79**(1): p. 81-5.
227. Bach, F.H., et al., *Lymphocyte reactivity in vitro. II. Soluble reconstituting factor permitting response of purified lymphocyte.* Cell Immunol, 1970. **1**(2): p. 219-27.
228. Liossis, S.N., et al., *Altered pattern of TCR/CD3-mediated protein-tyrosyl phosphorylation in T cells from patients with systemic lupus erythematosus. Deficient expression of the T cell receptor zeta chain.* J Clin Invest, 1998. **101**(7): p. 1448-57.
229. Maurice, M.M., et al., *Defective TCR-mediated signaling in synovial T cells in rheumatoid arthritis.* J Immunol, 1997. **159**(6): p. 2973-8.
230. Mizoguchi, H., et al., *Alterations in signal transduction molecules in T lymphocytes from tumor-bearing mice.* Science, 1992. **258**(5089): p. 1795-8.
231. Stefanova, I., et al., *HIV infection--induced posttranslational modification of T cell signaling molecules associated with disease progression.* J Clin Invest, 1996. **98**(6): p. 1290-7.
232. Chen, S., et al., *Upregulated TCRzeta improves cytokine secretion in T cells from patients with AML.* J Hematol Oncol, 2015. **8**: p. 72.
233. Zha, X., et al., *Upregulated TCRzeta enhances interleukin-2 production in T-cells from patients with CML.* DNA Cell Biol, 2012. **31**(11): p. 1628-35.
234. Deng, G.M., et al., *T cell CD3zeta deficiency enables multiorgan tissue inflammation.* J Immunol, 2013. **191**(7): p. 3563-7.
235. Benzer, S., *On the Topography of the Genetic Fine Structure.* Proc Natl Acad Sci U S A, 1961. **47**(3): p. 403-15.
236. Hwang, D.G. and P. Green, *Bayesian Markov chain Monte Carlo sequence analysis reveals varying neutral substitution patterns in mammalian evolution.* Proc Natl Acad Sci U S A, 2004. **101**(39): p. 13994-4001.
237. Keightley, P.D., et al., *Inference of mutation parameters and selective constraint in mammalian coding sequences by approximate Bayesian computation.* Genetics, 2011. **187**(4): p. 1153-61.
238. Siepel, A. and D. Haussler, *Phylogenetic estimation of context-dependent substitution rates by maximum likelihood.* Mol Biol Evol, 2004. **21**(3): p. 468-88.
239. Nachman, M.W. and S.L. Crowell, *Estimate of the mutation rate per nucleotide in humans.* Genetics, 2000. **156**(1): p. 297-304.
240. Coulondre, C., et al., *Molecular basis of base substitution hotspots in Escherichia coli.* Nature, 1978. **274**(5673): p. 775-80.
241. Knezetic, J.A. and D.S. Luse, *The presence of nucleosomes on a DNA template prevents initiation by RNA polymerase II in vitro.* Cell, 1986. **45**(1): p. 95-104.

242. Segurel, L., M.J. Wyman, and M. Przeworski, *Determinants of mutation rate variation in the human germline.* Annu Rev Genomics Hum Genet, 2014. **15**: p. 47-70.
243. Brutlag, D. and A. Kornberg, *Enzymatic synthesis of deoxyribonucleic acid. 36. A proofreading function for the 3' leads to 5' exonuclease activity in deoxyribonucleic acid polymerases.* J Biol Chem, 1972. **247**(1): p. 241-8.
244. Boulikas, T., *Evolutionary consequences of nonrandom damage and repair of chromatin domains.* J Mol Evol, 1992. **35**(2): p. 156-80.
245. Hodgkinson, A. and A. Eyre-Walker, *Human triallelic sites: evidence for a new mutational mechanism?* Genetics, 2010. **184**(1): p. 233-41.
246. Andrews, D.W., et al., *Sequences beyond the cleavage site influence signal peptide function.* J Biol Chem, 1988. **263**(30): p. 15791-8.
247. Blobel, G. and B. Dobberstein, *Transfer of proteins across membranes. I. Presence of proteolytically processed and unprocessed nascent immunoglobulin light chains on membrane-bound ribosomes of murine myeloma.* J Cell Biol, 1975. **67**(3): p. 835-51.
248. Sunder-Plassmann, R., et al., *Functional analysis of immunoreceptor tyrosine-based activation motif (ITAM)-mediated signal transduction: the two YxxL segments within a single CD3zeta-ITAM are functionally distinct.* Eur J Immunol, 1997. **27**(8): p. 2001-9.
249. Wallin, E. and G. von Heijne, *Genome-wide analysis of integral membrane proteins from eubacterial, archaean, and eukaryotic organisms.* Protein Sci, 1998. **7**(4): p. 1029-38.
250. Braakman, I. and D.N. Hebert, *Protein folding in the endoplasmic reticulum.* Cold Spring Harb Perspect Biol, 2013. **5**(5): p. a013201.
251. Guo, Y., D.W. Sirkis, and R. Schekman, *Protein sorting at the trans-Golgi network.* Annu Rev Cell Dev Biol, 2014. **30**: p. 169-206.
252. Babst, M., *Quality control: quality control at the plasma membrane: one mechanism does not fit all.* J Cell Biol, 2014. **205**(1): p. 11-20.
253. Koenig, P.A. and H.L. Ploegh, *Protein quality control in the endoplasmic reticulum.* F1000Prime Rep, 2014. **6**: p. 49.
254. Wang, S. and D.T. Ng, *Evasion of endoplasmic reticulum surveillance makes Wsc1p an obligate substrate of Golgi quality control.* Mol Biol Cell, 2010. **21**(7): p. 1153-65.
255. Briant, K., N. Johnson, and E. Swanton, *Transmembrane domain quality control systems operate at the endoplasmic reticulum and Golgi apparatus.* PLoS One, 2017. **12**(4): p. e0173924.
256. Call, M.E., et al., *The structure of the zetazeta transmembrane dimer reveals features essential for its assembly with the T cell receptor.* Cell, 2006. **127**(2): p. 355-68.
257. Senes, A., D.E. Engel, and W.F. DeGrado, *Folding of helical membrane proteins: the role of polar, GxxxG-like and proline motifs.* Curr Opin Struct Biol, 2004. **14**(4): p. 465-79.
258. Bonifacino, J.S., et al., *Role of potentially charged transmembrane residues in targeting proteins for retention and degradation within the endoplasmic reticulum.* EMBO J, 1991. **10**(10): p. 2783-93.
259. Petersen, M.T., P.H. Jonson, and S.B. Petersen, *Amino acid neighbours and detailed conformational analysis of cysteines in proteins.* Protein Eng, 1999. **12**(7): p. 535-48.
260. Parsegian, A., *Energy of an ion crossing a low dielectric membrane: solutions to four relevant electrostatic problems.* Nature, 1969. **221**(5183): p. 844-6.
261. Wiener, M.C. and S.H. White, *Structure of a fluid dioleoylphosphatidylcholine bilayer determined by joint refinement of x-ray and neutron diffraction data. III. Complete structure.* Biophys J, 1992. **61**(2): p. 434-47.
262. Serdiuk, T., S.A. Mari, and D.J. Muller, *Pull-and-Paste of Single Transmembrane Proteins.* Nano Lett, 2017. **17**(7): p. 4478-4488.